THESIS

THE EFFECT OF FUEL ADDITIVES IN A NATURAL GAS AND GASOLINE ENGINE

Submitted by

Thomas Falloon

Department of Mechanical Engineering

In partial fulfillment of the requirements

For the Degree of Masters of Science

Colorado State University

Fort Collins, Colorado

Fall 2016

Master's Committee:

Advisor: Anthony Marchese
Co-Advisor: Daniel Olsen

Kenneth Reardon

ABSTRACT

THE EFFECT OF FUEL ADDITIVES IN A NATURAL GAS AND GASOLINE ENGINE

Fuel additives are used worldwide for a variety of applications including increasing fuel efficiency, decreasing emissions, decreasing knock propensity and/or modifying storage/handling properties. Because of the high percentage of global fossil fuel consumption attributed to internal combustion engines, fuel additives that increase the efficiency of fossil fuel powered internal combustion engines can greatly impact global fossil fuel consumption and greenhouse gas emissions. In this study, the effect of various fuel additives on spark ignited natural gas and gasoline internal combustion engines was examined. The natural gas work focused primarily on using fuel additives to extend the lean limit, while the gasoline additives work focused on lean limit extension, decreased knock propensity and increased power. Experiments were performed in using a constant speed, single cylinder, variable compression ratio Cooperative Fuel Research (CFR) engine, which has the capability to operate with both gaseous and liquid fuels. The gaseous fuel system used compressed air to simulate a turbocharged engine, while the liquid fuel system used a naturally aspirated carburetor. In-cylinder pressure data were acquired using a high-speed piezoelectric pressure transducer, which is used to calculate indicated power, peak pressure and to quantify engine knock.

In this study, four natural gas and three gasoline additives were considered. For the natural gas fuel additives, the primary hypothesis for the fuel additives was that the lean limit would be decreased with the addition of the additives. By holding the power of the engine constant and decreasing the equivalence ratio, this hypothesis was tested and it was concluded

that the additives had a negative impact on the lean limit. For the gasoline additives, the hypothesis was that the additives would either increase engine power, decrease the knock propensity (i.e. increase the octane number), or decrease the lean limit. It was found that one of the additives increased engine efficiency slightly and decreased the knock propensity, while the other two gasoline additives had negative impacts on both metrics. One of the gasoline additives appeared to slightly extend the lean limit, but further testing will be required to confirm this result.

ACKNOWLEDGEMENTS

This work would still be in the planning stages if not for the help of many people. First, thank you to my adviser Dr. Anthony Marchese, who has been patient, humorous and extremely kind since bringing me onto the team. Thank you to Dr. Daniel Olsen for continually answering all of my questions at all times of the day and night, and Azer Yalin for bringing me onto the project as well as keeping the project moving. Andrew Boissiere and Colin Gould, thank you for the continual flow of ideas, both ridiculous and practical. Thank you to Max Beard for the insane amount of time you dedicated to testing and improving the testing apparatus. Also thank you to Kirk Evans and Mark James for helping me with all of the issues that I encounter. Finally, thank you to my friends and family that put up with my, at times, less than great mood and for encouraging me to keep going.

TABLE OF CONTENTS

ABSTRACT ii
ACKNOWLEDGEMENTS iv
LIST OF TABLES vii
LIST OF FIGURES viii
1 Introduction 1
1.1 Engine Knock 2
1.2 Advanced Compression Ignition Engines 4
1.3 Previous Additive Research at CSU 5
1.4 Problem Statement and Research Objectives 9
1.5 Literature Review 9
1.5.1 Natural Gas Fuel Additives 10
1.5.2 Gasoline Additives 21
1.6 Repeatability and Variance within a Single Cylinder Engine 24
2 Experimental Apparatus and Methods 33
2.1 Safety 46
2.2 Methods for Additive Injection 46
2.2.1 Natural Gas Fuel Additives Injected as Liquids 46
2.2.2 Liquid Fuel Injection for Gasoline Additive Tests 50
2.3 Fuels 52
2.3.1 Liquid fuel 53
2.3.2 Gaseous Fuel 53
2.4 Natural Gas Fuel Additives 54
3 Results 57
3.1 Gasoline Fuel Additive Testing 57
3.1.1 Engine Stability Testing 57
3.1.2 Base Fuel Testing 68
3.1.3 Commercial Fuel Additives 76
3.1.4 Experimental Additive Testing 81
3.2 Natural Gas Additive Results 104
4 Conclusions and Future Work 122

4.1 Further Engine Improvements and Testing 122
Bibliography 125

LIST OF TABLES

Table 1: Natural gas liquid additive vapor pressures at 0°C. 50
Table 2: Shows engine parameters taken during uncertainty testing. 58
Table 3: Data taken during uncertainty testing, data represents 60 points taken over two days. . 59
Table 4: Uncertainty data collected with dehumidifier. 60
Table 5: Uncertainty data collected with heat tape and zero pressure regulator. 62
Table 6: Engine conditions used when comparing base fuels. 70
Table 7: Engine conditions during commercial additive testing. 78
Table 8: Engine conditions used during experimental additive testing. 81
Table 9: Shows the percentage change that each additive has on the base fuel. 95
Table 10: Engine conditions use for lean limit testing of gasoline fuel additives. 97

LIST OF FIGURES

Figure 1: Auto-ignition of end gas that results in engine knock. 3
Figure 2: Cylinder pressure traces that increase in knock from left to right versus time in a spark ignited engine. 4
Figure 3: Variation in combustion efficiency (X), as a function of equivalence ratio for laser spark ignited mixtures of methane/air (red line, red circles), methane/1%NM/air (blue line, blue triangles), methane/1%DMM/air (black line, black diamonds) and methane/1%DTBP/air (green line, green circles) (Dumitrache, 2016). 7
Figure 4: Ignition Delay as a function of compressed temperature in the rapid compression machine for stoichiometric mixtures of isooctane/O2/inert (blue triangles) in comparison to the same fuel/air mixture with addition of 1000 ppm of Diphenyl Amine fuel additive (red squares). Experimental compressed pressures vary from 19 to 28 bar, as the temperature varies from 655 to 870 K. Green and orange lines correspond to CHEMKIN computations with detailed chemical kinetics (Boissiere, 2016). 8
Figure 5: Lean limit of methane/air/H_2 blends in a 6-cylinder natural gas with H_2 port injection as a function of manifold pressure (Ma, 2008). The addition of hydrogen allows for leaner engine operation. 11
Figure 6: Spark to 10% MFB versus excess air ratio for methane and hydrogen mixtures. The addition of hydrogen decreases the amount of time between spark and MFB 10% (Ma, 2008).. 13
Figure 7: The effect of hydrogen and ignition timing on average maximum in-cylinder peak pressure. The addition of hydrogen causes the peak pressure to be higher when compared with pure methane. The leaner the mixture the more profound the effect the hydrogen has on the peak pressure (Ma, 2008). 14
Figure 8: The effect of hydrogen and ignition timing on the coefficient of variance of peak pressure (Ma, 2007). Hydrogen addition reduces the COV of peak pressure. 15
Figure 9: The effect on emissions of enriching natural gas with hydrogen (Verma, 2016). The addition of hydrogen causes a decrease in carbon based emission and an increase of NO_x at high engine load. 18
Figure 10: NOx production is greatly reduced when the engine is operating under lean conditions (Sierens, 2000). While operating at the lean limit of the fuel, the cases with hydrogen produce less NO_x emissions. This is the case due to cooler in cylinder temperatures. 19
Figure 11: Small variations in ignition timing can translate to large changes in cylinder pressure (Binjuwair, 2016). This is observed due to the changing volume during the expansion stroke... 25
Figure 12: Depicts how the initial fuel air mixture temperature affects the flame speed observed within a gasoline engine (Binjuwair, 2016). All of the fuels show the same property of increasing flame speed with increasing initial temperature. 27

Figure 13: Laminar flame speed versus equivalence ratio for a methane hydrogen mixture. The flame speed reaches a peak at an equivalence ratio of 1.1. From the pinnacle, there is a steep drop off in flame speed when the mixture is made richer or leaner (Ji, 2016). 28
Figure 14: Cylinder and clamping sleeve sections (Wise, 2013). Releasing the clamping sleeve and rotating the worm wheel allows the shroud to move up and down. The motion is also present for the valves, oil tray, jacket coolant condenser and valve rotator. 34
Figure 15: Representative pressure versus volume for the CFR engine. Area "A" represents the NMEP that the engine can produce. Area "B" represents the pressure that the piston exerts on the residual gas during the exhaust stroke to clear the cylinder. 37
Figure 16: CFR engine exhaust schematic (Wise, 2013). 38
Figure 17: Turbo charger schematic (Wise, 2013). 39
Figure 18: Custom exhaust components (Wise, 2013). There is custom piping in order to replicate an engine that uses a turbocharger. 39
Figure 19: Test cell fuel blending schematic (Wise, 2013). 43
Figure 20: Original CFR engine knock meter setup. 44
Figure 21: Sectional view of original CFR detonation pick up (Wise, 2013). 45
Figure 22: Updated CFR detonation pick up system (Wise, 2013). 45
Figure 23: Low flow atomizing nozzle bench test set-up. 48
Figure 24: Carburetor schematic (Waukesha, 1998). The fuel level is the same in the float chamber, the sight glass and the vertical jet. Adjusting the height of the float chamber allows for fuel flow adjustments. 52
Figure 25: EHN chemical structure. 54
Figure 26: Nitromethane chemical structure 55
Figure 27: DTBP chemical structure. 55
Figure 28: DMM chemical structure 56
Figure 29: Shows the comparison between NMEP and intake venturi temperature. 61
Figure 30: Bar charts showing how the run-to-run NMEP COV, peak pressure COV, and location of peak pressure COV change with each iteration of engine air intake. 63
Figure 31: Shows how the cycle-to-cycle NMEP COV changes with the changing engine configuration. 64
Figure 32: Shows how the cycle-to-cycle peak pressure COV changes with the changing engine configuration. 65
Figure 33: Shows that the intake pressure is more variable when the zero pressure regulator is used compared to ambient air. 66
Figure 34: Cycle-to-cycle location of peak pressure COV changes with the changing engine configuration. 67
Figure 35: Critical compression ratio of all of the base fuels. 68
Figure 36: Compares NMEP versus equivalence ratio for all of the liquid base fuels. TRF and 3:1 have the highest NMEP of about 570 kPa, Isooctane is producing and NMEP of 550 kPa, and the refinery and pump gasoline produce an NMEP around 530 kPa. 70

Figure 37: Compares brake thermal efficiency for all base fuels. TRF is the highest due to a high density of the fuel as well as a high NMEP, as seen in Figure 36. 71
Figure 38: Peak pressure and location of pressure differences between all of the base fuels. Generally, fuels with a low peak pressure, also have a late location of peak pressure. 72
Figure 39: NMEP changes over an equivalence ratio sweep. 74
Figure 40: Polynomial fitted lines through NMEP COV versus equivalence ratio. The point where each fitted line crosses the NMEP COV = 10% line is deemed the lean limit. 75
Figure 41: Commercial fuel additives. The additive on the left is the VP Racing Maddditive. The additive on the right is the Lucas Oil Octane Booster. 78
Figure 42: Brake thermal efficiency comparison between the baseline fuel and the consumer additives. 79
Figure 43: Peak pressure comparison between the baseline fuel and the consumer additives. 79
Figure 44: Critical compression ratio comparison between the baseline fuel and the consumer additives. The Lucas Oil Octane Booster increases the critical compression ratio of the 3:1 baseline fuel. 80
Figure 45: Shows impact that additive 1b has on AFR control. Each point is a 20 point moving average, each band represents a three-minute test point. The points with the additive present show larger deviation. 83
Figure 46: Shows the effect that additive 1b has on NMEP. 84
Figure 47: Additive 1b has as positive impact on average maximum peak pressure. 85
Figure 48: Additive 1b reduces the time from TDC to the location peak pressure. 86
Figure 49: Additive 2 and 3 impact brake thermal efficiency. 88
Figure 50: Additive 2 and 3 impact on NMEP. 89
Figure 51: Shows the low temperature pressure rise rate of pure isooctane. 91
Figure 52: Shows the low temperature pressure rise rate of isooctane with 1000 PPM of additive 2 91
Figure 53: Impact of additive 1b and additive 2 on the critical compression ratio of refinery gasoline. 93
Figure 54: Impact of additive 3 on the critical compression ratio of refinery gasoline. 94
Figure 55: Shows how NMEP changes with equivalence ratio from 0.98 to 0.82. 97
Figure 56: Shows how NMEP COV changes with equivalence ratio. Misfire begins to occur between an equivalence ratio of 0.86 and 0.88. Misfire has a drastic impact on NMEP COV. ... 98
Figure 57: Shows how a linear interpolation method can be used to determine the lean limit. ... 99
Figure 58: Polynomial fit method can be used to determine the lean limit. The point where the curve fit lines cross the NMEP COV = 10% line are deemed the lean limit of the fuel. 100
Figure 59: NMEP COV versus equivalence ratio for the baseline refinery gasoline and additive 1. The additive causes large fluctuations in the AFR control which makes pinning the equivalence ratio down difficult. This is represented by the Additive 1 points lined up horizontally. 102

Figure 60: NMEP COV% versus equivalence ratio comparison between the baseline refinery gasoline and additive 2 in 10000PPM concentration. 103
Figure 61: NMEP COV% versus equivalence ratio for additive 3. Additive 3 extends the lean limit. 104
Figure 62: Knock integral versus additive mol% for natural gas fuel additives. The additives cause knock when in high concentrations. 105
Figure 63: Peak pressure versus equivalence ratio for methane and methane with additive. 106
Figure 64: Shows how cycle-by-cycle NMEP changes with different equivalence ratios. There is a large different between the 0.66 points and the 0.62 points 107
Figure 65: NMEP versus Equivalence Ratio. The hydrogen additive allows the engine to hold load at leaner conditions while the other additives tend to richen the point at which the engine can hold load. 108
Figure 66: Peak pressure versus equivalence ratio for comparison pure methane and all additives. Hydrogen increases the peak pressure. The novel fuel additives decrease the peak pressure at lean conditions. 111
Figure 67: Location of peak pressure versus equivalence ratio comparison for pure methane and all additives. 111
Figure 68: Peak pressure COV versus equivalence ratio comparison for pure methane and all additives. 112
Figure 69: THC production versus equivalence ratio comparison for pure methane and all additives. 113
Figure 70: NOx production versus equivalence ratio comparison for pure methane and all additives. 114
Figure 71: Carbon Dioxide production versus equivalence ratio comparison for pure methane and all additives. 116
Figure 72: Production of water versus equivalence ratio comparison for pure methane and all additives. 117
Figure 73: Production of volatile organic compounds versus equivalence ratio comparison for pure methane and all additives. 118
Figure 74: Production of Formaldehyde versus equivalence ratio comparison for pure methane and all additives. 119
Figure 75: Production of Carbon Monoxide versus equivalence ratio comparison for pure methane and all additives. 121

1 Introduction

In 2015, Americans used 140 billion gallons of gasoline and 27.47 trillion cubic feet of natural gas (U.S. DOE, 2016). This economic value of this market represents a substantial fraction of the U.S. economy since gasoline averaged $2.50 a gallon and natural gas averaged 1.2 cents per cubic foot. For the consumer, increased engine efficiency results in decreased operating costs and there is substantial room for improvement in engine efficiency. For example, the average consumer vehicle only converts 14-30% of the chemical energy in the gasoline to kinetic energy of the vehicle; nearly 75% of these inefficiencies occur in the engine (U.S. EPA, 2016). Therefore, an engine improvement of only 2% could save Americans $10.2 billion annually. One method for increasing the efficiency of an engine is to improve the fuel quality through adding additives that enable the engine to operate on less fuel than when there are no additives present.

While future engines might be optimized to operate on future fuel/additive combinations, it is imperative for the current engine market that a fuel additive does not require engine modification. Engine modifications would require substantial upfront costs, which would greatly reduce the number of engines that would benefit from the fuel additive. This thesis explores the effect of both natural gas and gasoline fuel additives on combustion properties that could increase engine efficiency without the requirement for engine modification.

Natural gas engines typically operate under lean-burn conditions to achieve higher fuel efficiency and lower NOx emissions, so the primary purpose of the natural gas fuel additives that were evaluated is to allow the engines to operate under leaner conditions. Hydrogen is the most widely studied natural gas additive because it has been shown to allow significantly leaner

operation while decreasing emissions (Verma, 2016). However, gaseous hydrogen is difficult to use because it has a very low mass density, making it difficult and costly to store and transport, and low molecular weight and wide range of flammability limits, which contributes to leak propensity and safety issues. So, it would be beneficial to find another natural gas additive that can provide the same positive benefits of hydrogen without the problems. The natural gas additives that are analyzed in this work are liquid, so storage and transportation is much easier than the gaseous hydrogen.

Fuel additives for gasoline engines have widespread applications, such as fuel injector cleaning, fuel vaporization or fuel dying. This work is focused on inhibiting engine knock, thereby increasing octane number. Tetra-ethyl lead (TEL) was used as an anti-knock fuel additive until the mid-1970s, when it was discontinued because of health implications such as abdominal pain, vomiting and neuropathy (Beattie, 1972). Do to the large economic impact that a safe octane-booster TEL substitute additive could represent, research is ongoing globally from the small markets of Malaysia (Rahmat, 2010) and Jordan (Al-Hasan, 2003) among others, to the large markets of the United States and China. The main focus for the gasoline additives considered in this study is inhibiting knock and increasing power, as well as lean limit extension. In this way, the full effects of these additives can be quantified.

1.1 Engine Knock

Atypical combustion, or knock, events in spark ignited (SI) engines occur in two forms of auto-ignition, spark knock and surface ignition knock. Auto-ignition is the spontaneous combustion of fuels. Given enough time, this phenomenon occurs at elevated pressures (above 10 bar) and temperatures (above 400C) (Silva, 2005). Auto-ignition causes extreme in cylinder pressure fluctuations as seen in Figure 2 below. Spark knock is the repeatable knock that is

rhythmic and audible. Surface ignition knock is the result of the air-fuel charge being exposed to a hot surface. Surface ignition knock may occur before the spark ignites the charge of after the spark-originated flame has passed (Jang, 2016). Spark knock is affected by the spark timing. Sustained operation with heavy knock, spark or surface ignition, can result in accelerated engine damage. Figure 1 shows how the auto-ignition event differs from the controlled combustion event.

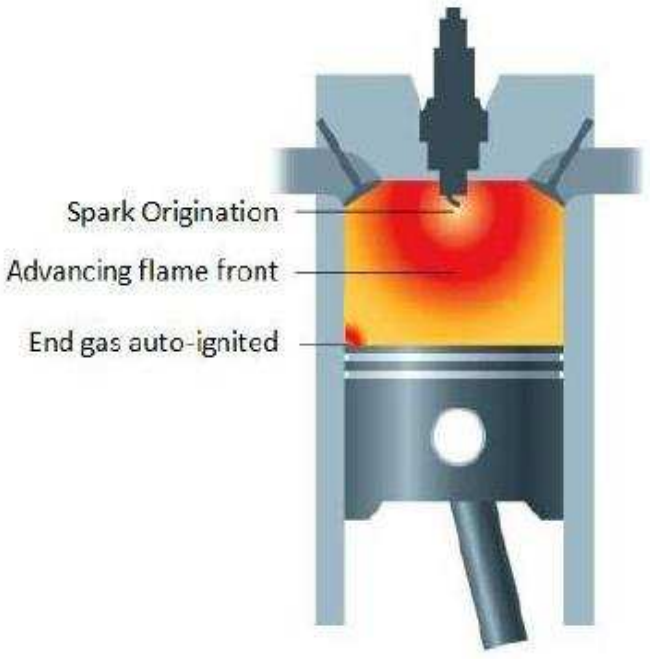

Figure 1: Auto-ignition of end gas that results in engine knock.

The combustion is controlled when the flame propagating from the spark, the large red area in Figure 1, reaches the end gas before auto-ignition occurs. Figure 2 shows how the engine cylinder pressure trace is affected by knock (Wise, 2013). The rapid fluctuations cause high pressure rise rates. The pressure rise rate is the time derivative of the shown graphs. High pressure rise rates are exceedingly hard on piston rings in Internal Combustion Engines (ICEs) and lead to shortening the usable lifetime of the machinery (Wise, 2013). The goal of the knock

tests will be to determine if these additives can be used immediately without having to modify the engine. The CFR engine provides an ideal test bed as the compression ratio and spark timing can be changed in order to induce knock.

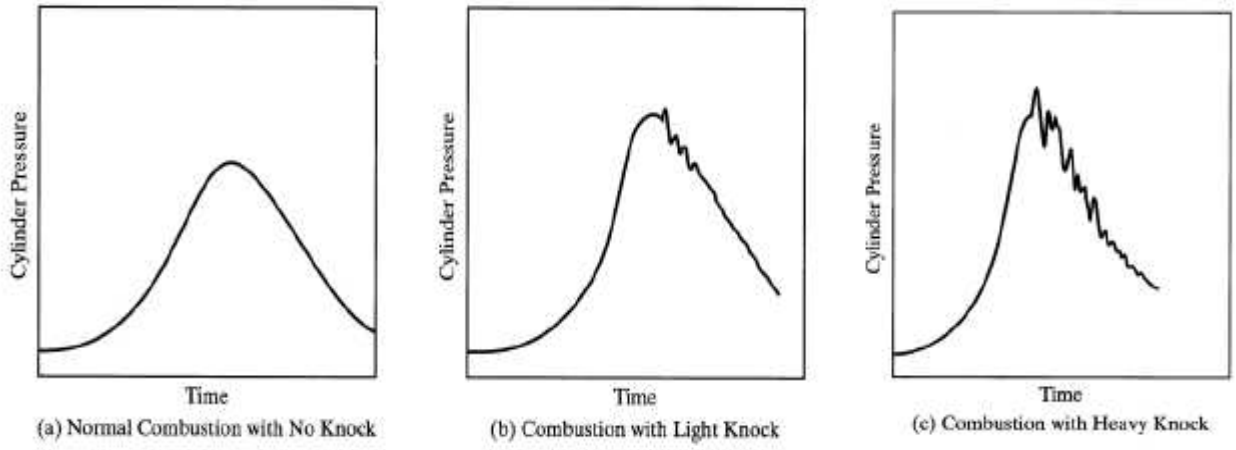

Figure 2: Cylinder pressure traces that increase in knock from left to right versus time in a spark ignited engine.

1.2 Advanced Compression Ignition Engines

Another potential application for gasoline additives is to tailor the fuel reactivity for use in future advanced compression ignition engines (ACI). Many ACI strategies have been proposed in recent years, including homogeneous charge compression ignition (HCCI), premixed charge compression ignition (PCCI), and reactivity controlled compression ignition (RCCI) (Dec, 2009). All of these strategies rely on the chemically kinetic-controlled autoignition of a premixed or partially-premixed fuel-air mixture. Current challenges with these strategies include difficulty in controlling the start of ignition over a wide range of operating conditions and, in some cases (e.g., HCCI), excessively rapid pressure rise rates during the ignition event and, in the case of RCCI, the use of two separate fuels (i.e. gasoline and diesel). Although RCCI has shown promise in terms of engine efficiency and control [(Reitz, 2015), (Kokjohn, 2011), (Hockett, 2016)], use of two separate fuels represents a unique challenge. It may be possible, however, to

instantaneously control the reactivity of a single fuel by the addition of an additive at low concentrations, thereby achieving the same objectives as RCCI but requiring only a small volume of liquid additive to be stored on the vehicle. Accordingly, a secondary objective of the gasoline research was to examine the possibility of some additives to *increase* gasoline reactivity for potential use in ACI engines.

1.3 Previous Additive Research at CSU

The fuel additive engine research presented herein was part of a larger effort at Colorado State University (CSU) that also included fundamental combustion studies conducted in the CSU Rapid Compression Machine (RCM) [(Boissiere, 2016), (Dumitrache, 2016)], . The RCM studies showed that certain fuel additives have the potential to produce the desired results discussed above (e.g., extension of lean limit for natural gas, modification of reactivity for gasoline, etc.). The CSU RCM is a duel piston cylinder system that rapidly compresses a gaseous mixture, creating an environment of elevated pressures and temperatures, and holds the pistons in the compressed position to allow the observation of high temperature chemical kinetics. See (Sung, 2014) for a more detailed description. The benefits that natural gas fuel additives have shown in RCM testing include reduced minimum ignition energy and extension of the lean limit. The extension in the lean limit can be seen in figure 3. On the x-axis is the equivalence ratio (ϕ) which is defined as the fuel /air mass ratio as compared to the stoichiometric fuel/air mass ratio. The y-axis is the overall combustion efficiency, which is defined as ratio of total heat release to the initial energy content (χ). Every RCM test was conducted with the same input energy to avoid the need to normalize the data. The input energy is the sum of fuel energy content, additive energy content, and energy supplied by the spark. The latter two components are very small in comparison to the fuel energy content. All trials were

ignited via laser, so ignition energy was precisely known. All of curves max out at about 0.95 on the y-axis due to incomplete combustion. The red curve is the baseline methane/air while the green, blue, and black curves each have 1%, by energy content of Di-tertbutyl peroxides (DTBP), Nitromethane (NM) and Dimethoxy Methane (DMM), respectively. Using these additives is correlated with getting a higher percentage of the fuel energy to being released at leaner conditions. For example, the baseline methane/air (red curve) achieves a combustion efficiency of 90% at an equivalence ratio of 0.45, whereas when certain additives are a present (the blue and black curves) a combustion efficiency of 90% can be achieved with a ϕ of approximately 0.37. This result leads to a 17.7% decrease in the amount of fuel needed to achieve the same energy output. These RCM tests show the promise of these liquid fuel additives to extend the lean limit for natural gas. However, the RCM is an idealized version of an engine where many transients (air swirl, residual gases, temperature gradients, turbulence, etc) are not present. Moreover, in the RCM the lean limit extension was quantified by the overall combustion efficiency, which is not strongly influenced by the speed at which the flames propagate through the RCM after spark initiation. As discussed below, the lean limit under engine operating conditions in the CFR is quantified by measuring the variation in cycle-to-cycle pressure history, which is much more strongly influenced by the flame propagation velocity than in the RCM.

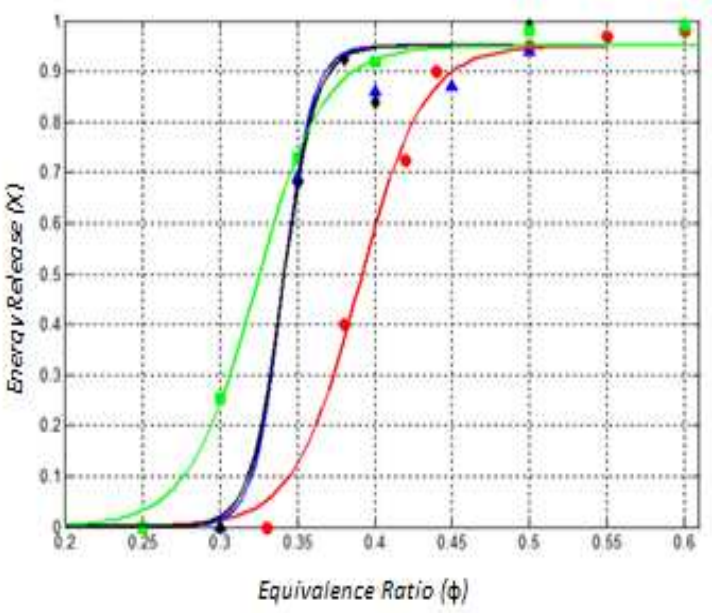

Figure 3: Variation in combustion efficiency (X), as a function of equivalence ratio for laser spark ignited mixtures of methane/air (red line, red circles), methane/1%NM/air (blue line, blue triangles), methane/1%DMM/air (black line, black diamonds) and methane/1%DTBP/air (green line, green circles) (Dumitrache, 2016).

Figure 4 shows how the gasoline fuel additives affected ignition delay in the RCM. In the gasoline additive RCM tests, the ignition delay was defined as the time period from when the pistons reach the middle of the RCM combustion chamber to the point in time where homogeneous autoignition occurs as evidenced by the maximum pressure rise rate.

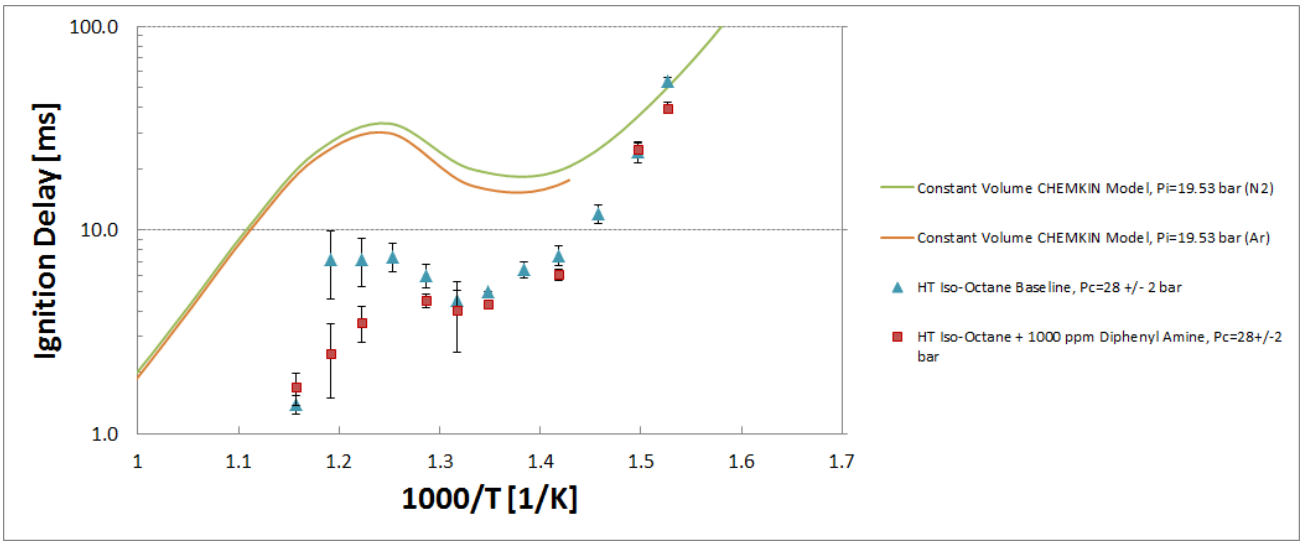

Figure 4: Ignition Delay as a function of compressed temperature in the rapid compression machine for stoichiometric mixtures of isooctane/O2/inert (blue triangles) in comparison to the same fuel/air mixture with addition of 1000 ppm of Diphenyl Amine fuel additive (red squares). Experimental compressed pressures vary from 19 to 28 bar, as the temperature varies from 655 to 870 K. Green and orange lines correspond to CHEMKIN computations with detailed chemical kinetics (Boissiere, 2016).

Figure 4 is a plot of ignition delay period as a function of compressed temperature in so-called Arrhenius form in which the ignition delay period is plotted on a log scale and the temperature is inversely expressed as (1000/T). In this form, the high temperatures are on the left side while the cooler temperatures are on the right. In the experiments plotted in Fig. 4, the experimental compressed pressures vary from 19 to 28 bar, as the temperature varies from 655 to 870 K. The green and orange lines correspond to constant volume CHEMKIN computations with detailed chemical kinetics, conducted at varying initial temperatures and two different initial pressures. The additive, at lower temperatures, had no discernable effect from the baseline. But at higher temperatures, the additive begins to have a significant impact on the ignition delay. For the temperatures between 760K and 870K, the Diphenyl Amine reduces the ignition delay. This result suggests that, at high temperatures the additive increases the reactivity of the fuel, while at low temperatures the additive does not have a discernable effect. The result suggests that the effect of these additives could differ at low temperature conditions in

comparison to high temperature conditions. Since low temperature heat release increases the temperature of a fuel/air mixture during the compression cycle and thereby increases the maximum temperature of the fuel/air mixture prior to ignition (Baumgardner, 2013), modification the reactivity of the fuel at low temperatures represents a means of enhancing or suppressing ignition at higher temperatures.

1.4 Problem Statement and Research Objectives

The problems for which solutions are pursued in this research effort are stated separately as follows:

(1) Determine effectiveness of liquid fuel additives of extending the lean limit in natural gas.

(2) Determine effect of additives on engine knock properties of natural gas.

(3) Determine effect of additives on emissions for natural gas.

(4) Determine effectiveness of liquid fuel additives of increasing engine output power for gasoline.

(5) Determine effect of additive on knock propensity in gasoline.

(6) Determine effect of additives on lean limit extension in gasoline.

This research will add to the knowledge base through testing Dimethoxy Methane (DMM), Ethylhexyl Nitrate (EHN), Nitromethane (NM), and Di-tertbutyl Peroxide (DTBP) as natural gas fuel additives as well as commercial and private gasoline fuel additives.

1.5 Literature Review

The literature reviewed in support of this project and detailed herein address two general subject areas:

(1) Previously used fuel additives for both gasoline and natural gas

(2) Repeatability and variance within a single cylinder engine.

Each of these subject areas will be address in detail below.

1.5.1 Natural Gas Fuel Additives

In the published literature, there are not many alternatives to hydrogen for use as a natural gas fuel additive. The reason for a lack of interest in natural gas additives might be because natural gas is a relatively inexpensive fuel source, which minimized the financial incentive to improve efficiency for natural gas engines. So, the research that is presented in this thesis is relatively novel since little previous work on liquid fuel additives for natural gas appears in the literature.

When hydrogen is used as a natural gas additive, the energy efficiency increases, but the operating costs increase dramatically because of the cost to produce, transport and store hydrogen. Hydrogen has been shown to increase engine power, extends the lean limit and reduces exhaust emissions (Ma, 2008). All of these characteristics will be discussed below.

Hydrogen allows an engine to be run at much lower equivalence ratios while still producing the same output power. This result has been shown in multiple studies [(Ma, 2007), (Ma, 2008), (Dillon, 1997)] and the published research is in agreement that hydrogen has a positive impact on extending the lean limit. In a study conducted by Ma et al, a 6-cylinder natural gas engine was modified such that hydrogen could be port injected. It was found that the percentage of the fuel that is hydrogen is directly proportional to the lean limit extension that the fuel exhibits. This can be clearly seen in Figure 5 (Ma, 2008).

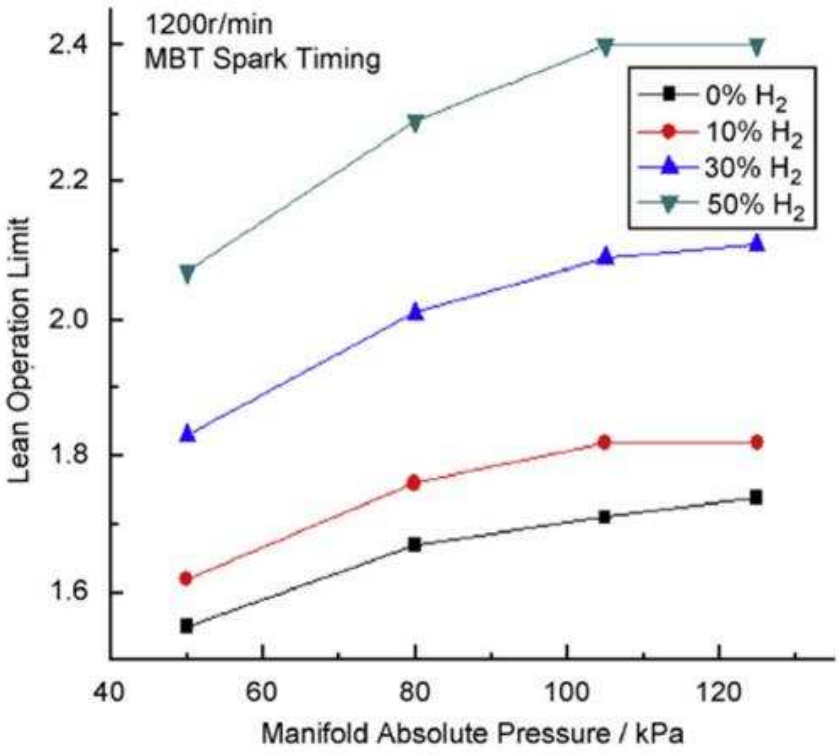

Figure 5: Lean limit of methane/air/H_2 blends in a 6-cylinder natural gas with H_2 port injection as a function of manifold pressure (Ma, 2008). The addition of hydrogen allows for leaner engine operation.

Figure 5 shows the lean operation limit (given as excess air ratio) versus the manifold pressure. An increasing lean operation limit, as shown this figure, suggests that the engine is capable of running under conditions in which less fuel is used. This chart shows that at conditions slightly above sea level (manifold pressure of 105 kPa), that the lean limit of natural gas is at an excess air ratio of 1.68. This ratio continually increases with the increasing percentage of hydrogen. When hydrogen accounts for 10% of the fuel, the lean operation limit increases by about 3% and continues to increase until the hydrogen accounts for 50% of the fuel at which point the lean operation limit of the fuel has increased by 10%. This result clearly shows how the addition of hydrogen affects the lean operation limit of a natural gas engine. Figure 5 shows how the hydrogen, even in relatively small amounts, can have a noticeable effect on the lean limit of natural gas and in larger amounts has an even larger effect. Because the

effect of hydrogen addition on combustion in natural gas engines has appeared extensively in the literature and because its effect is very pronounced, the additive work presented in this thesis will be compared against the effect of hydrogen. In addition to comparison against the literature data, comparisons are also made below against new experiments conducted in the CFR with hydrogen addition to natural gas.

Hydrogen also has the benefit of increasing the rate at which the turbulent flame propagates through the engine after spark initiation. A high turbulent flame speed will result in more complete combustion, higher pressure rise rate as well as higher bulk mean temperatures at the end of combustion. If the pressure rise rate is uncontrolled, as with engine knock, there can be significant implications with regard to engine wear. But if the engine is designed for consistently high pressure rise rates, then the engine can harness the power of hydrogen without inflicting mechanical harm. The following figure is from (Ma, 2008) and shows the burn duration from ignition to the location of mass fraction burned (MFB) 10% versus the excess air ratio and compares between methane and methane with varying levels of hydrogen. It can be seen that at conditions very near stoichiometric, that the time from spark to MFB 10% is reduced by about 6 CA, or over 25% when 50% of the fuel is hydrogen. This will drastically change the location of peak pressure as well as in-cylinder temperatures. This plot again shows that adding hydrogen to the fuel mixture will allow the engine to operate at leaner conditions. In following the MFB 0-10% of 32 CA line horizontally, it can be seen that the pure methane reaches this flame speed at an excess air ratio of 1.55 while this same flame speed does not occur in the 50% hydrogen enriched fuel until an excess air ratio of 2.07. This is a substantial difference in excess air ratio to achieve the same flame speed. Again, the correlation between MFB and excess air ratio is directly correlated to the percentage of hydrogen in the fuel.

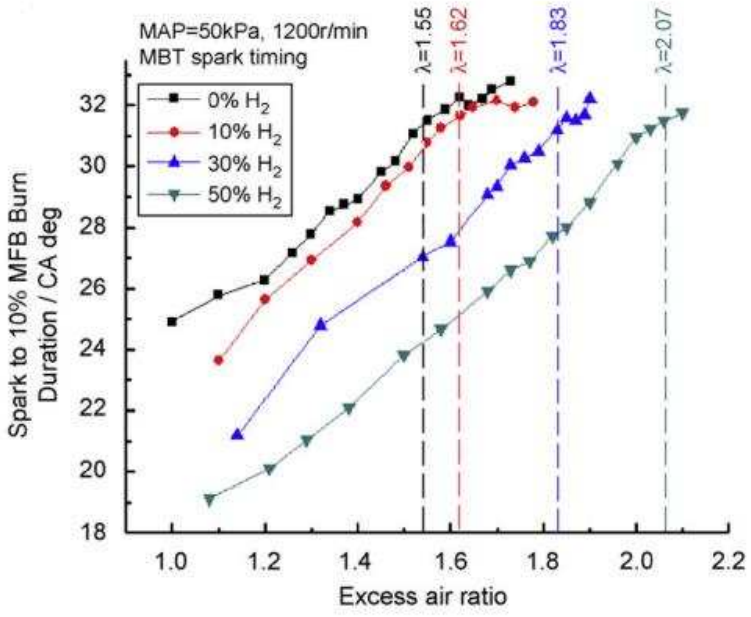

Figure 6: Spark to 10% MFB versus excess air ratio for methane and hydrogen mixtures. The addition of hydrogen decreases the amount of time between spark and MFB 10% (Ma, 2008).

In addition to extending the lean limit and increasing flame speed, hydrogen also has the capability to increase the maximum peak pressure that is observed within the cylinder. This effect happens because hydrogen burns faster as well as hotter than pure methane. Both of these parameters are important as they both affect the magnitude of peak pressure. All else being equal, the mixture with the higher temperature will have the higher pressure. Also, the flame speed is of utmost importance due to the fact that the volume is expanding during the expansion stroke. So if the flame propagates faster than the volume will be smaller and thus the pressure will be accordingly higher. These are two separate effects that both contribute to lean limit extension. Looking at the data reported by Ma [(Ma, 2007), (Ma, 2008)], it can be seen that hydrogen addition to methane has a strong impact on in-cylinder pressure. Looking at the black points that correspond to a close to stoichiometric fuel air mixture, the hydrogen case consistently displays a peak pressure that is 500 kPa higher than the methane alone. At leaner conditions such as the excess air ratio of 1.6, the difference ranges from 500 kPa to nearly 1000

kPa. This is a difference of 20% to over 30%, through adding 20% hydrogen to the fuel. Hydrogen has the ability to improve all pressure-based measurements of a natural gas engine.

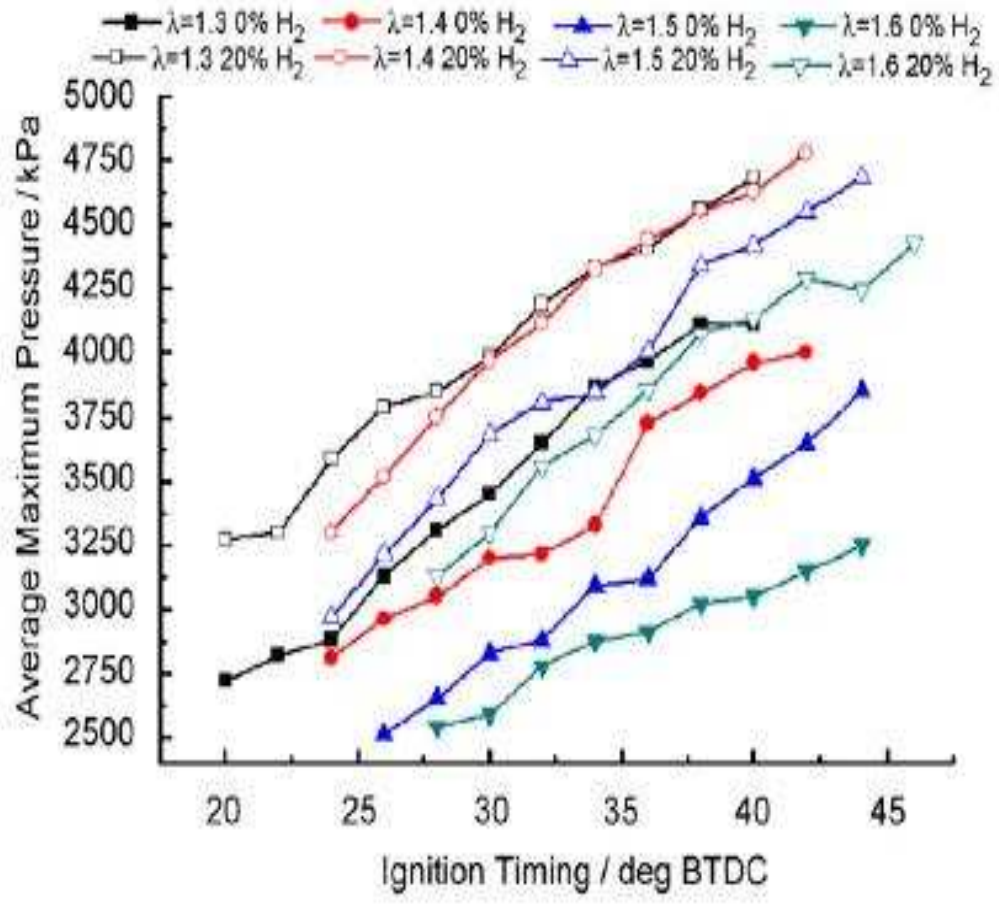

Figure 7: The effect of hydrogen and ignition timing on average maximum in-cylinder peak pressure. The addition of hydrogen causes the peak pressure to be higher when compared with pure methane. The leaner the mixture the more profound the effect the hydrogen has on the peak pressure (Ma, 2008).

Substantial research has been done that examines the effect of hydrogen addition on engine stability. This can be done in a few ways, the first of which is to look at how much the engine peak pressure changes from cycle-to-cycle. This is typically expressed as a coefficient of variance (COV) which is the percentage of the standard deviation compared to the full value. A small standard deviation compared to a large average value will produce a very small COV and a small COV is associated with small engine variation. The COV method can be applied to all major engine metrics, so variation can be quantified in many different ways. The second method

for examining engine stability is to look at the percent of cycles that the engine experiences misfire. Misfire is when one cycle produces much less power than the average cycle, or the mixture does not ignite entirely. This can be caused by many reasons, such as inadequate fuel or air supply, or a faulty spark plug. However, the percent misfire method is more suited towards two stroke engines, as two stroke engine experience higher rates of misfire.

Hydrogen enriched natural gas has be analyzed for engine stability improvements. In a study conducted by Ma (Ma, 2007), it was found that hydrogen significantly improves the peak pressure COV of a 4-stroke compressed natural gas engine. This can be seen from the following figure that was taken from (Ma, 2007):

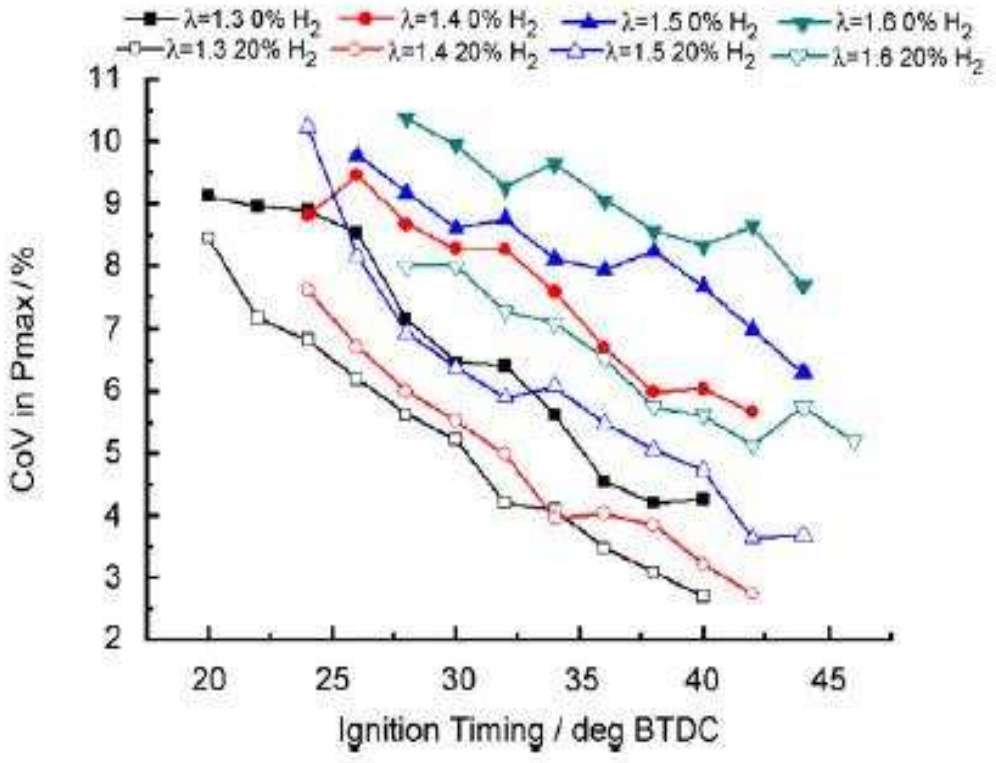

Figure 8: The effect of hydrogen and ignition timing on the coefficient of variance of peak pressure (Ma, 2007). Hydrogen addition reduces the COV of peak pressure.

This figure shows how the peak pressure COV changes with different excess air ratios, ignition timing and percent hydrogen in the fuel. Each connected data set represents one excess

air ratio, if the points are filled in then the fuel has 20% hydrogen by volume, but if the points are hollow then the fuel is only methane. It can be seen that all of the COVs decrease as the ignition timing get earlier. This is less an effect of stabilizing combustion and more of an effect of an effect that the average peak pressure is increasing as discussed above. Also, as the fuel air mixture gets leaned out, the peak pressure COV tends to increase. This shows how the pressure within the cylinder is more prone to fluctuations when the mixture is lean. It can be seen from the above data, that the addition of hydrogen can significantly lower the COV when the engine is operating lean. While looking at the green points of λ=1.6 and an ignition timing of 25 °BTDC, that the addition of 20% hydrogen reduces the peak pressure COV from 10.5 to 8. This drop is greater than 20% which shows how hydrogen can affect the behavior of a fuel at lean conditions. The effect of hydrogen enrichment is also prominent nearer to stoichiometric conditions; this can be seen when looking at the black lines in Figure 8 and an ignition timing of 25 °BTDC. With pure methane the peak pressure COV is just over 7 while the hydrogen enriched case this number drops to 5.5. Again this effect is larger than 20%. Hydrogen will impact the Peak pressure COV because it will increase the peak pressure, which will drive down the COV.

It has been discussed that hydrogen increases the flame speed, it also has been found that hydrogen promotes early flame growth. In the vicinity of the spark it is paramount that there is enough fuel and air to support combustion. If the ratio of fuel and air is not right, then no flame can exist. Hydrogen helps at the moment of the spark because H_2 has a relatively weak bond that breaks easily, and once this bond is broken two radicals are made. So, hydrogen helps with creating the initial flame kernel. However, when the flame kernel is small it is vulnerable as it loses heat to the spark plug. In order to continue propagation, the flame must produce more heat than it loses to the spark plug. Again hydrogen helps as it quickly makes a lot of radicals which

can decompose fuel and air molecules quickly to release a lot of heat in a short period of time. This helps the lean flames exist while losing heat to the spark plug. Once the flame leaves the vicinity of the spark plug it will expand rapidly. It is thought that hydrogen is so beneficial to extending the lean limit because of the rapid heat release that is hydrogen is capable of just after the spark.

Hydrogen has the capability to reduce emissions from a natural gas spark ignited engine. This research has been conducted multiple times and has been conclusive across numerous studies. For example, two studies [(Verma, 2016), (Sierens, 2000)] were focused on dissecting how the addition of hydrogen affects the emissions of natural gas. Theoretically, the emissions of hydrogen gas should be only water. This study found that CO, HC, and CO_2 emissions were reduced when hydrogen was added to the fuel in varying concentrations. It makes sense that the carbon based emissions decrease because less carbon is entering with the fuel when there is hydrogen instead of natural gas. However, the combustion temperatures that are produced when hydrogen is burned are relatively high, so the burned gas tends to cause nitrogen to deteriorate, which in turn will create NOx emissions. There is some debate in the literature about how much NOx emissions there will be in the exhaust gas when hydrogen is used as a fuel. It has been found that the amount of NOx emissions is related to the engine load, as seen in the following figure taken from (Verma, 2016):

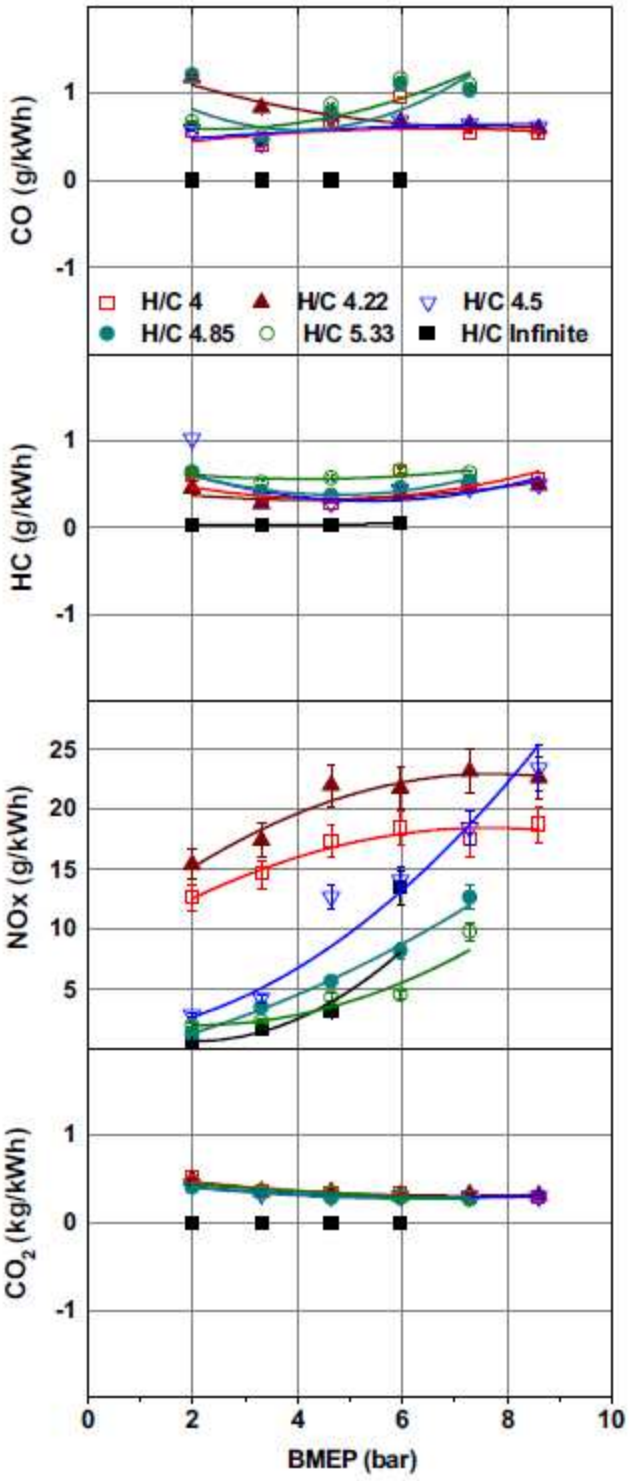

Figure 9: The effect on emissions of enriching natural gas with hydrogen (Verma, 2016). The addition of hydrogen causes a decrease in carbon based emission and an increase of NO_x at high engine load.

This data clearly show that when the engine load (BMEP) starts to increase beyond 5 bar, that the NOx emissions from the 100% hydrogen case begins to create more NOx emission than the other test cases where hydrogen is less prevalent. This is a clear sign that the effect of hotter combustion temperatures is beginning to take over at these higher engine loads. For comparison purposes, this research found that there was a crossing point. When the load of the engine was low, the pure methane and the low percent hydrogen cases produced more NOx than the high percent hydrogen cases. This result was not reflected in other studies. In another study (Sierens, 2000) it was found that the NOx emissions from the engine were always less from the natural gas with no hydrogen. This can be seen from the following plot which compares the NOx output versus the lambda value (lambda is equal to 1 divided by the equivalence ratio).

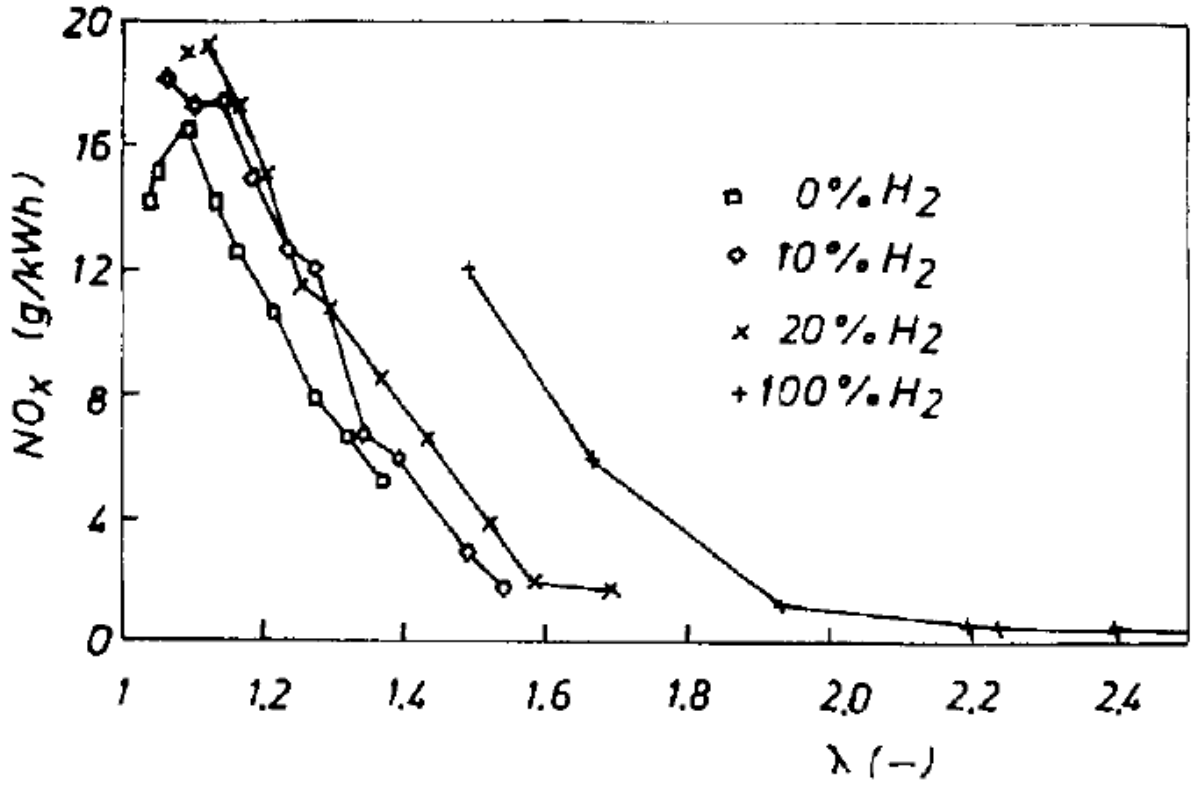

Figure 10: NOx production is greatly reduced when the engine is operating under lean conditions (Sierens, 2000). While operating at the lean limit of the fuel, the cases with hydrogen produce less NO_x emissions. This is the case due to cooler in cylinder temperatures.

This result is interesting as both research parties used methane as a natural gas representative as natural gas is primarily methane. So the base fuel is the same and the amount of hydrogen in the fuel is the same, but the amount of NOx emissions shows slightly different trends. However, it is standard that at the lower equivalence ratios that the NOx production is significantly less than at stoichiometric conditions. The only way to create NOx when burning any combination of methane and hydrogen is to create enough heat such that a N_2 bond breaks and creates nitrogen radicals. When the engine is operating under lean conditions, the mixture tends to cooler for two reasons. The first is that the heat is released from the decomposition of the fuel and air, and there are fewer reactions happening as there is less fuel so there is less energy being released. And the second reason is that the energy that is released is more or less evenly distributed among all of the species present in the chamber, so a smaller amount of energy is dispersed amongst the same amount of air, resulting in a lower air temperature. So, the lean mixture combustion tends to be much cooler than the stoichiometric mixture combustion, which causes fewer N_2 bonds to break and thus the amount of NOx emissions found in the exhaust are significantly lower.

Although hydrogen is a great fuel additive in the sense of performance, there are also challenges to implementing hydrogen. These include safe storage and transportation as well as economic problems. As discussed above, hydrogen is a very small and reactive molecule. The size of hydrogen is important when considering storage and transportation because hydrogen will escape through extremely small holes that even methane cannot escape from. There is already a problem with a leaky infrastructure around natural gas, and using a molecule that is much smaller than natural gas will only exacerbate the problem. There has been a lot of research done that focuses on safely storing hydrogen [(Rosi, 2003), (Dillon, 1997)]. The storage methods that

offer excellent hydrogen retention are expensive. This is an issue due to the propensity of hydrogen to ignite. So, hydrogen is not quite ready for the market yet. Once the transportation and storage issues are solved from an economic standpoint, and then hydrogen will most likely enter the market in higher concentrations.

Over all hydrogen is an effective fuel additive, but needs better infrastructure to be developed until widespread usage can be considered safe and economical. This leaves the door open for additional natural gas fuel additives. There is a scarcity of published research regarding liquid fuel additives for use in natural gas engines. This must be explored as a means to increase power and reduce emissions in natural gas emissions without the need for large scale infrastructure change.

1.5.2 Gasoline Additives

There have been numerous gasoline fuel additives that have been used in practice and/or experimentally. From the mid 1920's through the 1970's tetraethyl lead (TEL) was used as a gasoline fuel additive. With TEL in the fuel, the octane number increased dramatically which allowed for an increase in compression ratio which allows for an increase in engine power and efficiency. However, lead was found to cause brain damage so the large scale addition of TEL to gasoline was ceased (Beattie, 1972). This created a need to develop unleaded gasoline formulations and/or additives increase the octane number of gasoline without the use of TEL. A few potential additives are discussed below.

The most commonly used fuel additive in use today is ethanol. Ethanol is widely used because it is relatively cheap, is fully soluble in gasoline, is capable of increasing the global efficiency of an engine, and also reduces toxic pollutants [(Verma, 2016), (Schifter, 2016)]. Ethanol is commonly purchased at gas stations as either as E10 or E85 fuel. E85 fuel is 85%

ethanol and 15% gasoline by volume. Almost all gasoline purchased in the United States contains 10% ethanol while some engines are suited to run with E85. It has been found in multiple studies that ethanol tends to increase the average peak pressure and that the peak pressure increases with increasing ethanol percentage. It has also been reported that ethanol in the fuel decreases the particulate emissions that as engine emits. This benefit can be realized to the tune of a 90% decrease in PM1 (Schifter, 2016). Furthermore a decrease of the carcinogenic benzene rings was found to be around 50% when E85 fuel was used. The drawbacks to ethanol are that it has a low energy density and that it is more expensive to store as it tends to degrade when in the presence of water. The low energy density implies that a car running on fuel that has a high percentage of ethanol will have a significantly lower mpg rating than a car that is operating on pure gasoline. Ethanol is generally a less expensive than gasoline on a volume basis but the cost benefit is typically overcome by the lack of energy density. As of the time of writing, ethanol costs about 10% more per mile than pure gasoline. Also, storing ethanol becomes costly as it degrades when it interacts with water; many gas stations are not equipped with the equipment that will safely store ethanol. Using ethanol is a good start to supplementing fossil fuels with biofuels, but there are some key fuel parameters that must be fixed in order to enable the safe implementation of additives into the gasoline infrastructure.

A gasoline additive that has been studied is Di-tertbutyl peroxide (DTBP) (Splitter, 2010). This fuel additive is used as a cetane number (CN) enhancer. Like octane number, CN is a measure of the fuel's inclination to auto ignition. However, the CN is inversely proportional, so a low CN fuel will have a longer ignition delay while a fuel with a high CN is have a short ignition delay. In this study conducted by Splitter (Splitter, 2010), DTBP was used in a reactivity controlled compression ignition (RCCI) engine. The engine operated on gasoline. The majority

of the gasoline was port injected, while a small percent (up to 0.2%) of the gasoline entered the combustion chamber via direct injection. Of the fuel that is direct injected, between 0.75 and 3.5% is DTBP. The addition of DTBP causes the ignition delay of the mixture to shorten. So this fuel additive is used when the reactivity of the fuel needs to increase. A reactivity increase can lead to less fuel being used while still producing the same power. This study found that DTBP caused an increase in peak pressure and engine efficiency. When the DTBP was in a 3.5% concentration the deviation from the baseline gasoline was smaller than when in the 0.75% concentration. This result would indicate that the mixture became saturated when only a small amount of DTBP was present in the base fuel. This research has a direct link to the research presented in this thesis as DTBP is an additive that will be tested in natural gas.

In addition to using fuel additives that increase fuel reactivity, such as DTBP, fuel additives are used to decrease the reactivity of the fuel, such as Methyl-cyclopentadienyl Manganese Tricarbonyl (MMT) (Geng, 2015). MMT is used as an octane enhancer, which implies that the reactivity of the fuel is reduced, as the fuel will have a delayed onset of knock when compared to the base fuel. In one experimental study (Geng, 2015), MMT was used as a gasoline additive in a gasoline direct inject (GDI) engine. Previous research conducted on MMT (Splitter, 2010) has used a port injected engine and found that the additive tends to decrease catalyst life, as well as increase CO and HC emissions, which are both toxic to humans. However, a complete analysis of the additive had not been performed as it is possible that the additive could have a different effect on the engine properties when the fuel is injected in a different way. This study used the additive in varying concentrations from 0% to 18%. It was found that the additive tended to reduce knocking tendencies, increased cylinder peak pressure, increased combustion rate and decreased HC emission when compared with the base fuel.

However, this additive also increased the emission of CO and NOx. This research did not find the MMT additive to be safe enough for commercial use. However, this previous research is relevant to the research presented herein as it highlights that fuel additives can have a different effect in different engines when the engine parameters change. This is important to note because one positive or negative test is not enough to fully classify any one additive. The CFR currently has no way to vary load or engine speed with the current gasoline configuration, which represents a limitation of the present study and it is important to note that the results presented herein might differ from experiments with the same additives conducted in other engines.

There have been many gasoline fuel additives that have been tested and documented, but there have not been the same additive impacts seen with gasoline as hydrogen impacts natural gas. There is still a large window for gasoline fuel additives to fill. Currently almost all North American cars are run off of gasoline. This presents a very large market, so improving gasoline will have positive economic and environmental impacts. Further research must be conducted in order to find a gasoline fuel additive that fits this bill.

1.6 Repeatability and Variance within a Single Cylinder Engine

The repeatability of the engine can be analyzed in several different ways. The engine power output, peak pressure, location of peak pressure and emissions have been analyzed previously at other research firms and those results will be presented here as a means for a launching point for high engine repeatability for a high degree of accuracy in this research.

The location of peak pressure is mostly dependent on spark timing, mixture temperature and pressure, as well as equivalence ratio. The spark is the initiator for all of the combustion events that follow. In order to keep a constant location of peak pressure the ignition timing must also be very consistent cycle to cycle. As shown in Figure 11, a spark timing change of only 2

crank angle degrees has been shown in (Binjuwair, 2016) to alter the location of peak pressure by as much as 6 crank angle degrees.

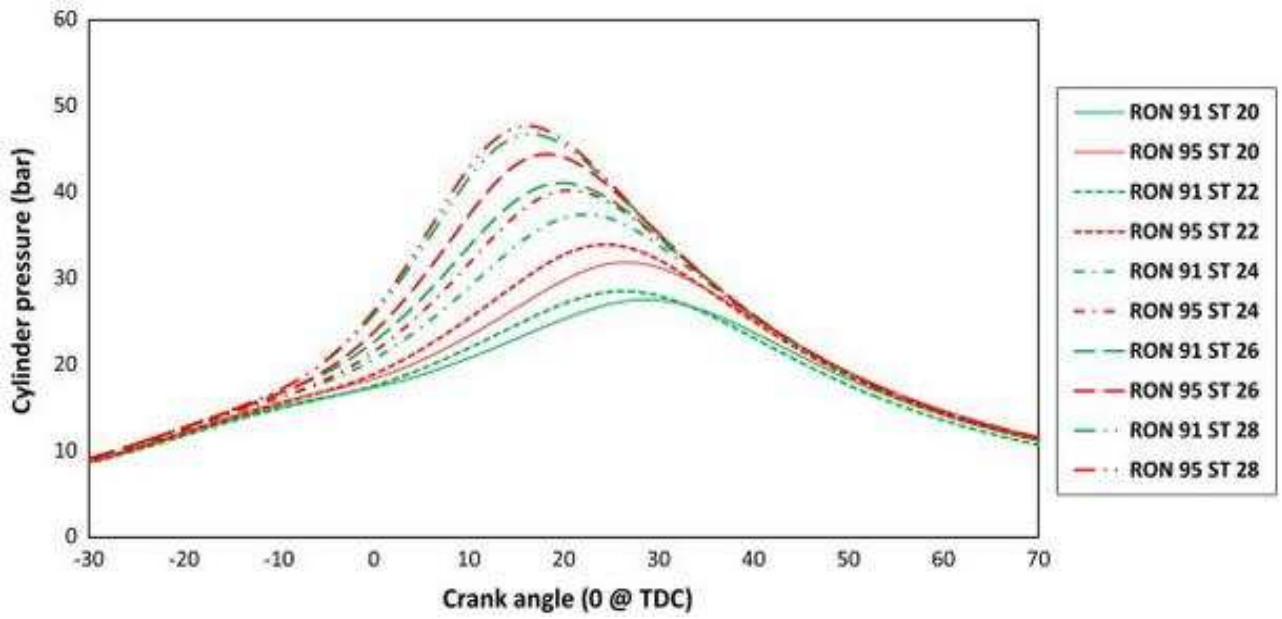

Figure 11: Small variations in ignition timing can translate to large changes in cylinder pressure (Binjuwair, 2016). This is observed due to the changing volume during the expansion stroke.

All of the green lines represent the same fuel with a research octane number (RON) of 91. Through analysis of looking the curves of the of the RON 91 ST (spark timing) 22 and RON 91 ST 24 cases, it can be seen that this two degree shift in ignition timing leads to a location of peak pressure change of 5 crank angle degrees. This leads to the conclusion that the location of peak pressure and spark timing are not linearly coordinated, which is the conclusion to be expected when the geometry of the engine is considered. This can be explained through examining one case where the spark timing is advanced and the other where the spark timing is retarded. After top dead center, in both cases, the flame is expanding in the cylinder and the piston head is moving away from the cylinder head. The main difference is that the advanced spark timing flame is larger as it has had more time to combust in the cylinder compared to the flame that was ignited with the retarded timing. If the piston head were to be stationary, than the

flames would reach the piston head in a time that differed by the same amount as the ignition timing. However, the piston head is moving away from the flame front. So the flame that exists from the retarded spark timing will have to travel further than the flame from the advanced spark timing. It is through this added distance is why the relationship between ignition timing and the location of peak pressure is nonlinear. Therefore, constant location of peak pressure readings requires a spark timing that is as constant as possible.

Another aspect of location of peak pressure repeatability is the air and fuel, or mixture, temperature at the inlet of the cylinder. The turbulent flame speed is a function of the laminar flame speed, which is a function of temperature. The turbulent flame, which is present in the cylinder of an engine, is therefore affected by the initial mixture temperature. This is due to basic chemical kinetics, when a gas is hot, the molecules in the gas move faster. When a gas is cold, the molecules move slower. Combustion requires the collision of molecules to occur in order to release the stored chemical energy, so this process will happen faster when the molecules of the gas are moving faster and bumping around more. A study by Binjuwair et al (Binjuwair, 2016) looked at quantifying how mixture temperature affected flame speed. The results can be seen in Figure 12.

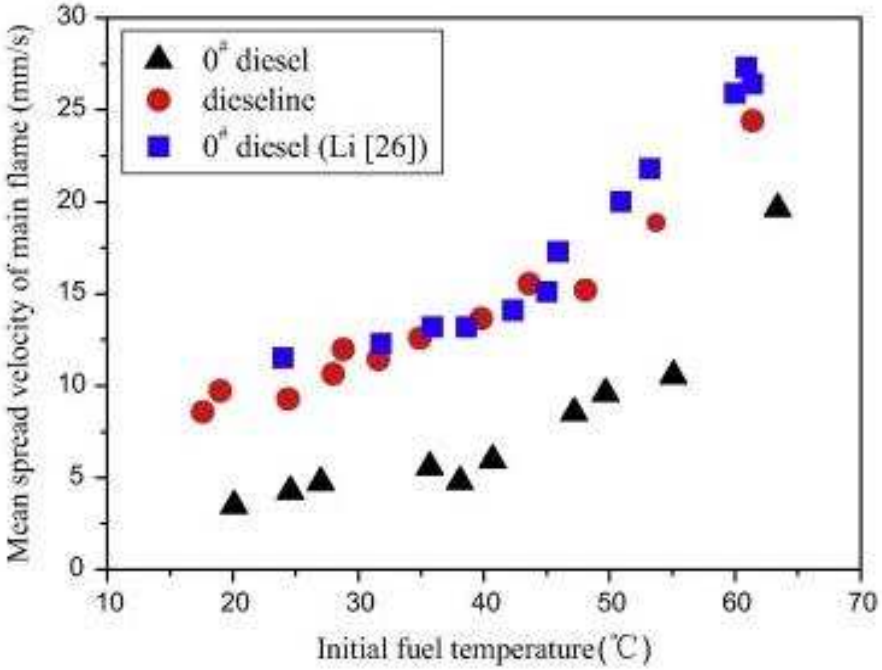

Figure 12: Depicts how the initial fuel air mixture temperature affects the flame speed observed within a gasoline engine (Binjuwair, 2016). All of the fuels show the same property of increasing flame speed with increasing initial temperature.

This plot shows how the mixture temperature (initial fuel temperature in the plot above) affects the flame spread rate in the cylinder, higher initial temperatures result in faster flames. Flame spread rate will show the same speed varying properties as the in cylinder pressure as the pressure rises with temperature through a flame surface. This fundamental study has real world applications in terms of engine operation. If the mixture temperature is varying widely in temperature, the mixture flame speed as well as the pressure rise rate will vary widely. This will mean that the location of peak pressure will vary widely. So, for increasing the repeatability of an engine in terms of location of peak pressure, the inlet temperature must be held constant.

The final aspect of the repeatability of the location of peak pressure rests with the consistency of the equivalence ratio. The amount of fuel that is injected into each cycle of the engine must be controlled very accurately as to minimize cycle-to-cycle variation. Many experiments have been done to quantify the change in flame speed with changing equivalence

ratio. These experiments tend to find that the maximum flame speed occurs at slightly rich conditions while both lean and rich conditions produce slower flame speeds. A plot that is seen in these experiments holds the parabolic shape found in the following Figure 13 (Ji, 2016):

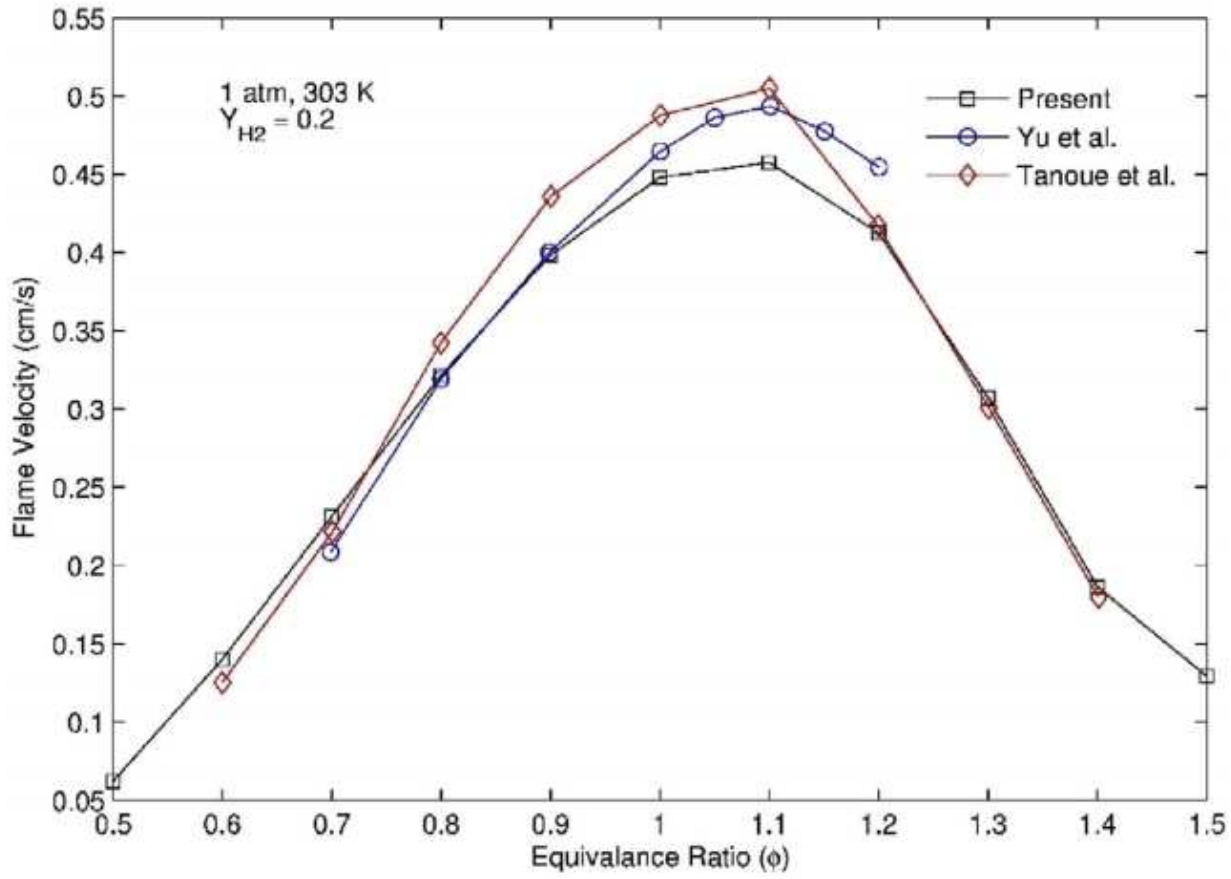

Figure 13: Laminar flame speed versus equivalence ratio for a methane hydrogen mixture. The flame speed reaches a peak at an equivalence ratio of 1.1. From the pinnacle, there is a steep drop off in flame speed when the mixture is made richer or leaner (Ji, 2016).

This plot shows that as the mixture gets richer, the flame will begin to move faster, until the chart tops out at an equivalence ratio of about 1.1. After this point, the flame begins to slow. In terms of engine operation and location of peak pressure it is crucial to keep the cycle-to-cycle variation in equivalence ratio constant as small changes in equivalence ratios can have large impacts on the flame speed and thus the location of peak pressure, especially when the engine is operating at leaner equivalence ratios where the curve is the steepest. When the equivalence

ratios are leaner, the curve is nearly linear. So a change in cycle to cycle equivalence ratio of 5% will also change the flame speed by 5%, this effect can be magnified when looking at peak pressure as the engine geometry will come into play as discussed above.

For all of the location of peak pressure repeatability analysis, the variables that are of importance are ignition timing, inlet temperature and pressure, and equivalence ratio. All of these variables are important to be aware of in regards to flame speed as flame speed is an important factor in location of peak pressure, peak pressure as well as mass fraction burned measurements.

The magnitude of peak pressure accounts for the same parameters as location of peak pressure, however the end result is different. Peak pressure relies on spark timing, mixture temperature and pressure, as well as equivalence ratio. All of these parameters are linked for peak pressure as they are for the location of peak pressure. As for spark timing effect, the main difference in the thinking is that as time goes on in the cylinder, the volume is getting bigger. So a flame that would have a late location of peak pressure, all else being equal, will also have a lower peak pressure. This is because the same amount of fuel and air are burning at the same rate, but the flame with a late location of peak pressure will also have to fill larger volume. This is the result of the piston moving away from the cylinder head after the piston hits top dead center. This can be seen in Figure 13 above.

The peak pressure will be significantly affected by the inlet temperature and pressure as both of these parameters affect the air density of the engine. According to the ideal gas law, when air is heated, the density of the air decreases. When the pressure of the ambient air is higher, the density of the air is also higher. A naturally aspirated engine can only pull in a volume of air that is as big as the volume that the piston displaces. Therefor the mass of fuel and air that the engine can pull in is highly dependent upon the density of the air. This error

manifests itself as cold air being able to produce more power in an engine simply because there is more fuel and more air, and thus more chemical potential energy, in the cylinder. So, controlling inlet temperature will have the double effect of controlling location and magnitude of peak pressure. The pressure will also be monitored in the following experiments as a means to track the peak pressure as well as the location of peak pressure.

The repeatability of engine power will be important to enhance so that data that is collected on different days can be compared. Controlling the inlet and spark conditions will go a long way towards controlling the engine power as power will be found primarily through calculations on the in-cylinder pressure trace. The external factors that contribute to the engine power that have not already been discussed are valve timing, valve lash, oil temperature, and exhaust pressure and temperature.

Valve timing is important to engine performance and repeatability as this timing is the only time that fuel and air can enter and exit the chamber, and the only time that exhaust products can exit the chamber. For both of these instances the timing must be held constant. If the inlet valve timing were to change from day to day, then there would be a variable amount of time that the fuel and air mixture would have to spread around the cylinder. Similarly, if the exhaust valve timing were to change from day to day then there is a possibility that the air exiting the cylinder would be hotter on one day compared to the other. This would mean that there would be a significant change in the exhaust residual gases remaining in the cylinder after the exhaust stroke as the air density at the valve would vary. Variable valve timing is not of much concern for the CFR engine as the valves are controlled by a cam shaft and not through electronics. This means that there is a mechanical system that is connected through gears that controls the valve timing. There is negligible change in day to day valve timing.

Valve lash is the amount that the valves open. This is a very important parameter because it can again affect how much fuel and air mixture can enter and exit the chamber. This parameter is checked regularly to make sure that the valve lash did not change over a period of testing.

Oil temperature is a very important parameter to hold steady as the temperature of the oil will affect the lubricating properties of the oil. When the oil is cold, it is much more viscous and harder to move and pump which results in more friction for the piston to overcome. So for testing it is important that the oil be heated to the same temperature every day before any points are taken. For the CSU CFR engine, there is an oil plateau temperature of around 140 °C. This temperature takes considerable time to reach; the warm up period for the engine is paramount to consistent engine data.

The conditions of the exhaust are also important for engine power readings. If the pressure of the exhaust is high, then the engine has to do work to push the exhaust products out the cylinder and into the exhaust line and also push the exhaust products through the exhaust line. This is wasted work. Similarly, the exhaust temperature must be kept at a steady temperature to ensure repeatable results. If the exhaust temperature is changing during testing than the mixture density is also varying in the exhaust, which causes variations in the amount of work that the piston must do to clear the exhaust products on the exhausts stroke. The CFR hits an exhaust temperature plateau around 240 °C.

Overall, the performance of the engine must be constantly monitored in order to ensure that there are not unrepeatable results being produced. As discussed above, a small change in exterior conditions can result in large output changes. This shows that it is very important to know the accuracy of the testing apparatus as to say what result is significant as an effect of the fuel and which result is not as an effect of experimental drift. It is critical to diagnose these

differences early. A good way to check is to run the baseline test many times, then run the new additive case, then run the baseline again. If the baseline case is producing the same values before and after the additive case, then it is likely that any measured difference is due to the fuel and not to the apparatus. However, when there is a difference noted between the baseline cases (either day to day or run to run) the problem may be any myriad of the issues discussed above. Engine accuracy is critical for analyzing engine data, especially when only small variations between fuel blends are expected.

2 Experimental Apparatus and Methods

The type of engine used in this project is a Cooperative Fuel Research (CFR) F-2 model manufactured by Waukesha Engine at Dresser Industries. It is a single cylinder, constant speed (~930 rpm), un-throttled, 4-stroke engine with a cylinder bore of 3.250 inches (8.255 cm) and piston stroke of 4.500 inches (11.43 cm). The displacement volume of the engine is 37.33 in^3 (611.7 cm^3). To enable operation at a range of compression ratios from 4:1 to 18:1 the engine is constructed with the cylinder and cylinder head as a single part that can be moved vertically independent to the piston/connecting rod assembly. By raising or lowering the cylinder, the clearance volume (the volume formed from the top of the piston at TDC and the cylinder head) is increased or decreased resulting in changing of compression ratio. The total vertical travel of the cylinder head is 1.235 inches. The engine is designed to allow adjustment of compression ratio while operating. Figure 14 provides a cut-away drawing of the piston-cylinder system. The particular engine used in this project was manufactured in 1957 and is a model still manufactured and sold today, which was designed specifically for testing knock tendencies of fuels. The primary difference of the models currently manufactured is that they have electronically controlled carburetors for gasoline operation, which the model used in this work does not. Originally configured for Octane Number testing of gasoline blends, the engine can currently be configured to burn gaseous fuels or liquid fuels. The engine is operated through a belt driven connection with a 5 horsepower synchronous motor. On start-up and while operating without producing power (motoring operation) the engine crankshaft is rotated by the motor. When fueled and producing power, the synchronous motor operates as a generator feeding power to the

electrical grid (powered operation). Engine speed is limited by the set constant motor speed during motoring operation and corresponding electric grid frequency during powered operation.

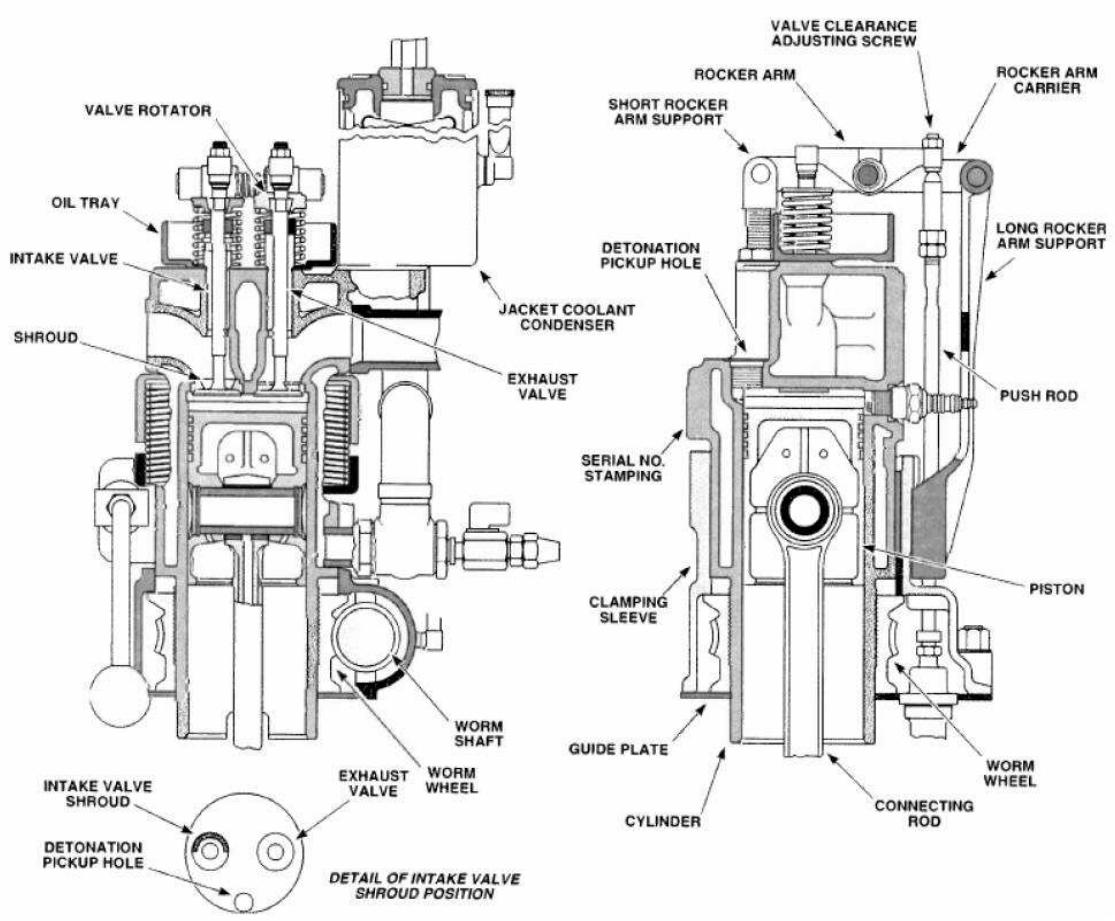

Figure 14: Cylinder and clamping sleeve sections (Wise, 2013). Releasing the clamping sleeve and rotating the worm wheel allows the shroud to move up and down. The motion is also present for the valves, oil tray, jacket coolant condenser and valve rotator.

A rotameter is installed in the system providing the test cell operator a visual flow indication for combustion air. An in-line mass flow meter (heated tube or calorimetric type electronic mass flow meter, Model FMA 1700 Series, 0-500 SLM, from Omega Engineering, Inc.) is installed to provide direct measurement of combustion air mass flow to the engine used to control the air fuel mixture. A pressure transducer mounted in the buffer volume of the intake system provides the signal to the controlling program used to trigger positioning of the intake air admission valve.

The in-cylinder pressure versus volume trace for a typical operating cycle of the CFR engine is shown in Figure 15. This cycle consists of two complete revolutions of the crankshaft which constitutes four strokes of the piston. The upper loop, area A, is formed during the compression and power strokes; the lower loop, Area B, is formed during the exhaust and intake strokes as the engine is aspirated. Area A is indicated work, the work delivered by the crankshaft is brake work which is slightly less than indicated work and includes losses due to friction. Brake work is given by Equation 1:

$$w_b = w_i - w_f \quad \text{Eq. 1}$$

where, w_i is the indicated specific work generated inside the cylinder and w_f the specific work lost due to friction. Area B formed during aspiration is called pump work. Net work is related to pump work as given by Equation 2:

$$w_{net} = w_b - w_p \quad \text{Eq. 2}$$

where w_p is the work performed by the engine during the exhaust and intake strokes.

The parameter mean effective pressure (mep) is used to facilitate the comparison of different engines because it is independent of both engine size and rotating speed. The definition of mep is given by the relationship in Equation 3:

$$w = (mep)\Delta v \quad \text{Eq. 3}$$

It follows that Equation 3 can be written as Equation 4:

$$mep = \frac{w}{\Delta v} = \frac{W}{V_d} \quad \text{Eq. 4}$$

where,

$$\Delta v = v_{BDC} - v_{TDC} \quad \text{Eq. 5}$$

and W is the work of one cycle, w the specific work of one cycle, v the specific volume of the cylinder contents, v_{BDC} the specific volume of the cylinder contents at bottom dead center, v_{TDC} the specific volume of the cylinder contents at top dead center and V_d the displacement volume. The definition of mep is often further distinguished by incorporating indicated work, gross work, brake work, friction work, and net work. For the purposes of this study, the following subsets of mep are defined and utilized:

Brake mean effective pressure (bmep): Defined in terms of brake work, given by Equation 6:

$$bmep = \frac{w_b}{\Delta v} = \frac{w_b}{V_d} \quad \text{Eq. 6}$$

Pump mean effective pressure (pmep): Defined in terms of the actual work available at the crankshaft lost to both pumping (aspiration) and friction losses, given by Equation 7:

$$pmep = \frac{w_p}{\Delta v} = \frac{w_p}{V_d} \quad \text{Eq. 7}$$

Net mean effective pressure (nmep): Defined in terms of net work, given by Equation 8:

$$nmep = \frac{w_{net}}{\Delta v} = \frac{w_{net}}{V_d} \quad \text{Eq. 8}$$

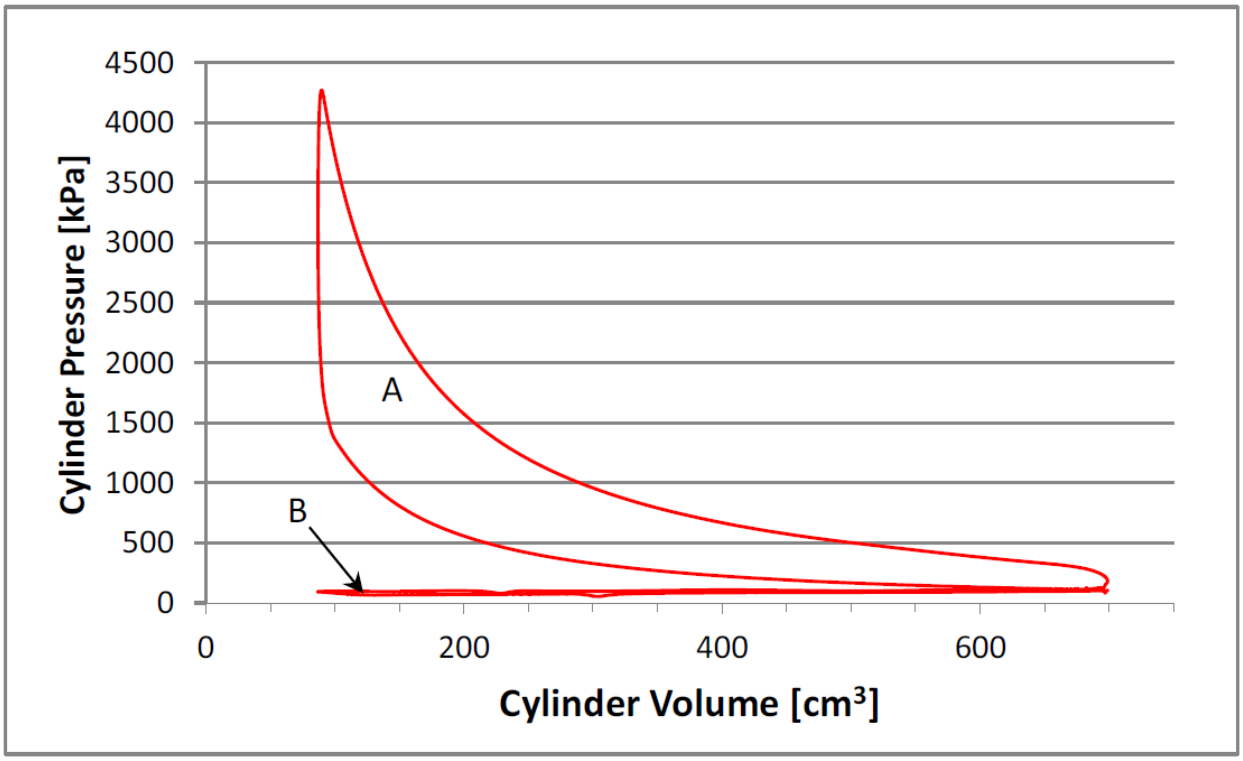

Figure 15: Representative pressure versus volume for the CFR engine. Area "A" represents the NMEP that the engine can produce. Area "B" represents the pressure that the piston exerts on the residual gas during the exhaust stroke to clear the cylinder.

Figure 16 shows a schematic diagram of the engine exhaust system for the test cell. Modifying the engine exhaust system to perform suitably for this test cell requires a number of specific design considerations when operating on natural gas in the boosted mode. The exhaust requires a buffer volume to dampen pressure fluctuations in the exhaust stream and sufficient, controllable, flow restriction is necessary to establish back pressure that mimics the parameters realized in a turbo charged engine. Figure 18 is a photograph of this custom piping. This piping was installed to have better control on the relationship between exhaust backpressure, intake pressure, and other engine parameters to mimic a typical turbocharger installation in an engine. Figure 17 shows a schematic depiction of a turbocharger where point (1) is the compressor inlet from the atmosphere, point (2) the engine intake at the compressor outlet, point (3) the engine exhaust to the turbine intake, and point (4) the turbine exhaust to ambient atmosphere. The

exhaust gas flows through the buffer volume to an orifice sized to allow minimal flow and maximum backpressure of approximately 2 atm (gauge). Bypass piping with an in-line manual valve is installed to allow sufficient flow, when fully open, to reduce backpressure to nearly ambient pressure. The gate valve is adjusted manually to control the amount of exhaust gas bypassing the orifice thus controlling backpressure.

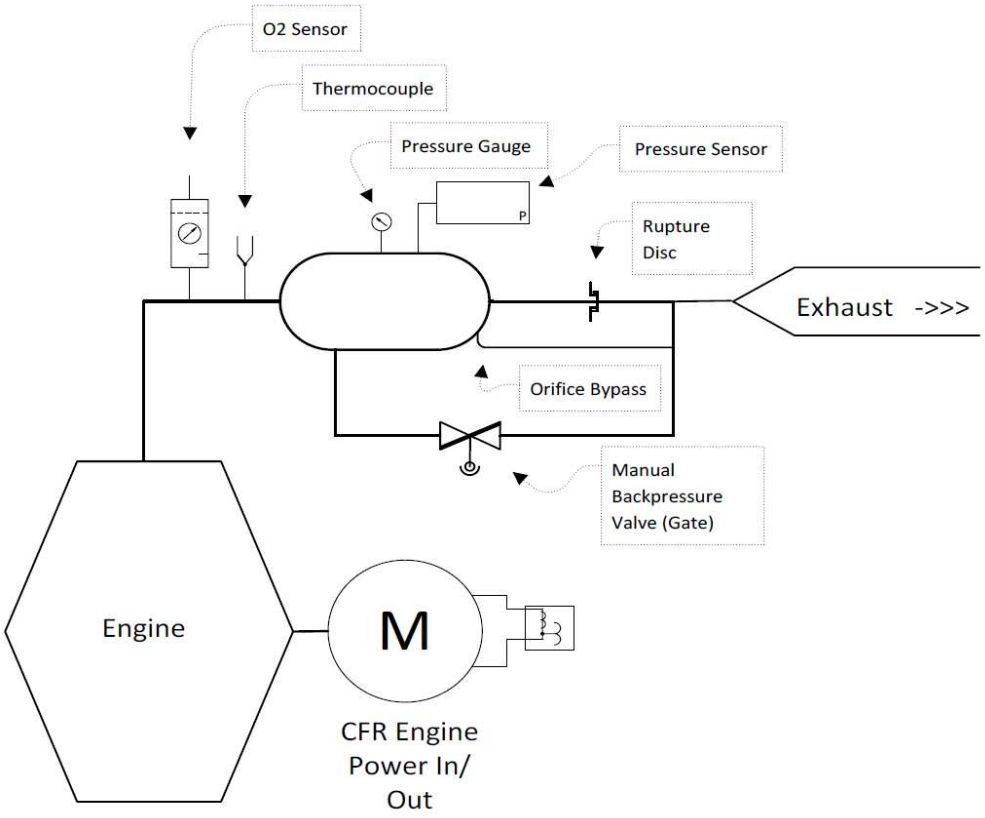

Figure 16: CFR engine exhaust schematic (Wise, 2013).

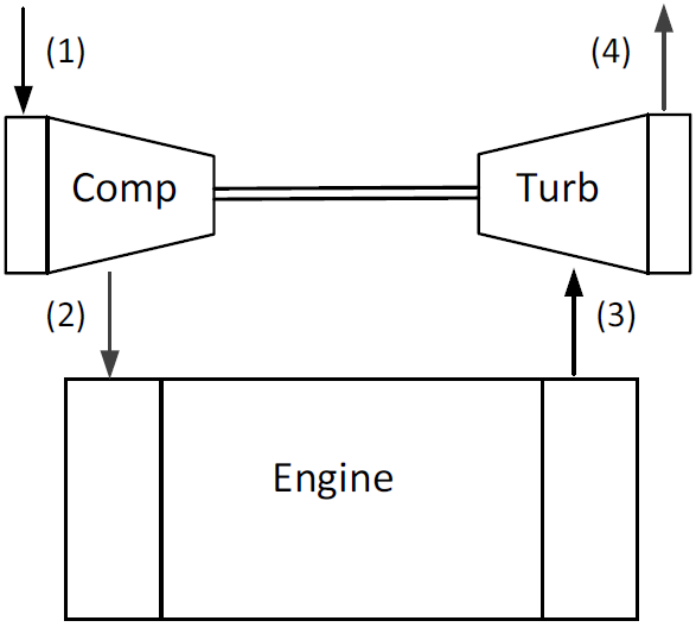

Figure 17: Turbo charger schematic (Wise, 2013).

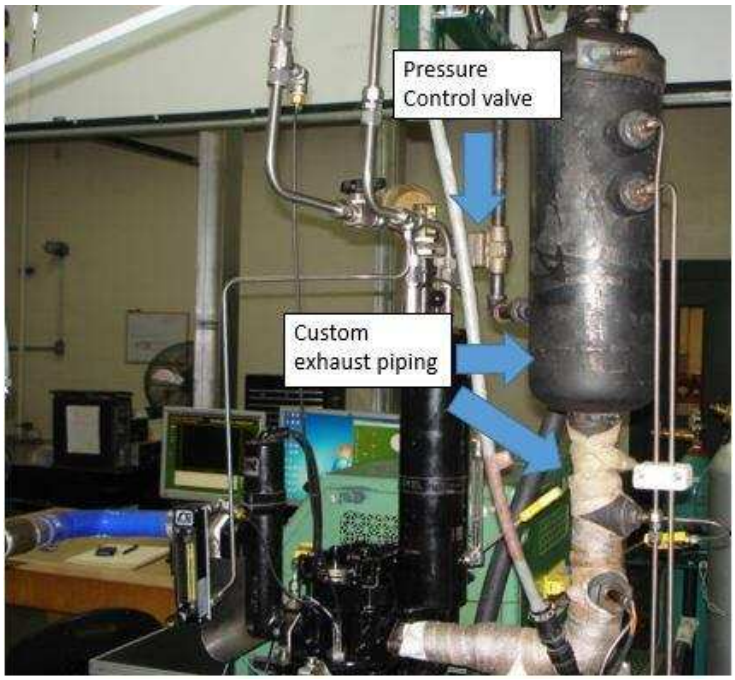

Figure 18: Custom exhaust components (Wise, 2013). There is custom piping in order to replicate an engine that uses a turbocharger.

For the CFR engine, the cylinder head is raised and lowered in order to adjust compression ratio and the exhaust port from the engine is fixed to the cylinder head, therefore the entire exhaust assembly must be able to travel vertically by roughly 1.25 inches (3.2 cm)

without imposing excessive stress on the exhaust piping or fasteners. In the original configuration of the engine the exhaust system consisted of a simple thin walled exhaust pipe bolted to the exhaust port of the engine with a total weight of approximately 5 kg. This test cell application increases the weight of the exhaust components to 50 kg of new materials. The new test cell is arranged to suspend the exhaust components from springs mounted overhead such that the bulk of the system weight is not assumed by the exhaust port bolts and adequate flexibility is afforded to allow free vertical travel when adjusting the cylinder head to vary compression ratio.

The engine, originally configured with a capacitive discharge type ignition system, is currently configured with an electronic ignition system (Altronic model CD200) adapted for use in a single cylinder engine. The system consists of a controller unit, magnetic pickup sensor, input and output harness and ignition coil. Software enables control of the system to allow ignition timing to be set and changed as desired during engine operation without mechanical adjustment

Because of the climate conditions in Fort Collins, Colorado the ambient air at the CSU Powerhouse is consistently at low relative humidity. The facility compressed air system contains in-line filters and desiccant air dryers to clean and condition the air prior to introduction to the system. As an added precaution, a separate filter and drier assembly is installed downstream of the test cell pressure regulator.

Additionally, the engine intake has an installed electrical resistance heater that heats the mixture just upstream of the intake valves. Intake heater operation is controlled by the LabVIEW© controller software, which cycles the heater on until the indicated minimum temperature is met.

For gaseous fuel operation, the fuel blending system is designed to allow any proportion of any combination of constituent gas desired to create specific fuel gas blends. The system consists of a number of compressed gas cylinders with regulators discharging flow first into mass flow meters, then into a buffer volume, then to the inlet of a pulse width modulated (PWM) injector for each gas. The PWM injectors introduce respective gases to a manifold and the blended gas mixture is then allowed to flow through a combination flash arrestors/check valves and finally mix with combustion air prior to entering the engine intake. The fuel air mixture passes through a static mixer prior to encountering the mixture heater. Figure 19 provides a schematic depiction of the test cell fuel blending system. The gases available for blending include methane (CH_4), ethane (C_2H_6), propane (C_3H_8), carbon monoxide (CO), carbon dioxide (CO_2), nitrogen (N_2), and hydrogen (H_2). In this study, for the natural gas additive work, only methane, ethane and hydrogen were used.

Accurate measurement of combustion air and fuel are necessary for accurate testing. So, an in-line mass flow meter (heated tube or calorimetric type electronic mass flow meter, Model FMA 1700 Series,0-15 SLM, 0-100 SLM, and 0-200 SLM, from Omega Engineering, Inc.) is installed for each constituent gas to provide direct measurement of net fuel gas flow to the engine. The operating range of the meters was selected based on the peak flow requirements identified by constituent percentage in projected producer gas blends.

As originally manufactured and configured, the knock measurement system on the CFR engine consists of a power supply, detonation meter, detonation pickup, and knock meter. The pick-up sensor, mounted through the head of the cylinder, offers a thin flexible diaphragm cover which is exposed to the combustion chamber. As the diaphragm surface reacts to combustion chamber pressure variation, the magnetic field varies around a magneto-restrictive alloy wound

with a copper wire coil. The magnetic field variance induces a voltage in the coil which is directly proportional to the rate of change of cylinder pressure, and is output to the detonation meter. The detonation meter is an analog device that is able to isolate the relative knock amplitude through averaging and filtering the received signal which is then transmitted to the knock meter. The knock meter display reflects the relative intensity of the knock event to establish a comparative scale used as the basis for measuring the intensity of knock experienced in the engine. An analog strip chart recorder may also be attached to provide a permanent record of a data set. Figure 20 shows a signal flow diagram for the original knock measurement system. Figure 21 provides a sectional view of the originally installed type D-1 detonation pickup. The original knock measurement system requires that the operator determine the onset of knock audibly and then adjust the meter reading and spread dial settings (controlling resistive networks that adjust the sensitivity of the instrument), establish an operate/zero point, and then select a time constant (1 of 6 positions determining the integration interval). The process and instrumentation force a subjective measurement of knock intensity which is certainly acceptable for comparing tested fuels to reference blends to assign an octane number.

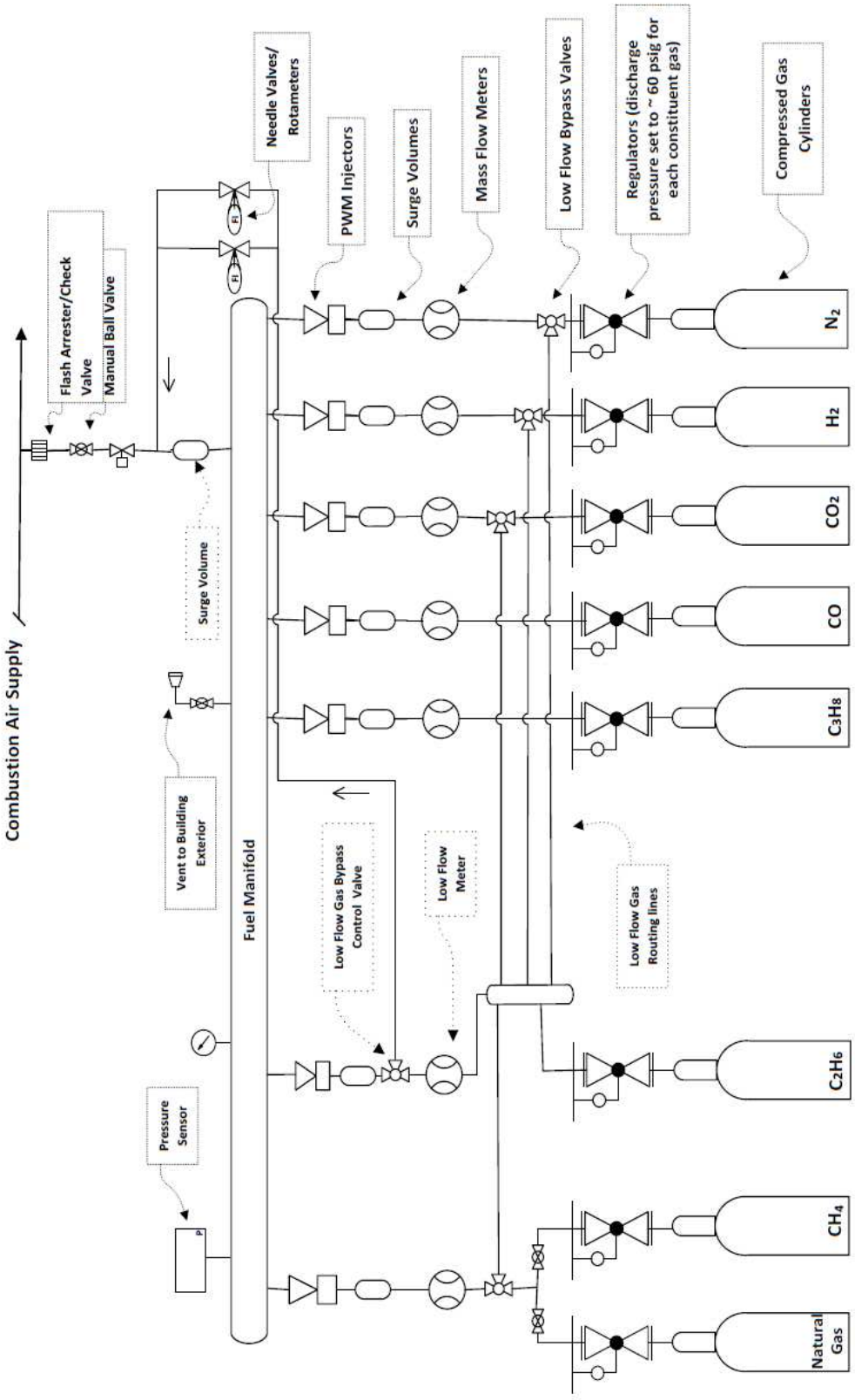

Figure 19: Test cell fuel blending schematic (Wise, 2013).

For this project, it was desired to establish an objective knock intensity measurement less prone to variability due to operator interpretation and sufficiently detailed to allow more refined analysis of the knocking phenomenon. The modified knock measurement system begins with a water-cooled, piezoelectric transducer (Kistler model 6061A) mounted in the same cylinder detonation port previously housing the Type D-1 pickup. The signal from the transducer is fed to a charge amplifier which relays pressure signal input to the controlling software. A rotary 0.1° incremental optical engine encoder (BEI model L25) provides positive crank angle position indication enabling real-time display of cylinder pressures as a function of crank rotation. Due to high dynamic response and resolution (3600 discreet data points per engine revolution) detailed pressure history is available allowing direct analysis of the combustion event in the cylinder. Figure 22 provides a signal path depiction of the post-modification knock measurement system.

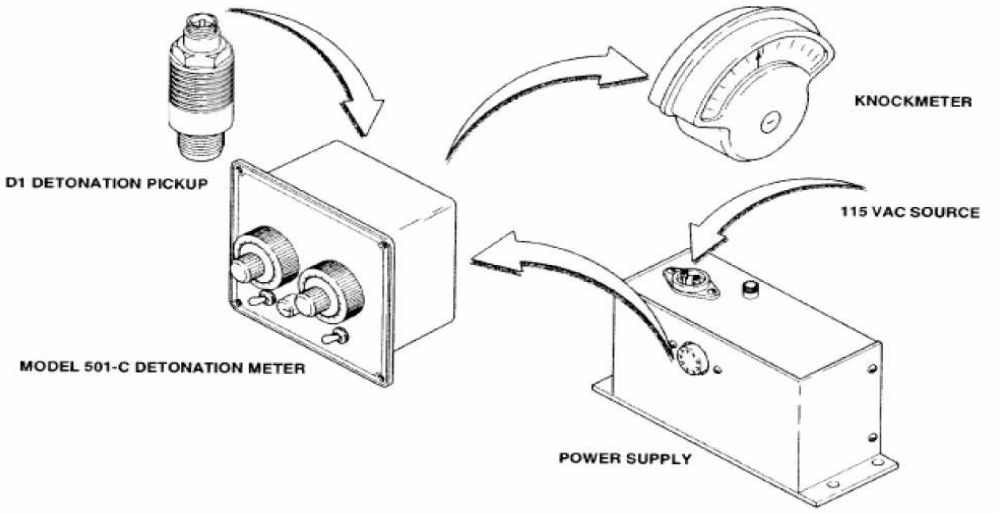

Figure 20: Original CFR engine knock meter setup.

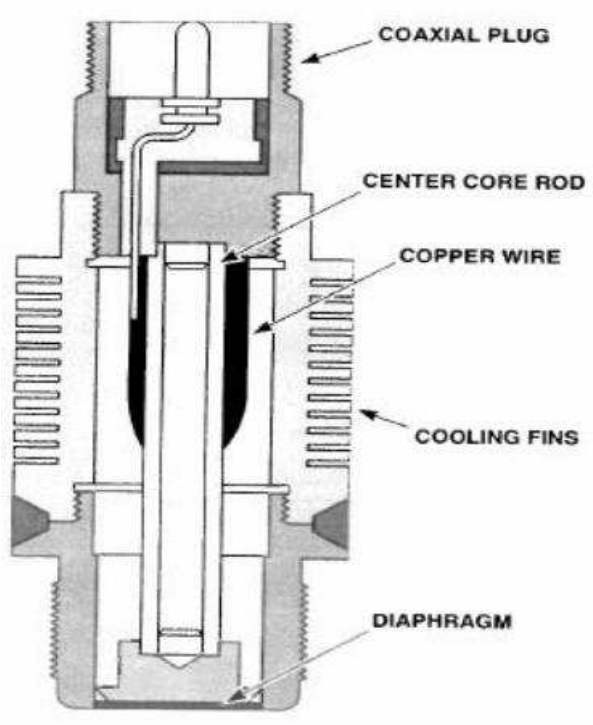

Figure 21: Sectional view of original CFR detonation pick up (Wise, 2013).

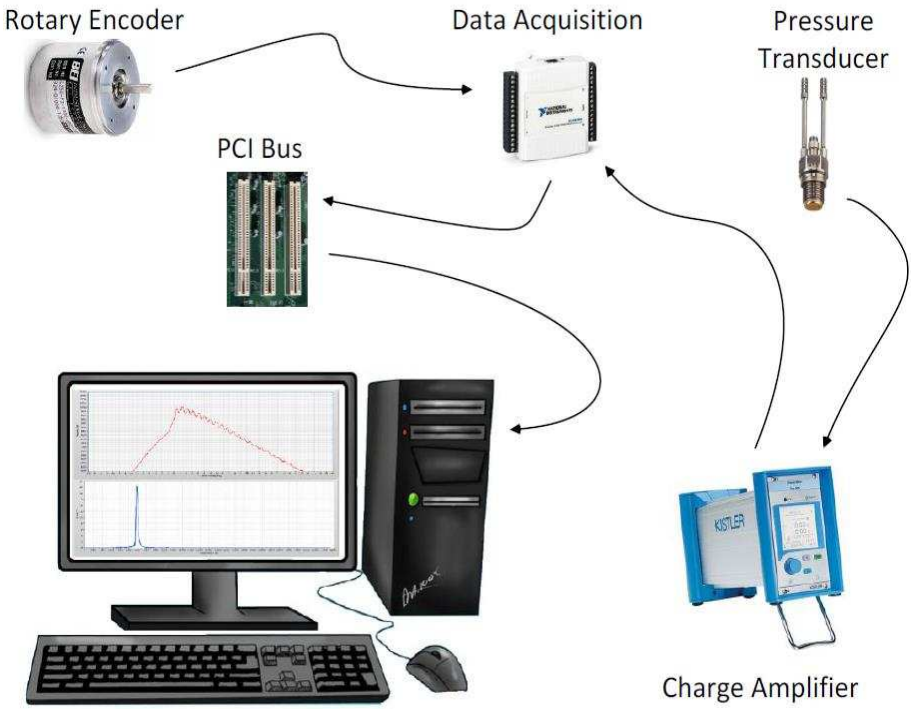

Figure 22: Updated CFR detonation pick up system (Wise, 2013).

2.1 Safety

The intake system can be isolated from the facility compressed air system by two valves in series. The first isolation valve is a hand operated ball type valve. The second isolation valve is a normally shut solenoid operated diaphragm type valve.

In the event of interrupted power to the solenoid operated admission valve, whether through an inadvertent loss of power or intentional isolation of the system in the event of an emergency, the valve will fail shut isolating combustion air from the engine. Additionally, a normally open solenoid vent valve is installed in the proximity of the intake port venting to ambient air exterior to the building. As with the solenoid at the admission side, in the event of interrupted power to the solenoid the vent valve will position to its normal position (open) depressurizing the intake system.

2.2 Methods for Additive Injection

2.2.1 Natural Gas Fuel Additives Injected as Liquids

To inject the liquid additives into the air stream an Exair 35XT46 air assisted low-flow atomizing nozzle was used. Theoretically, the nozzle was to work by blasting a small amount of liquid fuel additive with air. The fuel would then be atomized into the fuel/natural gas mixture. There were two major drawbacks to the Exair nozzle. The first drawback was that the minimum recommended liquid flow rate was about double the flow rate required for additive injection, this problem manifested itself as the flow rate of fuel additive was not adequately controlled by the positive displacement syringe pump that was chosen to accurately pump and meter the volume flow rate of the liquid fuel additive. Instead, a siphoning effect was created at the nozzle exit which caused more fuel to flow than was desired. The second drawback was that, for the internal spring in the atomizing nozzle to compress and open the nozzle, the air pressure had to reach 30

psi which introduced 32 SLPM of air into the air stream. This resulted in about 18% of the air that the engine needed to operate came from the nozzle. These problems had to be rectified to allow for accurate testing.

To fix the siphon effect and excess air problem, the liquid control spring was removed and replaced with a threaded rod. The siphon effect was caused because of the low pressure region formed at the nozzle exit. By replacing the spring with a threaded rod the nozzle opening was no longer dictated by air pressure. Thus, less air could be introduced into the air stream, which had the secondary effect of not created a low-pressure region at the nozzle exit. It follows that the siphon effect and excess air problems were minimized. A flow visualization bench test setup was constructed to test the low flow atomizing nozzle before use on the engine. The bench test setup was constructed of clear PVC pipe with a static in-line mixer and an inner diameter similar to that of the air intake on the CFR. There was a gate valve at the exit of the bench test setup in order to control the pressure within the set up to mimic the effects of the boosted intake. In the CFR engine, the air/fuel mixture makes a 90 degree turn just before reaching the static mixer, to simulate this in the bench test set up a clear T-joint was used. It was found that running 5 slpm air through the low flow nozzle was adequate for fuel atomization. The bench top setup can be seen in the following Figure 23.

Figure 23: Low flow atomizing nozzle bench test set-up.

Some of the results found while using the low flow atomizing nozzle method were surprising in that the fuel additives were causing the engine to knock while not enhancing the functional operational parameters such as NMEP or peak pressure. This effect could have been the result of two possibilities: the first being the additives do not improve combustion, or the second being the fuel additive did not have sufficient resonance time in the CFR air intake before entering the cylinder and the liquid fuel additives were stratified in the air.

To eliminate the fuel stratification hypothesis, a new method for delivering the liquid fuel additives into the engine was developed, which was called the “bottle fill method”. The bottle fill method consisted of filling a 50 liter air gas bottle with a base fuel and additive combination instead of using the low flow atomizing nozzle. By filling this bottle, there was ample time for the fuel and fuel additives to mix, thereby eliminating the concern of stratification.

Calculating how much fuel additive and fuel to put into each bottle was done on a molar basis, and filling the bottle was done through using partial pressures. This relationship can be seen in Equation 9:

$$Mol\%\ Additive = \frac{Additive\ Vapor\ Pressure}{Total\ Bottle\ Pressure} \quad \text{Eq. 9}$$

The vapor pressure of the fuel additive was the limiting factor of how much additive could be put into the bottle as the maximum additive mol% is the vapor pressure of the additive divided by the final pressure of the bottle. Calculating the amount of fuel additive to put into the bottle required a desired additive mol% to be tested. This additive percent would dictate the final bottle pressure and thus the amount of methane and ethane that would also be put into the bottle with the additive. By rearranging the previous equation the maximum total bottle pressure can be found in Equation 10:

$$Total\ Bottle\ Pressure = \frac{Additive\ Vapor\ Pressure}{Mol\%\ Additive} \quad \text{Eq. 10}$$

This creates competition because filling a bottle with a high percent of the additive requires a low final bottle pressure, which results in a shorter run time as compared to a bottle with a low percent additive and a high final bottle pressure. The vapor pressures of the natural gas fuel additives at 0 °C are included in Table 1.

Table 1: Natural gas liquid additive vapor pressures at 0°C.

Additive	Vapor Pressure (Pa)
Nitromethane	5675
DMM	43080
DTBP	2500
EHN	27

As seen in Table 1, DMM has by far the highest vapor pressure and thus DMM filled bottles could either have the highest pressure or the highest mol%. If the desired mol% DMM was 0.5%, then the maximum bottle pressure could be (equipment permitting) over 1200 psi. A bottle at 1200 psi would be able to run for multiple hours without needing a new bottle. While EHN has an extremely low vapor pressure and the if the desired mol% EHN was 0.5mol% then the final bottle pressure could only be only 7.5 psi which would allow no run time to the engine (the engine requires a minimum of 60 psig to get significant fuel flow). Running the calculations from desired mol% to an actual volume requires the use of the ideal gas law, liquid fuel density and molar mass conversions.

2.2.2 Liquid Fuel Injection for Gasoline Additive Tests

A naturally aspirated carburetor was used for the gasoline portion of the project. There are three different fuel tanks to allow easy change between fuels. These fuel tanks flow into a float chamber that keeps the pressure head of the fuel at a relatively constant level. The float in a float chamber is a hollow piece of metal that floats atop the fuel. When the fuel level goes down too far the float will lower and this will open a valve that allows more fuel to enter the float

chamber. Once the level of fuel reaches the upper point, the float will close the valve. The float opens and closes the valve regularly so that the fuel stays at a consistent level.

From the float chamber, the fuel passes through nylon tubing and goes to the horizontal jets. The horizontal jets are just plugs that have a small hole drilled through them. The horizontal jets feed into the fuel selector valve. This valve can be rotated so that a desired fuel can be selected. The fuel selector valve also changes the fuel flow direction from horizontal to vertical. From the fuel selector valve the fuel enters the vertical jet. The vertical jet is a narrow 4" capillary. The fuel level within the vertical jet is the same as the sight glass and the float chamber. After the exhaust stroke of the engine, the inlet and exhaust valves will be closed and the piston will be moving down. The piston will pull a vacuum. When the intake valve opens fuel is pulled up through the vertical jet and into the air stream. To vary the equivalence ratio, each gas tank and float chamber is attached to a threaded rod so that the tank and float assembly can move vertically. The level of the fuel within the float chamber stays relatively constant, so moving the float chamber up will increase the fuel pressure head. The change in pressure from moving the float chamber height can be seen on the sight glass and the increased pressure will cause more fuel to flow through the horizontal jets, thus the fuel level will increase in the vertical jet and the equivalence ratio will change accordingly.

The vertical jet terminates into the air bleed tube. This is the first interaction of fuel and air. The fuel and air are both pulled into the engine by the vacuum created within the chamber. The fuel enters the air stream and evaporates. The air is heated prior to fuel interaction so that the air density is nearly constant between days, thus the fuel flow rate is also nearly constant. The fuel air mixture is then heated are then heated again prior to entering the chamber. The following figure depicts a schematic of the carburetor.

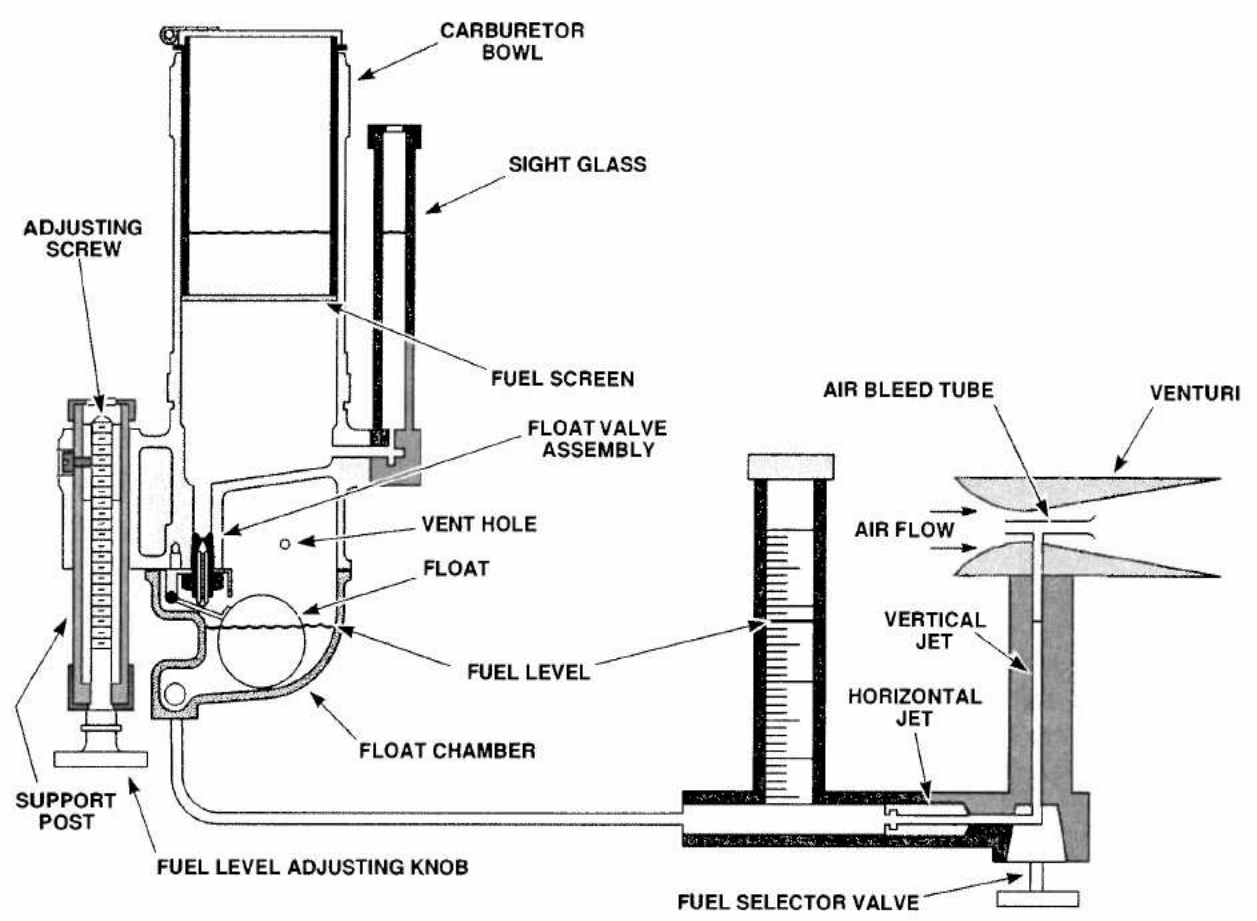

Figure 24: Carburetor schematic (Waukesha, 1998). The fuel level is the same in the float chamber, the sight glass and the vertical jet. Adjusting the height of the float chamber allows for fuel flow adjustments.

To determine the equivalence ratio of the fuel and air that the carburetor was providing, a AFRecorder 4800 was used on the exhaust constituents. The fuel reservoirs were moved up and down and the horizontal jets were changed until the AFRecorder 4800 reported an equivalence ratio of 1.

2.3 Fuels

The overarching goal of this research is to dissect the operational differences between different fuel compositions. The previous section discussed the equipment that was used, while the following section will discuss the base fuels as well as the differences between the additives.

2.3.1 Liquid fuel

There are multiple baseline liquid fuels used in this work as a means to classify additive impacts on a broad spectrum of base fuels. The baseline liquid fuels that were used during testing were Refinery Gasoline (blend created by sposor), a blend of 60% Toluene, 30% n-Heptane and 10% iso-octane (Toluene reference fuel, TRF), pure iso-octane and a 3:1 iso-octane : n-heptane blend.

The additives that were tested in the gasoline testing are proprietary and are referred to in this thesis as additives 1a, 1b, 2 and 3. Additives 1a and 1b come from the same chemical family and additive 1a was only tested in the CFR at a 200 PPM concentration while additives 1b, 2 and 3 were tested in all base fuels in both 200PPM and 1000PPM concentrations as well as 5000PPM and 10000PPM concentrations in the Refinery Gasoline blend.

2.3.2 Gaseous Fuel

Natural gas compositionally varies depending on where the gas was extracted and how it was processed. For example, natural gas extracted from Alaska typically is over 99.7% methane by volume and about 0.3% nitrogen while natural gas extracted from Algeria typically is about 87% methane, 10% ethane, and 3% propane. This demonstrates that using natural gas supplied by the city (typically used for natural gas water heaters) would not suffice for research purposes as, depending on point of extraction, the composition of the fuel would change regularly which would make comparing data taken at different times impossible. To circumnavigate this issue, a natural gas blend was originally created in house that consisted of 90% methane and 10% ethane by volume. This fuel blend was changed part way through testing to consist entirely of methane. This change was made because of the flame speed of ethane relative to pure methane. Ethane

burns much faster than methane so it was thought that the ethane may have been masking the effects of the liquid fuel additives.

2.4 Natural Gas Fuel Additives

The natural gas additives were selected by the sponsor as additives with potential to reduce the lean limit of natural gas. These additives were ethylhexyl nitrate (EHN), nitromethane (NM), di-tert-butyl peroxide (DTBP), and dimethoxy methane (DMM). EHN is typically used in as a fuel additive in diesel engines as a means to increase Cetane Number [6]. Cetane improvers typically decompose at lower temperatures,which allows for lower temperature combustion, and thus possibly lean limit extension because lean limit flames are typically colder than stoichiometric flames. EHN has the chemical formula $C_8H_{15}NO_3$ and the chemical structure can be seen in Fig. 25.

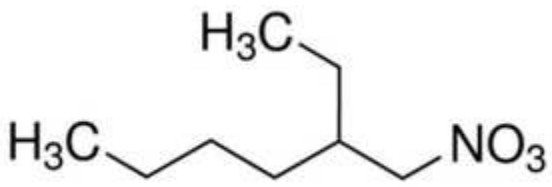

Figure 25: EHN chemical structure.

NM is typically used as a fuel component in automotive racing. Nitromethane showed promise for lean limit testing based on the propensity of nitromethane to decompose. Aso, NM carries a significant amount of oxygen. Because NM carries oxygen it will not need as much air to burn. This may help with initial flame growth and propagation as it would provide an additional source of oxygen within the area around the fuel. The chemical formula of NM is CH_3NO_2 and the chemical structure can be seen in Fig. 26.

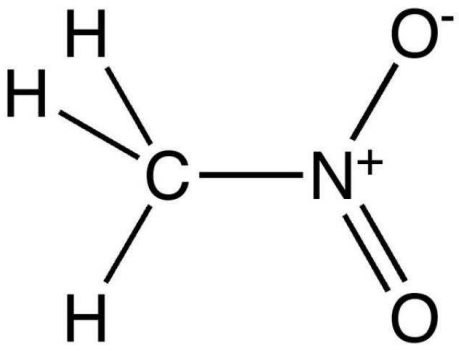

Figure 26: Nitromethane chemical structure.

DTBP is typically used as gasoline fuel additive as a radical initiator because it decomposes at relatively low temperatures (<100°C) [5]. This property could have an impact on the lean limit in much the same way as EHN as the flame may be able to initiate at the lower cylinder temperatures that are found in lean combustion. A secondary benefit to using DTBP is that the molecule is a stable organic peroxide at lower temperatures. The chemical formula of DTBP is $C_8H_{18}O_2$ and the chemical structure can be seen in the following figure.

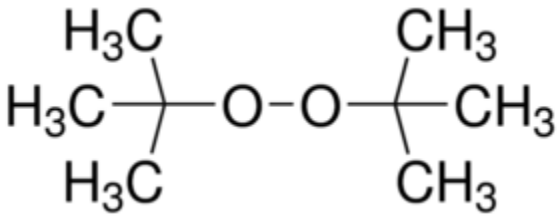

Figure 27: DTBP chemical structure.

DMM is typically used as a gasoline additive for increasing Cetane Number (Huang, 2006). Since high Octane Number means that a fuel has a low propensity to knock, the benefit of DMM is not found in increasing free radicals. Instead the primary benefit of DMM is that it has a very high vapor pressure, so a large amount of DMM can be put into the gaseous fuel before the additive starts to condensate out. The energy density of a liquid is much higher than that of a gas, so an engine would be able to carry more fuel energy on board in smaller tanks when using a

liquid fuel as opposed to a gaseous fuel. The chemical formula of DMM is $C_3H_8O_2$ and the chemical structure can be seen in Fig. 28.

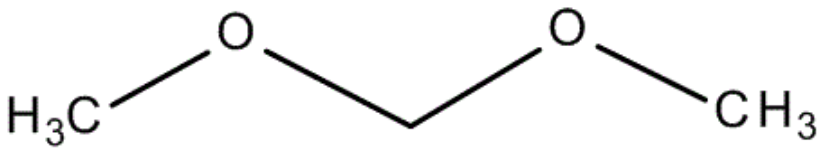

Figure 28: DMM chemical structure.

3 Results

3.1 Gasoline Fuel Additive Testing

The gasoline additive testing was conducted in two main phases. The first phase consisted of an uncertainty analysis in which the repeatability of the engine under liquid fuel operation was characterized. The second phase consisted of the gasoline additive testing.

3.1.1 Engine Stability Testing

Stability testing was done in order to quantify the uncertainty through observing the minimum change in engine output that was detectable by the equipment in use and also to determine the amount of drift that was observed from point to point. The first round of testing was conducted using the standard Waukesha liquid fuel setup. This setup uses ambient air, with no control over relative humidity, pressure or temperature. Comprehensive data analysis was conducted to determine which data were more prone to fluctuation and which data were most consistent between repeated tests. It was found that primary engine conditions such as intake and exhaust pressure and engine speed were held very constant throughout testing. It was then found that the engine conditions that are controlled either by a feedback loop or manual adjustments such as equivalence ratio and intake temperature, induced error. The errors compound, which affects engine output parameters, such as average peak pressure, location of peak pressure and NMEP. These data can be seen in Table 2. The data presented in Table 2 is the result of 30 consecutive tests. For these tests, refinery gasoline blend was used, the ignition timing was 23°BTDC, equivalence ratio was 1 and compression ratio was 8.

Table 2: Shows engine parameters taken during uncertainty testing.

Parameter	Mean	StD	COV (%)	Max Difference
Speed (RPM)	936	0.5	0.01	2.38
Ambient Pressure (kPa)	86	0.1	0.1	0.46
Intake Temp (°C)	36	0.1	0.4	0.5
Equivalence Ratio	1.00	0.005	0.5	0.02
Peak Pressure (kPa)	3390	22	0.6	74
Peak Location (°ATDC)	16.2	0.27	1.69	0.91
NMEP (kPa)	660	4	0.6	19

A metric to define repeatability in Table 2 is the maximum difference found within the 30 runs. For the primary engine conditions, such as speed, ambient pressure and intake temperature the maximum difference percent average is 0.74% as compared to 1.7% for manual engine input conditions, such as equivalence ratio and 3.57% for the engine output conditions such as peak pressure, location of peak pressure and NMEP. These results suggest that large variations in engine output can result as a consequence of relatively small engine input variations.

Further engine uncertainty testing showed that the engine operated differently from day to day. These data are very pronounced and can be seen in Table 3. This table includes 60 points taken over two days at the same engine conditions as those reported in Table 2. The key repeatability metric is again in the maximum difference percent average which is 1.15% for primary conditions, 1.8% for secondary conditions, and 18.6% for engine outputs.

Table 3: Data taken during uncertainty testing, data represents 60 points taken over two days.

Parameter	Mean	StD	COV (%)	Max Difference
Speed (RPM)	936	0.62	0.067	2.38
Ambient Pressure (kPa)	86	0.4	0.5	1.3
Mixing Temp (°C)	36	0.2	0.6	0.6
Equivalence Ratio	1.00	0.005	0.5	0.02
Peak Pressure (kPa)	3320	160	5	489
Peak Location (°ATDC)	16.9	1.8	10.6	5.3
NMEP (kPa)	650	20	3	62.8

These day-to-day inconsistencies were too large and would make it very difficult to elucidate the effect of the fuel additives on engine performance. The carburetor is naturally aspirated and naturally aspirated engines produce varying results based on the ambient air conditions due to changing air density that accompany temperature changes. In the carburetor, the fuel mixes with the air in the venturi tube, which is upstream of the heater. So, when the air and the fuel first mix, the air is at ambient temperature. Therefore, on a hot day the air will be less dense and less fuel will be needed to create a stoichiometric mixture with the volume of air in the venturi tube.

Downstream of the venturi tube and upstream of the cylinder, the fuel/air mixture is heated. This means that the temperature of the air entering the cylinder should be the consistent regardless of varying ambient air temperature. When the ambient temperature is higher, the density is lower and the velocity through the carburetor venturi and other components is higher. This effect increases the flow resistance and decreases the mass flow of air. To better control the upstream conditions, the carburetor air intake was modified such that the air was sent through a dehumidifier. The purpose of a dehumidifier is to remove water from the air by cooling the air so

that the water condensates out. This system provides control over air relative humidity as well as air temperature entering the carburetor. Controlling these variables allows for decreased run-to-run variations as well as allows for day-to-day test results to be compared regardless of the ambient air conditions.

The dehumidifier was an Energy Star 70-Pint Dehumidifier. The 70-pint designation indicates that is it capable of removing up to 70-pints of water from fully saturated air per day. It has a minimum temperature of 35°F, which suggests that the ambient air temperature must be over 35°F to control the intake air temperature. The engine parameters taken while using the dehumidifier can be seen in Table 4.

Table 4: Uncertainty data collected with dehumidifier.

	Mean	STD	COV (%)
Ambient Temp (F)	77	2.2	2.9
Ambient Pressure (kPa)	87	0.2	0.2
Loc. PP (°ATDC)	18.6	0.4	2.4
Equivalence Ratio	1.00	0.005	0.5
Fuel Flow Rate (ml/min)	17.6	0.08	5
Electrical Power (kW)	1.3	0.02	1.52
NMEP (kPa)	645	5	0.7

The key difference between the data in Table 3 and Table 4 is indicated in red. The NMEP was held much more constant over these two uncertainty testing days as seen in the NMEP COV drop from 3.2% pre-dehumidifier to 0.81% with the dehumidifier installed. This result stems from keeping the intake temperature more constant in the venturi tube of the carburetor. This is a large improvement; however, further analysis of these data indicate that the venturi temperature needs to be held more constant. Figure 29 shows the relationship between

venturi temperature and NMEP. There is a linear correlation (R^2=0.94) that indicates that NMEP fluctuations still result from small venturi temperature changes. A 6°F venturi temperature change resulted in an NMEP shift of 25kPa. To be able to conduct more comprehensive additive testing and have large values of statistical significance, the venturi temperature must be held more constant. Therefore, a temperature control loop was implemented between the dehumidifier and the carburetor intake.

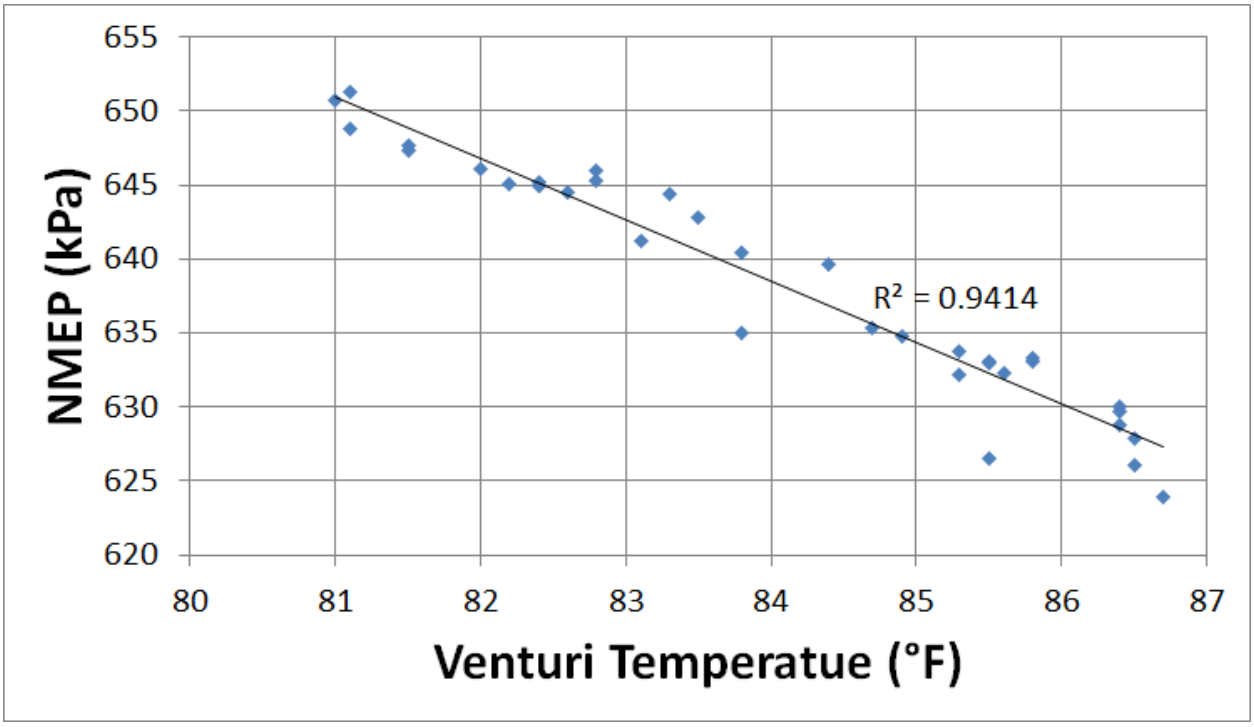

Figure 29: Shows the comparison between NMEP and intake venturi temperature.

The temperature control loop consists of a PID loop that reads thermocouple output voltage and adjusts the voltage applied to the heat tape accordingly. The heat tape was wrapped around the metal pipe that connects the air filter to the carburetor intake. It was found that ambient air with a temperature of 72°F could be heated to a temperature of 100°F when the carburetor intake wall temperature was controlled to 125°F.

In addition to this new temperature control loop, a zero pressure regulator was installed on the air intake line. A zero pressure regulator is a passive device that controls the air intake

pressure to 0.2 kPa above ambient pressure. This means that the performance of the CFR is still related to changes in the ambient barometric pressure. The following data in Table 5were taken over two days and fifteen points were taken on each day. The overall NMEP was lower on average as compared to the previous testing because the air at the venturi and at the cylinder intake was heated to a higher temperature than when the dehumidifier was being used. The higher temperature at this location resulted in decreased density, which resulted in a decreased mass of air entering the cylinder. This fuel and air mixture is then heated again before entering the cylinder, which means that the fuel/air mixture is less dense in this configuration than when the dehumidifier is being used. It was found that controlling the venture temperature helped to resolve day to day variation as seen in the following Table 5.

Table 5: Uncertainty data collected with heat tape and zero pressure regulator.

	mean	STD	COV
Ambient Pressure	87	0.25	0.3
Loc. PP	19.5	0.22	1.14
phi	1.00	0.01	1
fuel flow rate	17.2	0.1	0.6
Electrical Power	1.33	0.02	1.6
NMEP	620	5	0.8

Figure shows that through adding these improvements to the air intake system that the variation in ambient temperature and humidity are eliminated. Thus the variation in NMEP is reduced to variation in ambient pressure, spark timing and equivalence ratio. The reduction in COV's during this engine upgrade process can be seen in the following bar charts:

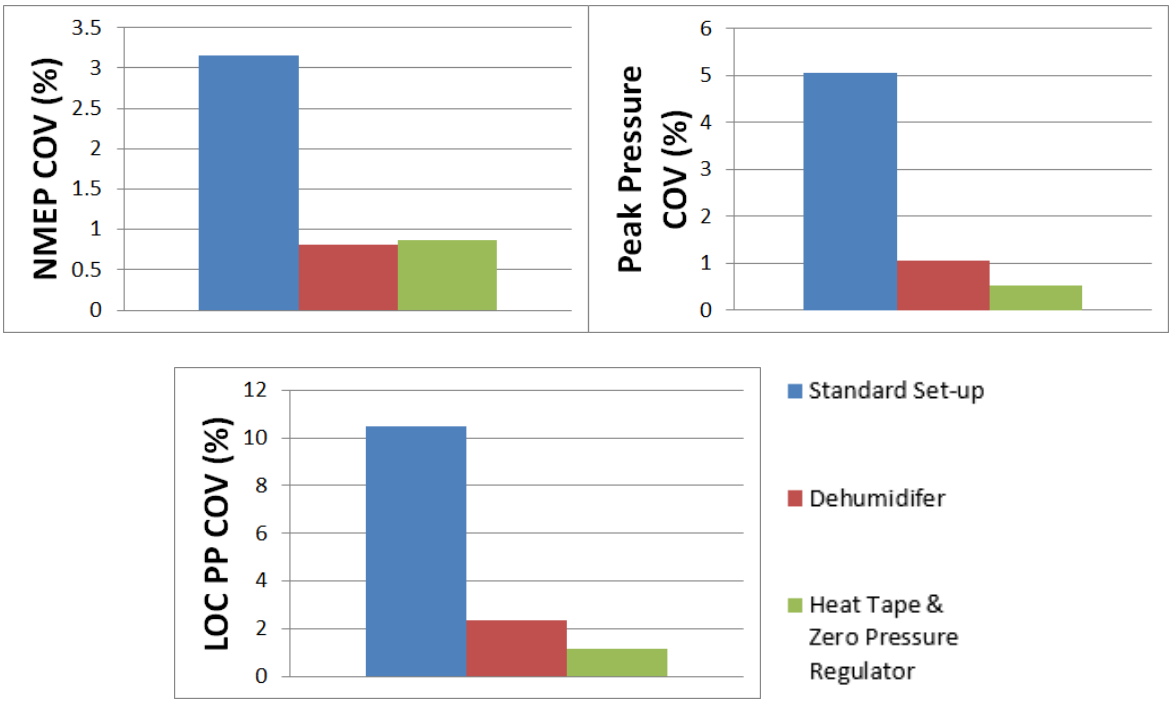

Figure 30: Bar charts showing how the run-to-run NMEP COV, peak pressure COV, and location of peak pressure COV change with each iteration of engine air intake.

The location of peak pressure also improved throughout this uncertainty testing as the temperature uniformity of the air was improved. As discussed above, the flame propagation velocity of the air/fuel mixture varies as a function of the temperature of the mixture at the start of ignition, which varies as a function of the intake temperature. By controlling the variation in intake temperature the location of peak pressure occurred at a more similar timing when compared to the engine configuration that had large temperature changes in the intake air.

Although the day-to-day variation in operating parameters decreased, the cycle-to-cycle variation increased slightly. This can be seen in Fig 32. These figures were constructed through viewing the average value and standard deviation for each individual 3-minute test point. A COV was then calculated with this information. These COV's were then compared and the average and standard deviations are found on the following plots.

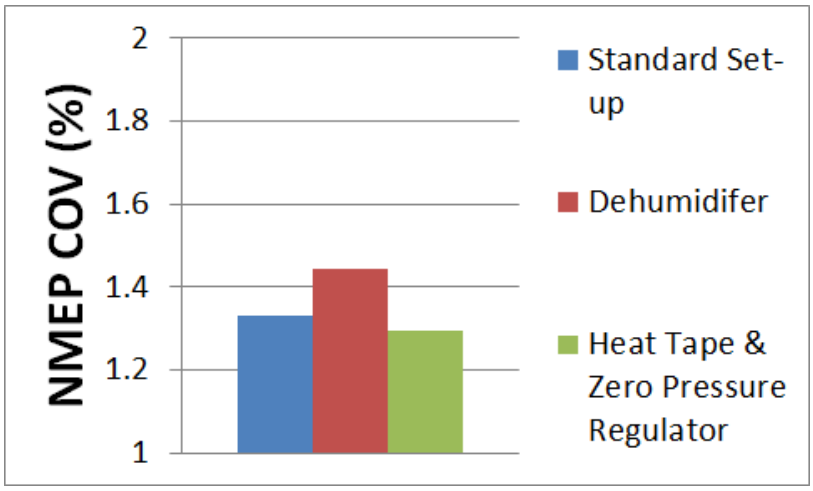

Figure 31: Shows how the cycle-to-cycle NMEP COV changes with the changing engine configuration.

Figure 31 shows the cycle-to-cycle COV for NMEP. It can be seen that the initial addition of using the dehumidifier decreased the engine stability. This occurred because the temperature at the exit of the dehumidifier was not controlled and thus the amount of air and fuel that entered the cylinder on a cycle-by-cycle basis was more variable than the relatively stable venturi air temperature set up as well as well as the temperature controlled heat tape method. Temperature in the venturi tube is very important to control as this dictates the air density. Air density directly impacts the amount of air (and thus the amount of fuel) that enters the cylinder each cycle. It follows that the standard setup and the temperature control set up controlled the NMEP better on a cycle to cycle basis as the venturi temperature in these configurations was more consistent. The NMEP COV was essentially the same between the standard and the temperature controlled set-ups.

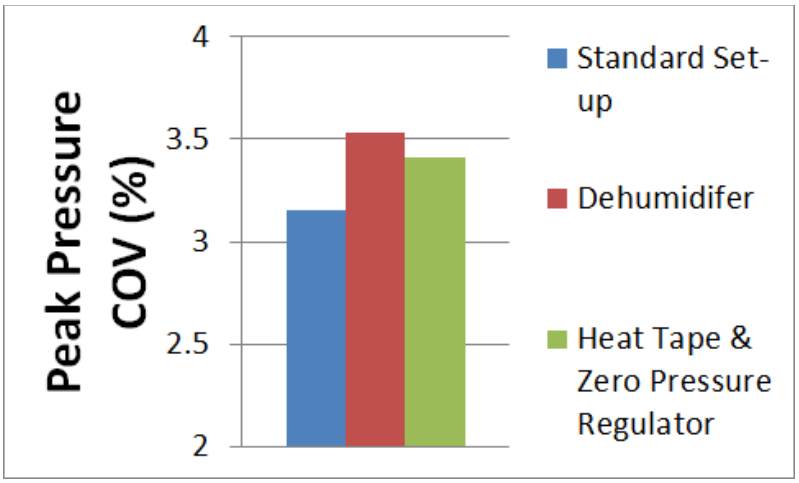

Figure 32: Shows how the cycle-to-cycle peak pressure COV changes with the changing engine configuration.

Figure 32 shows that the additions of the dehumidifier and the temperature control loop slightly increase the COV of peak pressure. For the dehumidifier setup, this is again the effect of the relatively variable venturi temperature. The highly variable intake temperature will result in a wide range of the equivalence ratio due to air density changes. The reason that the temperature control loop method affects the peak pressure COV is because of cycle-to-cycle pressure differences and changes in airflow rate. The zero-pressure regulator is slightly oversized for the CFR air requirements, which resulted in slight cycle-to-cycle pressure variations. This can be seen in Figure 33.

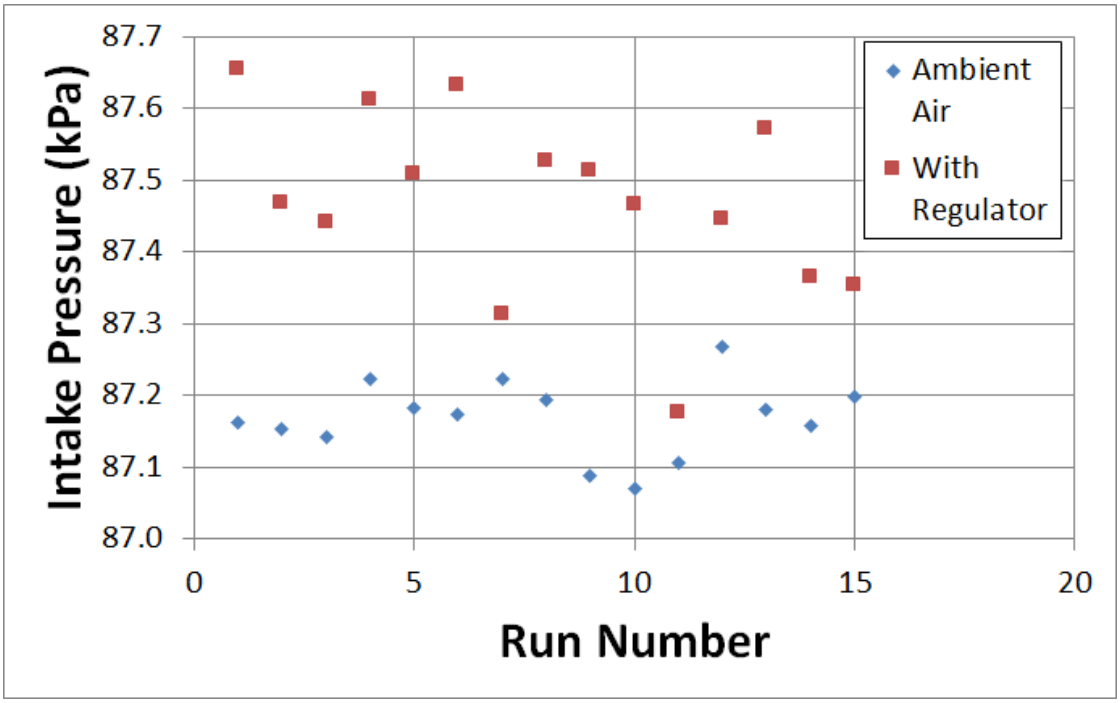

Figure 33: Shows that the intake pressure is more variable when the zero pressure regulator is used compared to ambient air.

Each of these data sets consists of 15 three minute points taken consecutively. It can be seen that, in the case when the regulator is used, there is more variation in the intake air pressure. Although some of this variation is caused by changing atmospheric conditions, there is more variability than the slow-changing atmospheric pressure would suggest. The standard deviation of the data shown in the previous plot is 0.13kPa for the "with regulator" case and only 0.05kPa for the ambient case. The higher peak pressure COV is also a byproduct of the temperature control loop. While the temperature control loop helps to control the average venture temperature, there are temperature cycles that will occur during one three-minute test point. The air temperature set point for the PID loop is 100F. The actual output temperature fluctuates between 98F and 101F during a three minute test point. As discussed previously, this small temperature fluctuation will cause small air density changes that affect both the amount of air in the cylinder as well as the equivalence ratio. These parameters will change over the course of

one point. The main conclusion from this graph is that the fluctuations in airflow from the zero pressure regulators in conjunction with small venturi temperature fluctuations results in a slight increase in the cycle-to-cycle variation of peak pressure. When these variations average out over a full three minute test point the result is smaller run-to-run variation when compared to the standard set up.

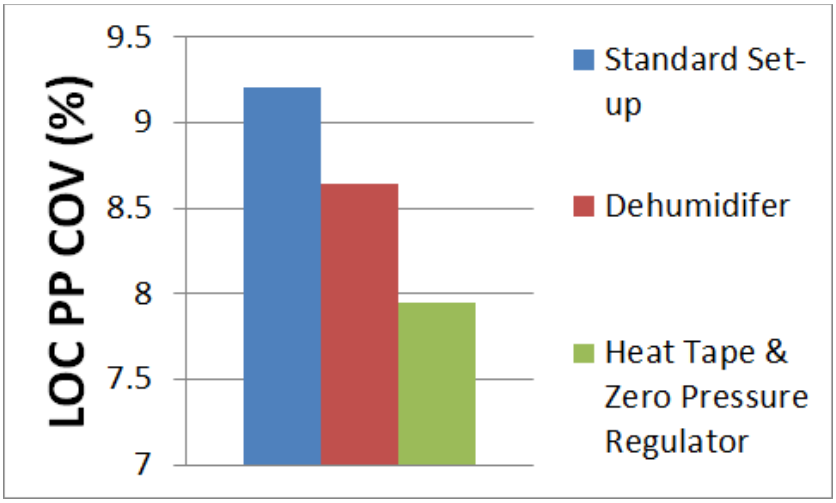

Figure 34: Cycle-to-cycle location of peak pressure COV changes with the changing engine configuration.

The cycle-to-cycle variation of the location of peak pressure was also steadily improved. This improvement is the result of more a consistent mixture temperature. As discussed previously, the location of peak pressure is related to flame speed, which is a function of initial temperature. For the standard setup there was only one heating element which was a coil heater. There was a solitary PID loop that must control the mixture temperature no matter the venturi temperature. For the dehumidifier and the temperature control loop setups. there was a more consistent air temperature reaching the mixture heater. This means that the mixture heater had to provide less heat to control the air. temperature For example, with the temperature control loop, the coil heater only needs to heat the air about 3F while it may need to heat the air 35F without the temperature control loop. The more consistent air temperature will result a more repeatable location of peak pressure.

The Location of Peak Pressure shows the highest COV values of any of the major engine parameters. This is because the Altronic ignition system exhibits cycle-to-cycle drift. When looking at the ignition timing using an ignition light, the timing drifts about 1 CA° over the course of a few cycles. This happens because the mag pick up that is used to control ignition only has one mag pickup port, so there is a predictive algorithm used that tries to identify the 23 °BTDC ignition timing. The resolution of one revolution should be improved.

3.1.2 Base Fuel Testing

Once uncertainty testing had revealed that the consistency of the engine had greatly improved, testing the different baseline liquid fuels began. This testing began by finding the critical compression ratio of each of the fuels. This provided a good launching point as the Octane Number of most of the fuels was known, so comparing the critical compression ratio showed if the results obtained from the CSU CFR compared favorably to results obtained on experimental apparatuses elsewhere. It should be noted that a higher Octane Number means that a fuel will have a higher critical compression ratio by definition. Therefore, this test served as a check for the critical compression ratio criteria as well as test method.

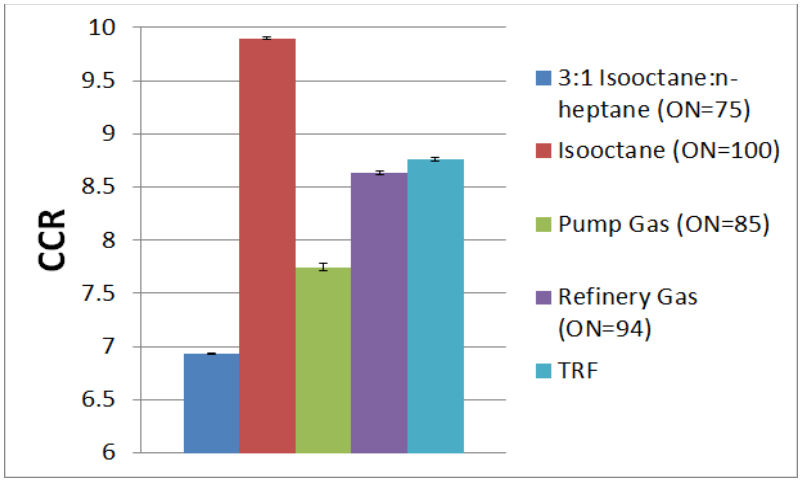

Figure 35: Critical compression ratio of all of the base fuels.

These data show that the fuels and apparatus performed as expected since the fuels with the lowest octane numbers had the lowest critical compression ratios while the fuels with the highest octane numbers have the highest critical compression ratio. The 3:1 blend which, by definition, has an octane number of 75 displays the lowest critical compression ratio, while isooctane has an Octane Number of 100, by definition, displays the highest critical compression ratio. The pump gasoline has an Octane Number of 85 and the critical compression ratio resides been the 3:1 blend and the pure isooctane. Furthermore, it can be concluded that the refinery fuel that was sent from the sponsor has an Octane Number that is about half way between 85 and 100.. The TRF fuel is an interesting case as it has a composition that is 30% isooctane, which has an octane number of 100, 60% toluene which has an octane number of 121, and is 10% n-heptane which has an octane number of 0. This 10% n-heptane is enough to significantly impact the knock properties of the fuel. If the fuel were to be all isooctane and toluene the octane number of the fuel would be expected to be greater than 100, and thus the critical compression ratio would be higher than that of isooctane. However, the 10% n-heptane is enough to drastically affect the critical compression ratio such that the critical compression ratio of TRF is approximately 10% less than that of pure isooctane. These tests showed that the CSU CFR has the resolution to show the difference in critical compression ratio between vastly different fuels.

All of the base fuels were tested on the same day at the same engine conditions (Table 6) so as to fairly compare each of the base fuels. This test was done to see what kind of power differences can be seen in the base fuels. As the critical compression ratio of the 3:1 blend is low, the compression ratio of the engine during this test was set to be 6 so as to avoid any knocking phenomena in any of the fuels that would impact the pressure trace and exaggerate power output.

Table 6: Engine conditions used when comparing base fuels.

Engine Conditions	
Equivalence Ratio	~1
Ignition Timing	23 °BTDC
Compression Ratio	6
Venturi Temp	38°C
Intake Pressure	Ambient
Intake Temperature	45°C

This testing revealed that the CFR apparatus can collect pressure data that can be easily distinguished to separate the different base fuels. This can be clearly seen from the NMEP vs Equivalence Ratio plot in Fig. 36:

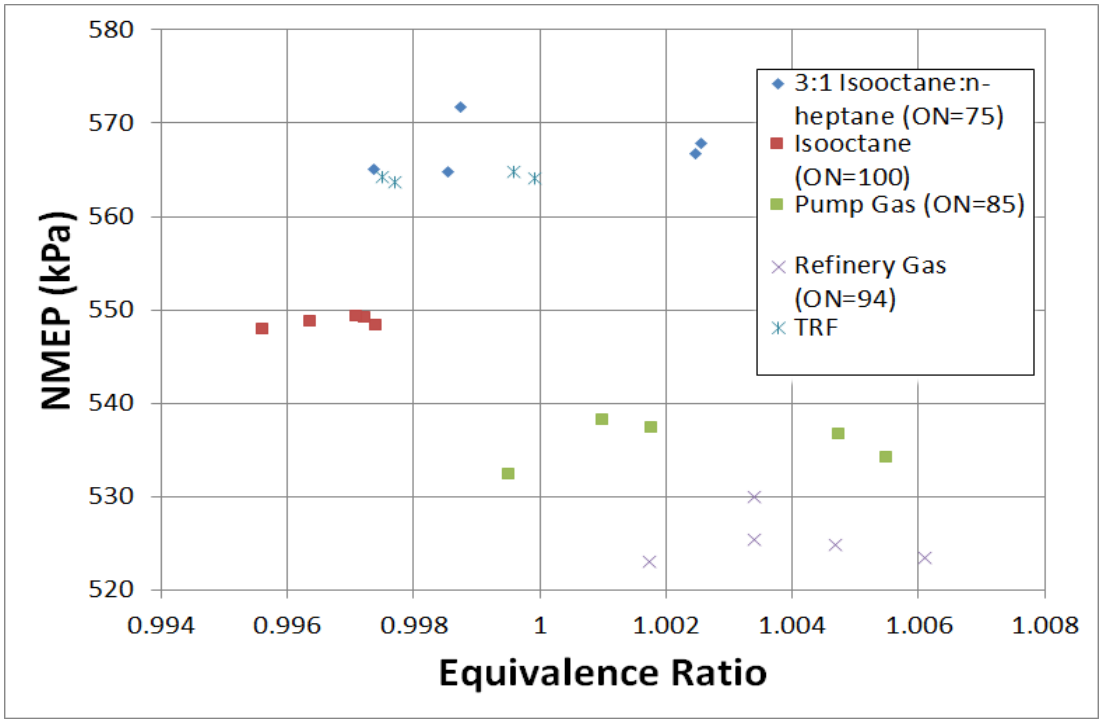

Figure 36: Compares NMEP versus equivalence ratio for all of the liquid base fuels. TRF and 3:1 have the highest NMEP of about 570 kPa, Isooctane is producing and NMEP of 550 kPa, and the refinery and pump gasoline produce an NMEP around 530 kPa.

The plot in Fig. 36 shows that all of the base fuels that the project sponsor provided (3:1 isooctane: n-heptane, isooctane, Refinery Gasoline, Toluene Reference Fuel) were tested. There

is also an additional fuel that was tested; this fuel was an 85 Octane fuel that was purchased from a local gas station. This plot shows that at standard engine conditions there are obvious differences between the fuels. The fuels that have the highest NMEP at these conditions are the 3:1 base and the toluene reference fuel. These fuels have n-heptane in common. As n-heptane is very prone to knock, these fuels will be experiencing higher combustion efficiency because some of the fuel (n-heptnae) is highly combustible at these engine conditions. It should be noted that all of these fuels could produce a higher NMEP with an expanded compression ratio. It is interesting that the refinery gasoline and the pump gasoline experience the lowest power out of all of the fuel tested. The iso-octane has a high critical compression ratio, which means that it can be ran at higher compression ratios than all of the other fuels. When fuels are run at higher compression ratios they produce more power. Since isooctane can be safely run at the highest compression ratio of all of the fuels tested it is interesting that isooctane still produces a higher power output than the gasoline fuels at this low compression ratio. The gasoline fuels produce a very similar power output.

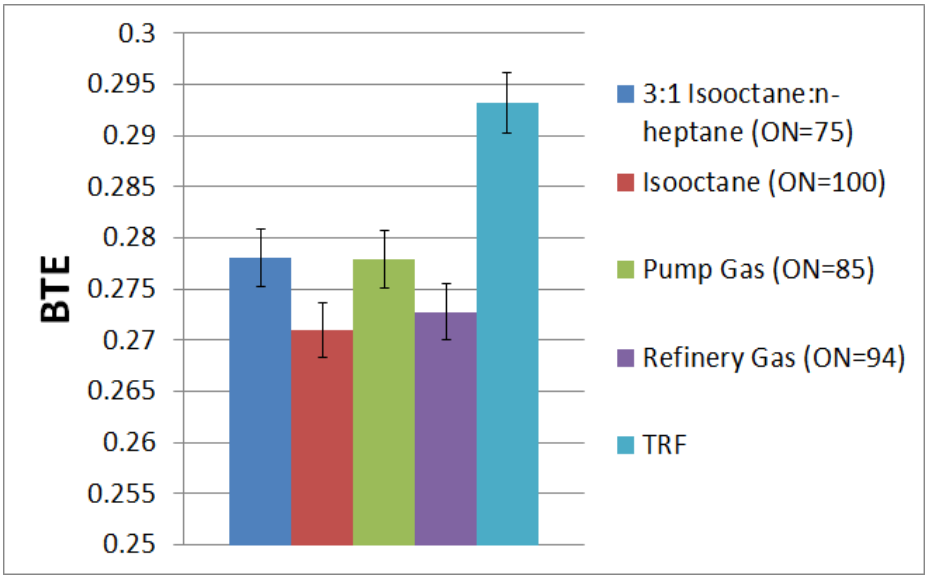

Figure 37: Compares brake thermal efficiency for all base fuels. TRF is the highest due to a high density of the fuel as well as a high NMEP, as seen in Figure 36.

In terms of brake thermal efficiency (BTE), the TRF fuel is the most efficient. This is the case because the two most likely candidates were the TRF fuel as well as the 3:1 blend due to the high NMEP each of these fuels produced. These fuels produced nearly identical power; however, the TRF fuel is much denser. This means that, volumetrically, less fuel is consumed when used the TRF fuel, also, at these engine conditions there will be the most power output per volume of fuel consumed for the TRF fuel. Most of the other base fuels are nearly identical. This represents a change in fuel efficiency that is more or less negligible between all of the fuels. A fuel that has high power output (the 3:1 blend) also will tend to be less dense. A less dense fuel will mean that a larger volume of fuel will need to be used in the engine to match the same power output. This is of significance because people tend to compare the miles per gallon (MPG) that a car gets. A gallon is a unit of measure of a volume, so a car that uses a less dense fuel will get lower MPG's. That being identified, the base fuel that, at these engine conditions, will produce the most miles per gallon would be the TRF fuel. If the engine conditions were to be configured to maximize the energy output of the fuel, then these efficiencies will change.

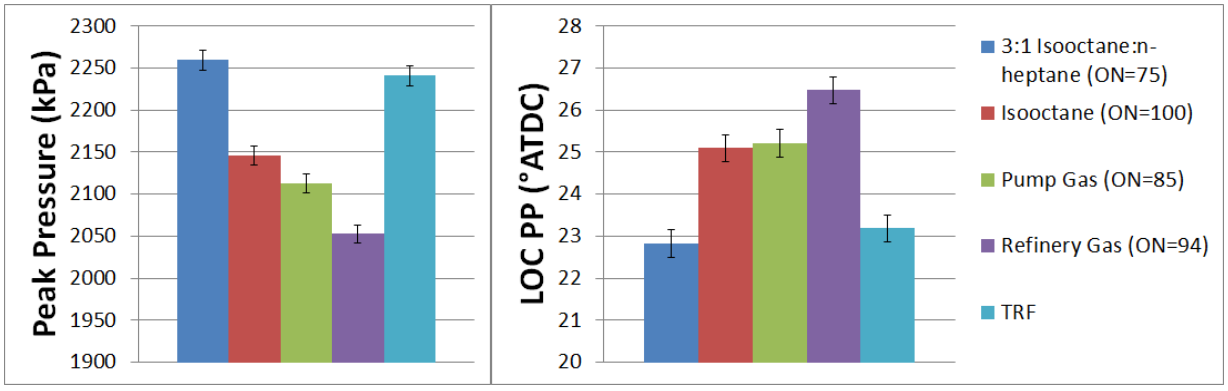

Figure 38: Peak pressure and location of pressure differences between all of the base fuels. Generally, fuels with a low peak pressure, also have a late location of peak pressure.

The peak pressure and the location of peak pressure for the baseline fuels is plotted in Fig. 38. The average peak pressure seen during these tests follows the same trend as the NMEP in that the TRF and the 3:1 blend have the highest values. This is expected as these fuels are

running closest to the optimal compression ratio in which they would show the most power. It can also be seen that the gasoline fuels produce the lowest average peak pressure. This plot in conjunction with the previous NMEP and critical compression ratio plots show that the isooctane fuel has the highest energy density. This is the case because isooctane is very far from its optimal compression ratio; however, it still produces high power as well as high peak pressure. Isooctane base fuel would have the ability to run with the most power of all of the base fuels that were tested. As observed previously, there is a correlation between the peak pressure and the location of peak pressure.

The 3:1 blend and the TRF exhibited the earliest location of peak pressure. This means that this flame is burning the quickest. Interestingly, the refinery gasoline has the latest location of peak pressure by a significant margin. These error bars come from the point-to-point COV's that were found from the uncertainty testing. For example, it was found the point-to-point peak pressure COV was 0.533%. This number is then divided by 100 and then multiplied by the average peak pressure for the baseline data. As the uncertainty testing included about 50 points, there is a significant sample size with which to analyze.

The final baseline fuel comparison experiment that was conducted was a lean limit test. This testing was done by systematically decreasing the amount of fuel that was used while keeping the air flow the same. This testing required that the engine configuration revert to the ambient air since the slight pulses in the air that are present when the building air is used could prove to be problematic when the engine is operating very lean. There was a high rate of misfires when the ambient set-up was being used and this problem was exacerbated when the building air was used. It should also be noted that the compression ratio was set to 7, which was consistent with the lean limit additive testing described below. This is a different compression ratio from

the other tests that were described above, which is why the average NMEP values that are shown are different from those in the preceding plots. Figure 39 is a plot NMEP versus equivalence ratio for each baseline fuel. The 3:1 isooctane: n-heptane blend has much fewer points than the rest of the fuels as this fuel had a knock integral greater than 1 when the equivalence ratio was over 0.9. The knock integral stipulation was held strict to facilitate interpretation of the data.

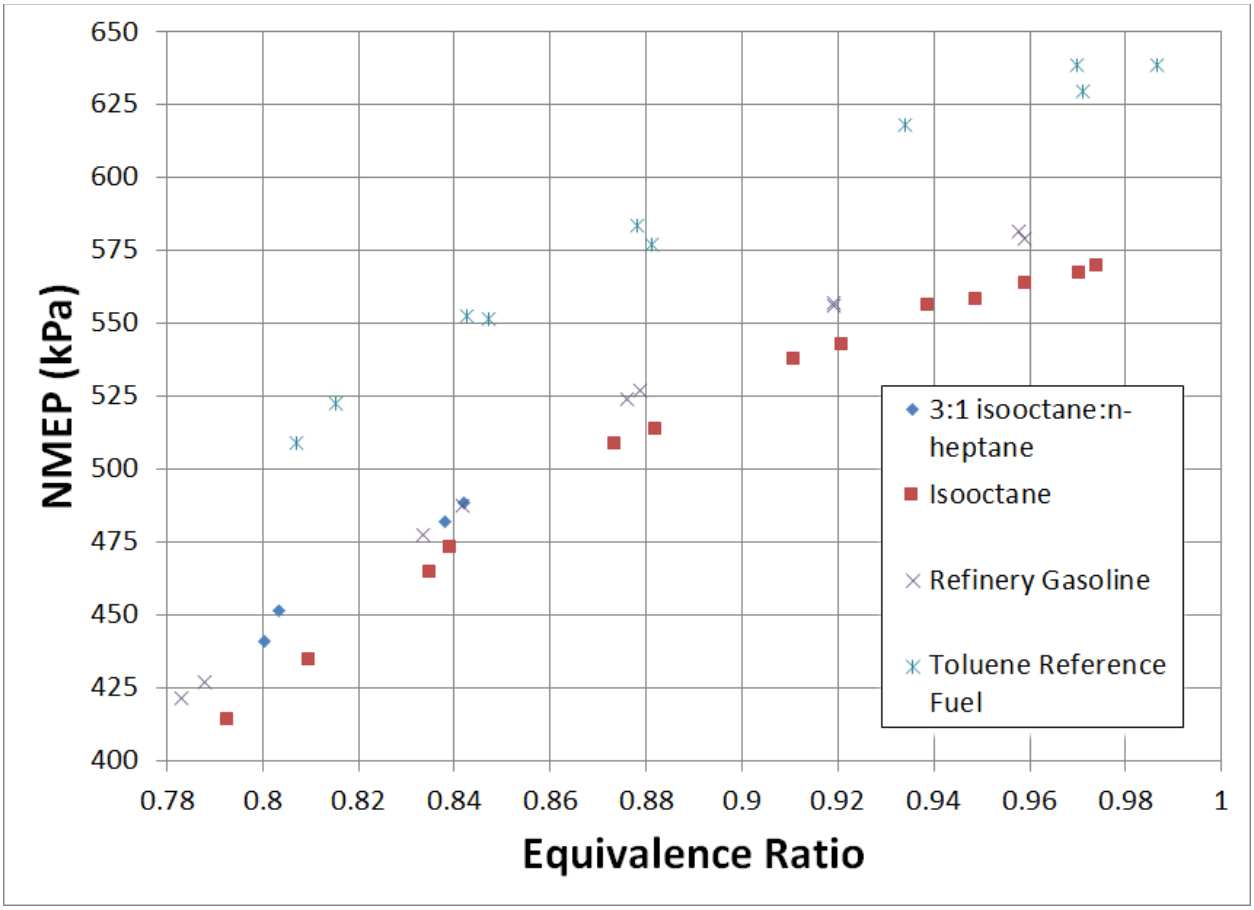

Figure 39: NMEP changes over an equivalence ratio sweep.

Figure 39 shows that all of the tested base fuels show the same trend in that the NMEP decreases with decreasing equivalence ratio at nearly the same rate for all fuels. This result is consistent with the previous result that the highest NMEP is seen with TRF, followed by isooctane and the refinery gasoline near stoichiometric conditions. It is important to note these trends on decreasing NMEP but NMEP is not an effective metric for identifying the lean limit as

evidenced by the steady decrease in NMEP as a function of equivalence ratio. To identify the lean limit, the COV of NMEP, which is a measure of engine stability, is a more effective metric than the average NMEP values. The NMEP COV versus equivalence ratio plot is shown in Fig. 40.

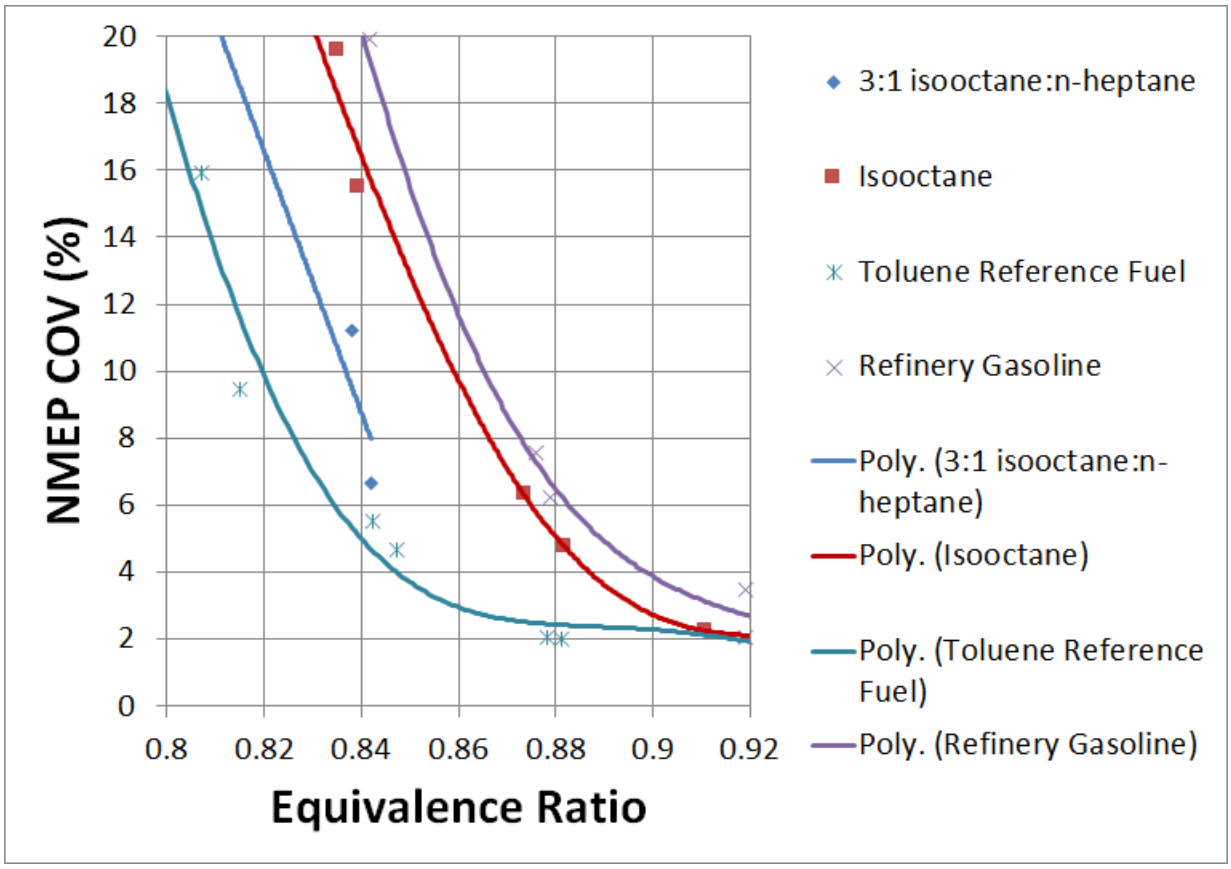

Figure 40: Polynomial fitted lines through NMEP COV versus equivalence ratio. The point where each fitted line crosses the NMEP COV = 10% line is deemed the lean limit.

To define a lean limit for each of the fuel types, a value of COV must be specified to define a level of engine misfire that is deemed unacceptable. For example, from Fig. 40, one might choose to define the lean limit based on a value of COV > 10%. To facilitate comparison of the lean limit COV among the fuels, 6th order polynomials were fit to the data as shown in Fig. 40. These polynomial curve fits show the separation that exists between the fuels at lean conditions. While the choice of lean limit NMEP COV is somewhat arbitrary, the literature

suggests a definition for the lean limit as the point at which either the NMEP, IMEP or peak pressure COV crosses the 10% threshold (Ma, 2008). For this study, the 10% NMEP COV was used as the defining variable for the lean limit for the liquid fuel additives. This process is described in greater detail below.

At the engine conditions that were used during this testing, it can be seen that the TRF had the leanest lean limit and the NMEP COV did not reach 10% until an equivalence ratio of 0.82. The next leanest was the 3:1 PRF blend, which held consistent load until an equivalence ratio of 0.835 was realized. The isooctane and the refinery gasoline exhibited lean limit equivalence ratios of 0.86 and 0.87, respectively. All of the curves, with the exception of the 3:1 PRF blend, show the same shape. All of the curves are relatively flat until the NMEP COV reaches approximately 6%. At this point, all of the fuels produce a rapid rise in NMEP COV. Also, all of the curves have a very similar slope above 6%. Overall, this experiment was beneficial to understanding the comparisons between all of the base fuels. The results also suggested that using the refinery gasoline would provide the best opportunity to produce measureable results with the additives since this fuel showed the worst lean limit performance of all of the baseline fuels tested.

3.1.3 Commercial Fuel Additives

After the base fuel comparison described above was completed, some tests were performed with commercially available gasoline additives. These additives were not provided by the sponsor, but rather they were commercial additives purchased locally from Autozone. The commercially available additives were tested as a benchmark against which to compare the experimental additives. The commercially available additives are claimed to increase the Octane Number and to deliver more power. The first additive tested was Madditive from VP racing. This

additive is purported to increase the Octane Number of the fuel while also increasing engine power and efficiency. It is also purported to clean injectors and other sludge build up. The second fuel additive is made by Lucas and it is primarily an Octane Number enhancer.

To give these additives the highest probably of affecting the fuel and combustion properties, the fuel additives were added to the 3:1 isooctane:n-heptane, which by definition had an Octane Number of 75. If the fuel additives were added to the other base fuels, then the Octane Number range that the additives would be able to impact would be minimized. It is much less likely to see an octane improvement when the Octane Number of the fuel was already at 90 or above. Keeping the baseline Octane Number lower provides the best chance to observe a positive effect from the additives.

The additive manufacturers recommend putting the entire bottle into a full tank of gas. It was assumed at a tank of gas was 16 gallons and the additive was added using that same blend ratio. The blend ratio came out to about a 0.75% additive concentration by volume or about 7500 PPM. It should be noted that the Lucas additive is not considered street legal, while the VP additive is street legal.

Figure 41: Commercial fuel additives. The additive on the left is the VP Racing Madditive. The additive on the right is the Lucas Oil Octane Booster.

Table 7: Engine conditions during commercial additive testing.

Engine Conditions	
Additive Concentration (volume)	0.75%
Equivalence Ratio	~1
Ignition Timing	23 °BTDC
Compression Ratio	6
Venturi Temp	38°C
Intake Pressure	Ambient
Intake Temperature	45°C

The engine conditions under which the additives were tested are included in Table 7. These conditions are the same conditions under which the base fuels were tested. The compression ratio was relatively low so that the fuel would not knock while running the baseline.

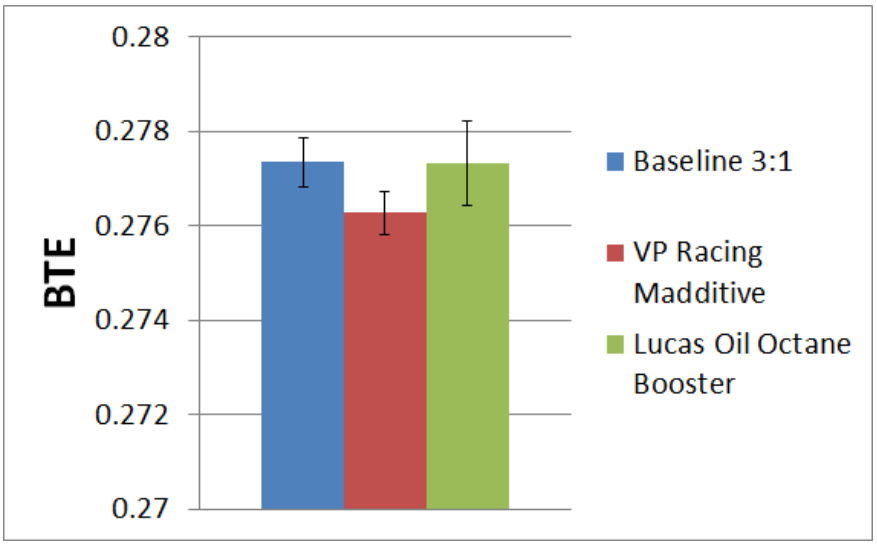

Figure 42: Brake thermal efficiency comparison between the baseline fuel and the consumer additives.

The additives did not have a large impact on the thermal efficiency of the base fuel. If the engine were actually producing more power as the additives claimed, then the thermal efficiency would be expected to be higher with the addition of the additives. This was not the case during testing. The additives did have a slight effect on the average peak pressure as shown in Fig. 43.

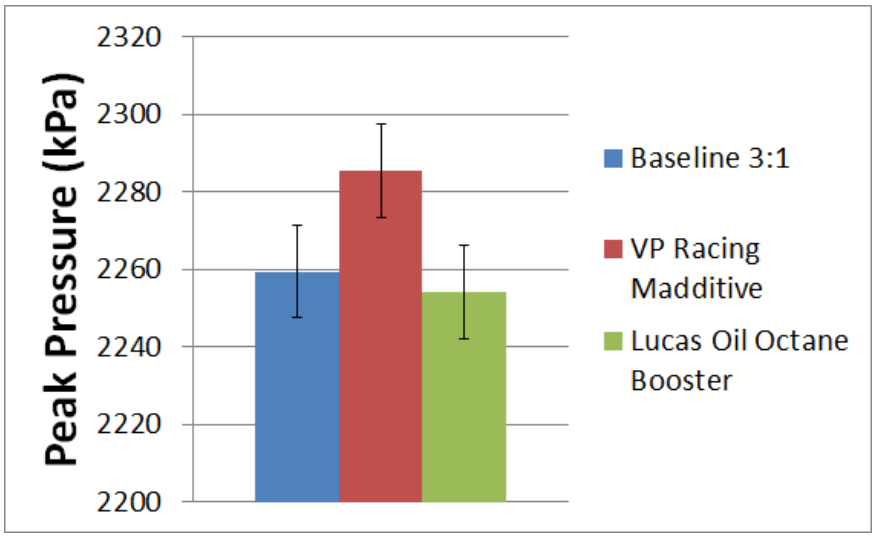

Figure 43: Peak pressure comparison between the baseline fuel and the consumer additives.

From analysis of Figure 43, the VP racing additive seems to have increased the peak pressure. However, most of this effect is likely due to the fact that this additive was running slightly rich. A better measure of how the additives impact combustion is found in the brake thermal efficiency plot. The peak pressure did, however, trend in the correct direction for the VP additive while the Lucas additive appears to not show any significant difference.

The only major statistically significant difference that was observed during this additive testing was the critical compression ratio. Both additives claimed to stop engine knock. This would imply that the additives would result in an increase in the critical compression ratio since they would delay the onset of knock. This result is clearly seen in Fig. 44 for the Lucas additive.

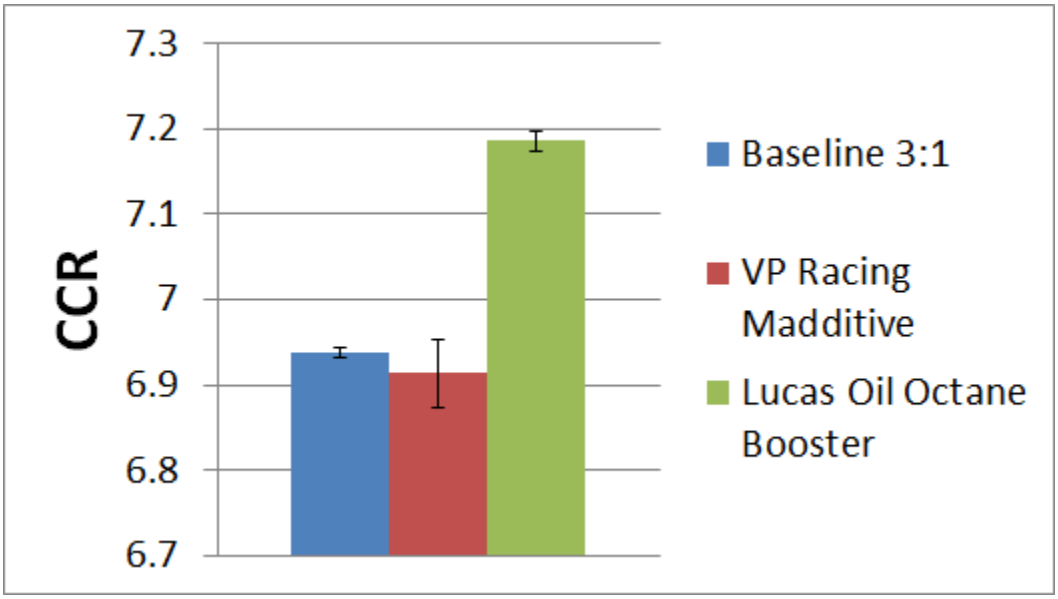

Figure 44: Critical compression ratio comparison between the baseline fuel and the consumer additives. The Lucas Oil Octane Booster increases the critical compression ratio of the 3:1 baseline fuel.

The critical compression ratio increased when the Lucas oil additive was present. This result shows that the additive does increase the Octane Number of the fuel as advertised. The increase in critical compression ratio was approximately 10%. On the bottle, the additive is claimed to increase the Octane Number of the fuel by up to 8 points. From the data that was collected, this could actually be true. However, the fuel to which the additive was added had an

Octane Number of 75, which was much lower than any commercially available gasoline. So, the effect of the additive on a commercial gasoline may be less than what was observed in this experiment. The VP additive did not display the same extension of the critical compression ratio. The VP additive had minimal impact on the state of the engine.

3.1.4 Experimental Additive Testing

Upon completion of testing with the commercially available additives, the additives supplied by the sponsor were tested. These tests represented one of the primary objectives of the research study, so the goal was to obtain a large sample size of all of the data. So, if there was a difference in any engine metric, then the sample size would be large enough to claim statistical significance. The engine was configured with the heat tape and with the zero-pressure regulator for the highest degree of accuracy attainable. The test matrix that was used for these tests is listed in Table 8.

Table 8: Engine conditions used during experimental additive testing.

Engine Conditions			
Additive	1b	2	3
Concentrations (PPM)	5000/10000	5000/10000	5000/10000
Equivalence Ratio	~1	~1	~1
Ignition Timing	23 °BTDC	23 °BTDC	23 °BTDC
Compression Ratio	7.5	7	7
Venturi Temp	38°C	38°C	38°C
Intake Pressure	Ambient	Ambient	Ambient
Intake Temperature	45°C	45°C	45°C

The key independent variables for these tests were the additive concentrations (ppm), equivalence ratio, and the compression ratio. The concentrations of the additives tested were 0.5mol% and 1mol%, respectively. There are a few equivalence ratio problems that arose during this testing. The first issue was that the high concentration of additive proved to have

complications when testing, which will be discussed in the next paragraph. The second problem was that the engine was configured such that the air flowed through multiple regulators before entering the carburetor. This configuration resulted in fluctuations in the air flow that were not present when the engine was operating on ambient air. The fluctuations in this configuration resulted from other happenings in the building as well as regulator error. So there was more drift in the air flow than when the engine was operating off of ambient air. The final key point of the above table is that the compression ratio was changed during this testing due to an operating error. However, the baseline refinery gasoline was run on both days, so the additive impact could still be compared to the baseline conditions.

As mentioned previously, the additives can impact the equivalence ratio stability of the engine. This result was most commonly seen with additive 1b for concentrations equal to or above 1000 PPM when the equivalence ratio control begins to falter. This result can be seen in Fig. 45, which shows the air fuel ratio versus time for the baseline refinery gasoline case and for the same fuel with 10000 PPM of additive 1b.

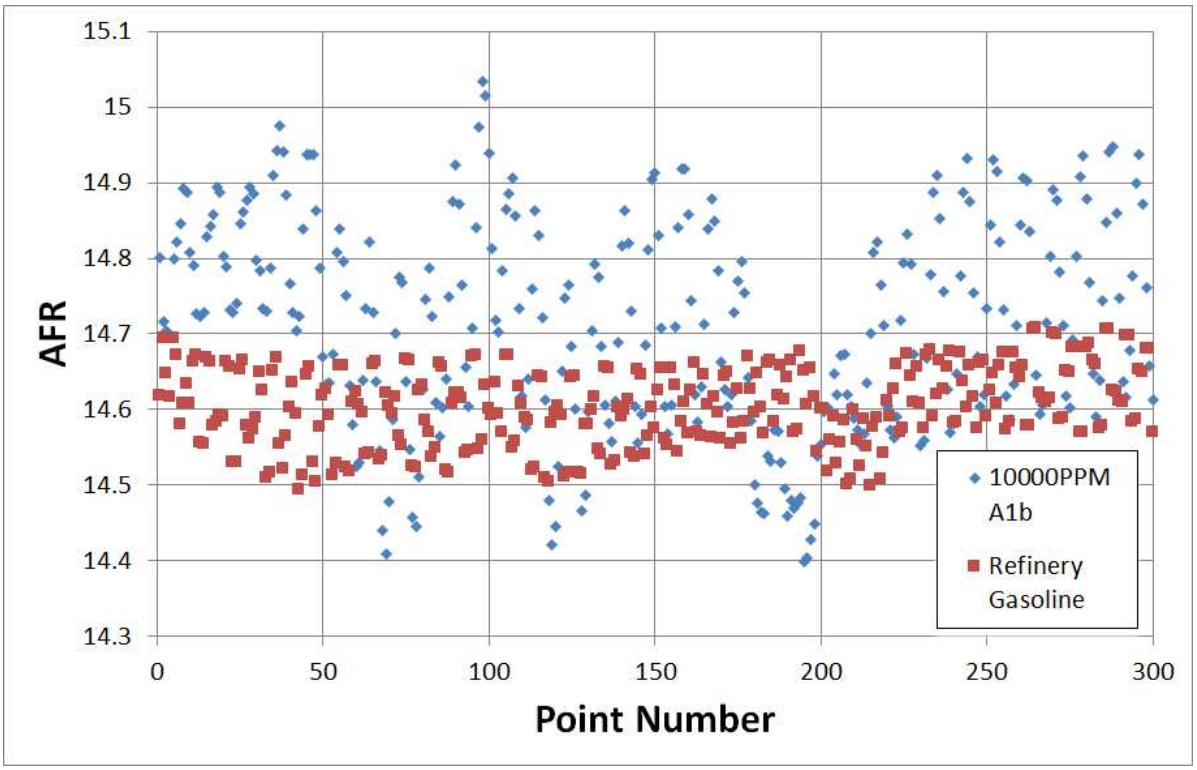

Figure 45: Shows impact that additive 1b has on AFR control. Each point is a 20 point moving average, each band represents a three-minute test point. The points with the additive present show larger deviation.

The red squares are the baseline refinery gasoline and the blue diamonds are the same base fuel with 10000PPM of additive 1b. Each point on the plot represents a 20 point moving average of the AFR when the building air and 0-pressure regulator were being used. It can be seen that the baseline condition shows much less fluctuation than the additive case. This phenomenon may be caused by the additive condensing in the fuel lines, which would cause slugging of the additive. So some cycles would have next to no additive while the next cycle would have a much higher concentration of additive than the desired amount. This may cause the AFR as measured by the AFRecorder 4800 to vary as the composition of the fuel is changing during testing. The secondary impact of this AFR fluctuation is that it made testing for a statistically large sample size difficult since data points taken consecutively did not always have the same equivalence ratio. When the baseline fuel was used, there was little fluctuation in the AFR, so many data points could be acquired consecutively. Conversely, when there was a high

concentration of additive, the AFR drifts, which creates difficulty in taking many points consecutively. This drift adds considerable time to the testing, which prohibits gathering as substantial quantity of data points. Still, even with the screening of these points, there was a large range of points that made it through the screening process. This can be seen in Fig. 46, which is a plot of NMEP versus equivalence ratio.

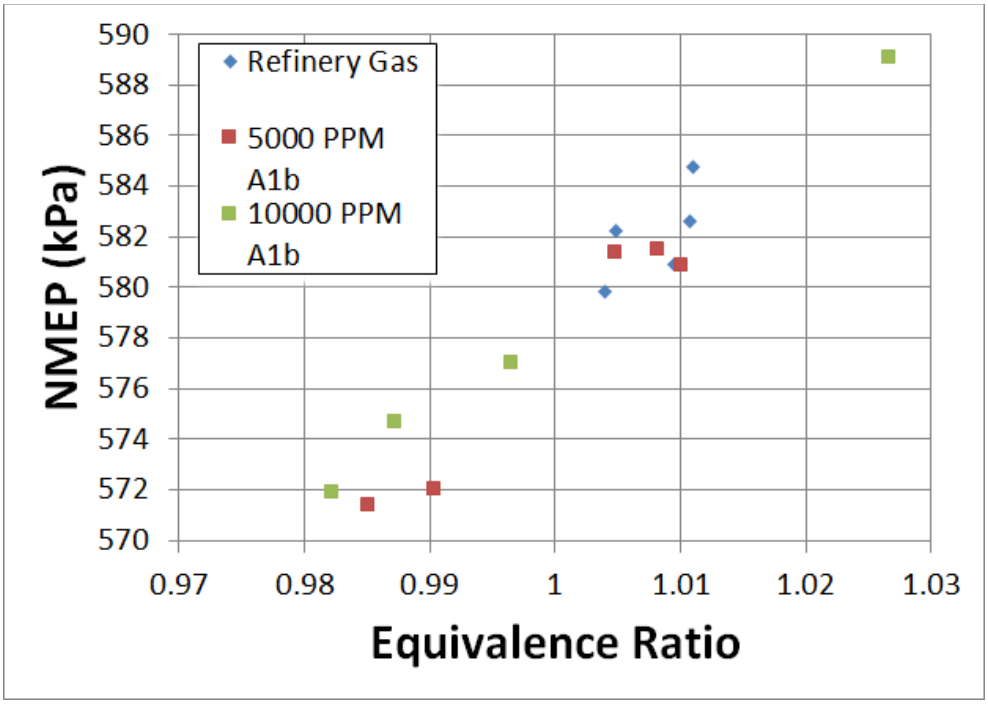

Figure 46: Shows the effect that additive 1b has on NMEP.

It can be seen that only a small amount of points are represented. In the high concentrations of additive 1b, there is a large range in the equivalence ratio. However, there is a cluster of data points at an equivalence ratio near 1.01 for both the refinery gasoline and the 5000 PPM additive 1b. These data points are nearly overlapped. This result would indicate that, at this equivalence ratio and these engine conditions, the additive has no effect on output power. Furthermore, fitting a line through the 10000 PPM points also intersects the cluster of points that resides at an equivalence ratio of 1.01. Any slight change that could be determined for output power from these data would be difficult based on the large range in equivalence ratio and the

small sample size of usable points. That said, there are certain metrics that indicate that additive 1b had a slight positive impact on combustion. These metrics are peak pressure and location of peak pressure. The peak pressure plot is shown in Fig. 47.

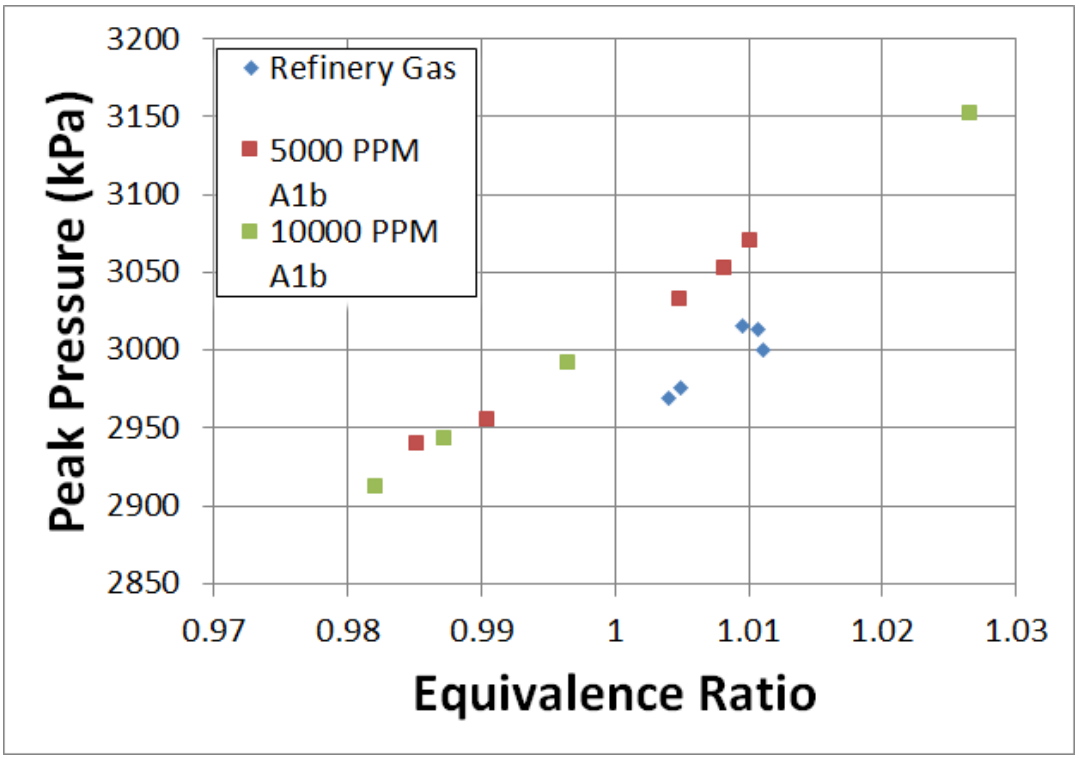

Figure 47: Additive 1b has as positive impact on average maximum peak pressure.

Figure 47 shows how the peak pressure varies with the equivalence ratio. These data, show that the peak pressure for the additive case is higher than for the baseline case. It appears that all of the baseline points follow a linear trend and the additive cases follow another higher linear trend. This results suggests that the additive increases the peak pressure by approximately 1%. This results shows that this 1% difference is very small but is most likely greater than the experimental uncertainty that was discussed earlier. All of the additive 1b points exhibit a higher peak pressure than the baseline case, indicating that additive 1b positively impacts the peak pressure. The location of peak pressure shows a similar trend (Fig. 48).

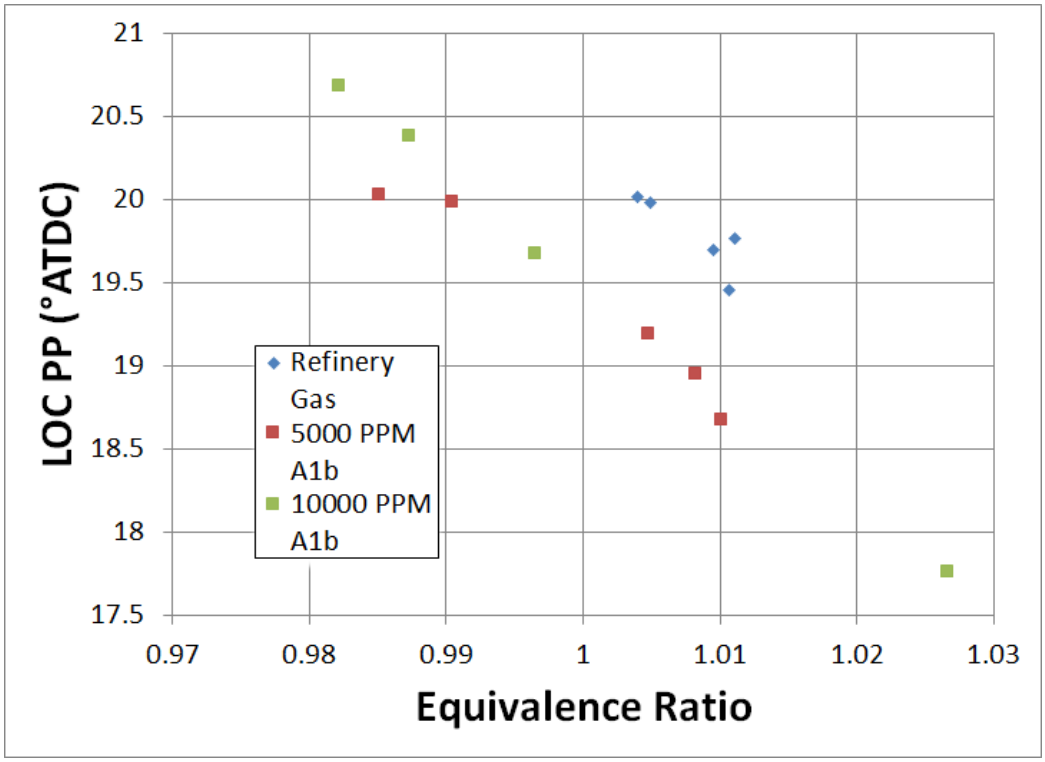

Figure 48: Additive 1b reduces the time from TDC to the location peak pressure.

The location of peak pressure shows the same type of trend as the peak pressure data. The additive cases follow a certain linear trend while the baseline data follows a different linear trend. In this case, however, is the results may not be statistically significantly different. The point-to-point location of peak pressure (LOPP) COV was reduced during uncertainty testing; however, the COV was still in the 5% range. In analyzing the change in location of peak pressure data at equivalence ratio of 1.01, it can be seen that the location of peak pressure advances about 1 full crank angle degree from the baseline case to the 5000PPM case. The LOPP COV of 5% covers a full crank angle degree. This means that the standard deviation bars for these points have a full degree of overlap. So, quantifying how much the additive is affecting the location of peak pressure is not possible with the current engine apparatus and test method. However, the claim can be made that the additive does have an effect on the location of peak pressure and it tends to speed up combustion. This can be seen from the difference of fitting lines through the

base line and the additive points. There is an obvious location where the location of peak pressure occurs for the baseline and a separate location for the additive case. One particular place of interest are the two baseline points at an equivalence ratio of about 1.005 and the two 5000 PPM additive points at about 0.99. All of these points represent nearly identical location of peak pressure at 20 degrees after top dead center. There is 1.5% more fuel in the cylinder for the baseline case. So, the baseline fuel should reach a peak pressure faster, but the presence of the additive causes the flame speed to increase. For the baseline case, when the fuel is increased by 0.5% the location of peak pressure advances by almost 0.5 crank angle degree. While examining the additive case, the numbers are similar (0.5% increase in fuel leads to a half crank angle degree change in location of peak pressure). Both the base fuel and the additive show the same location of peak pressure change versus equivalence ratio. So the result is that the two fuel blends show the same trend, but the additive shows a location of peak pressure that is always faster than the baseline condition.

Next, high concentrations of additives 2 and 3 in the Refinery Gasoline were tested. These tests went much smoother than the additive 1b testing in that there was no significant impact on the equivalence ratio stability, except for in the 10000 PPM concentration of additive 2. Even so, this effect was slight when compared to the effect that additive 1b had on the AFR. No such AFR instability effect was observed with additive 3. All of these data were acquired on the same day, so pressure variation was minimal, and the baseline was repeated regularly. Figure 49 is a bar chart of a thermal efficiency.

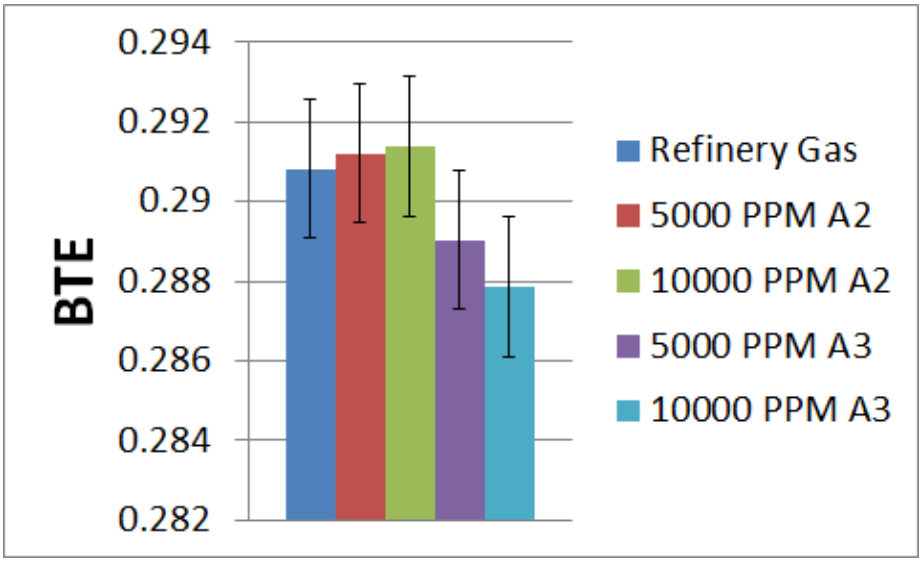

Figure 49: Additive 2 and 3 impact brake thermal efficiency.

For these additive cases, additive 2 had a minimal impact on the thermal efficiency of the engine, while additive 3 had a slightly negative impact on engine performance at these conditions. Although the data from additive 2 trended in the positive direction, the steps were incremental and were within the experimental uncertainty. These small steps also show that the point of diminishing returns had been reached. When additive 2 is in a 5000 PPM concentration, the average efficiency increases by 0.4%, while the increase from 5000 PPM to 10000 PPM only results in an additional efficiency increase of 0.03%. The increase in thermal efficiency that is seen between the 5000 PPM and 10000 PPM is negligible. So it is predicted that adding more additive beyond the 10000 PPM concentration would not substantially affect the brake thermal efficiency of the engine. When examining the results of additive 3, the results are clear. This additive negatively affected the thermal efficiency of the engine significantly. When this additive was added to the fuel in the 5000 PPM concentration, the thermal efficiency decreased by 0.3%. When another 5000 PPM of additive 3 was added to the refinery gasoline, the thermal efficiency decreased by another 0.44%. This shows that adding in additive 3 causes the engine to produce less power, and the trend continues at higher additive concentrations. There is still a possibility

that the additive will delay the onset of knock, so the engine could operate at a higher compression ratio and thus produce more power. The other engine parameters that were analyzed were the peak pressure and the location of peak pressure. The peak pressure trends are shown in Figure 50.

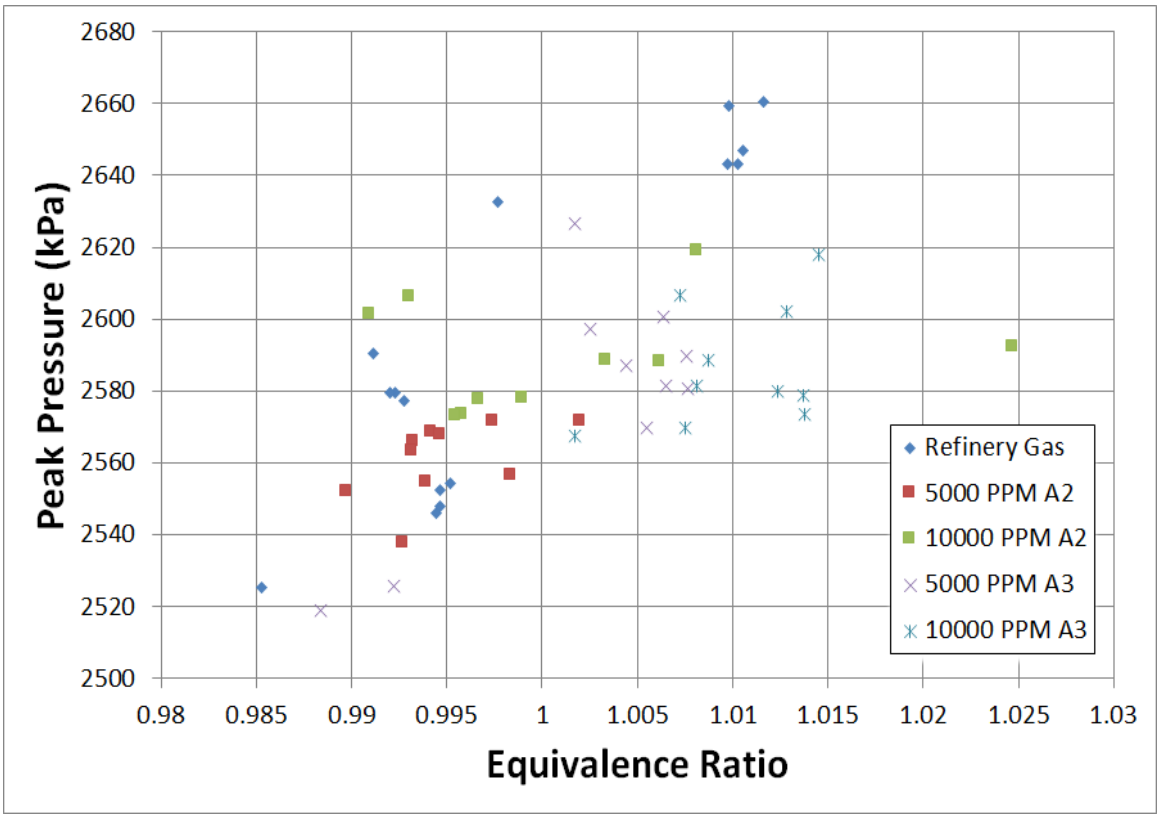

Figure 50: Additive 2 and 3 impact on NMEP.

Figure 50 has several key regions of interest. The first region of interest is the region between an equivalence ratio of 0.99 and 1. In this region, there are multiple baseline points, as well as many points that represent the 5000 PPM and 10000 PPM additive 2 points. It is important to see that these points have the same equivalence ratio and also the same peak pressure. This shows that additive 2 has no impact on the peak pressure. For additive 3, the key region of interest is the region of equivalence ratio from 1.005 to 1.015. In this region, we can see that the baseline peak pressure points are significantly above the case when additive 3 is

present. The baseline refinery gasoline had a peak pressure that ranged from 2640 and 2660 kPa while the cases with additive 3 (both the 5000 PPM and 10000 PPM concentrations) span from 2570 to 2620 kPa. This difference represents a significant difference. There are even additive 3 points that are richer than these highlighted baseline points, and the peak pressure magnitude is still lower than the leaner baseline points. This results suggests that additive 3 negatively affects the peak pressure that is seen at these engine conditions.

In a parallel study conducted by Boissiere (Boissiere, 2016), experiments were conducted to determine the effect of additive 2 on homogeneous autoignition in an RCM. The RCM data analysis showed that Additive 2 in 1000 PPM concentrations caused a lower amount of energy release in the low temperature regime. This can be seen in comparing Figure 51, which shows the low temperature pressure rise rate of pure isooctane in comparison with Figure 52, which is focused on the same low temperature pressure rise rate with 1000 PPM of additive 2 present in the isooctane.

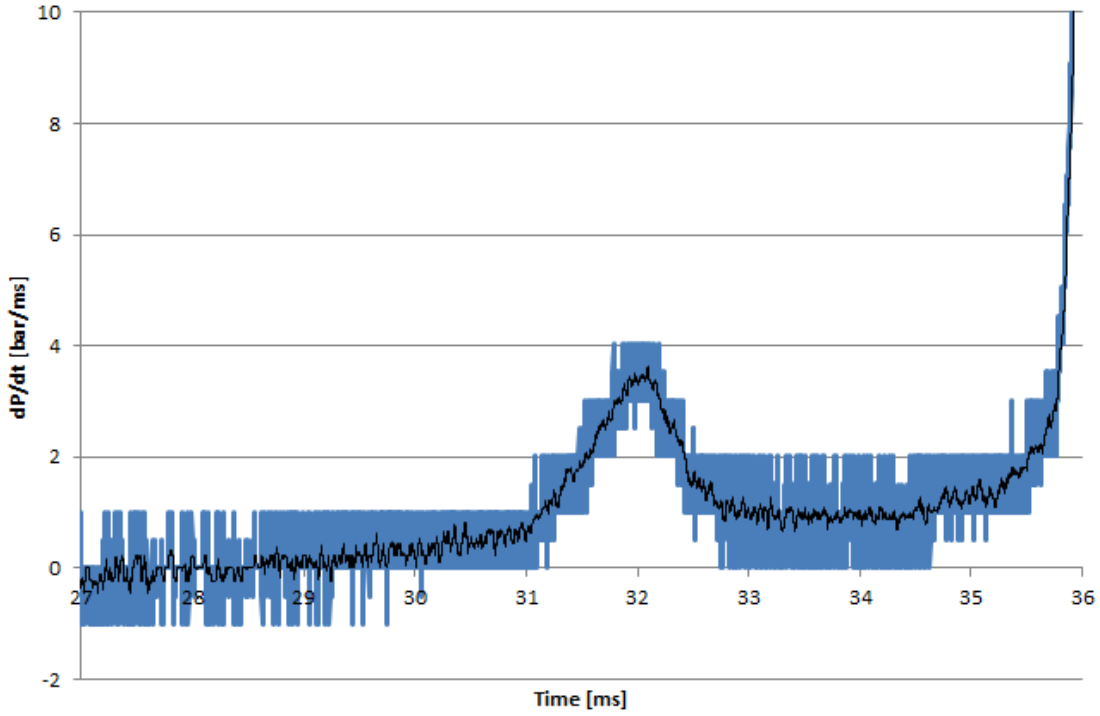

Figure 51: Shows the low temperature pressure rise rate of pure isooctane.

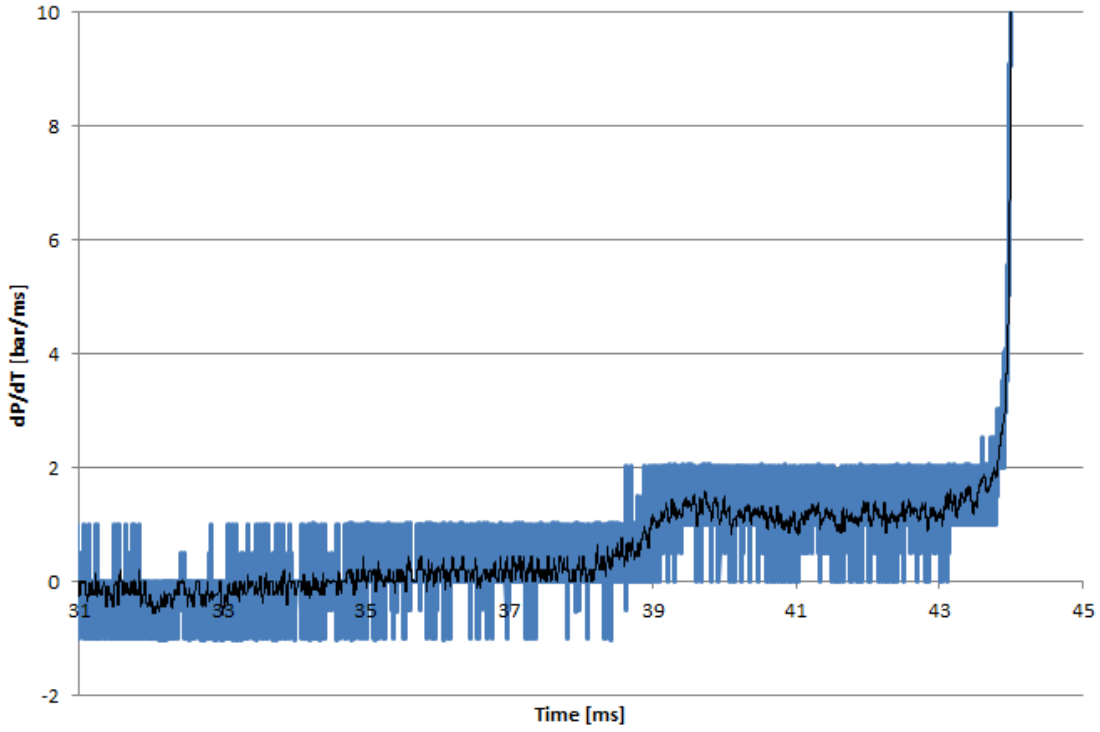

Figure 52: Shows the low temperature pressure rise rate of isooctane with 1000 PPM of additive 2.

The figures clearly show that there is less low temperature heat release when additive 2 is present. This result suggests that the fuel/air mixture will heat up slower and will be colder through the NTC region. This would imply that this additive would increase the critical compression ratio as the mixture is less likely to knock. In the present study, the critical compression ratio tests were re conducted with the refinery gasoline baseline and the repeatability improvements (zero pressure regulator and temperature control loop).

The next tests that were performed on the gasoline additives were high additive concentration (5000 and 10000 PPM) critical compression ratio tests. It should be noted that the data for these additives were acquired on different days. During this time off, there was a software issue that developed, which resulted in the critical compression ratio of the base fuel to be different. However, this problem was known during testing, so the base fuel was tested both days, and the critical compression ratio of the base fuel with additive can be compared to base fuel on each day. The first day consisted of testing additive 1b and additive 2. The results can be seen in Figure 53.

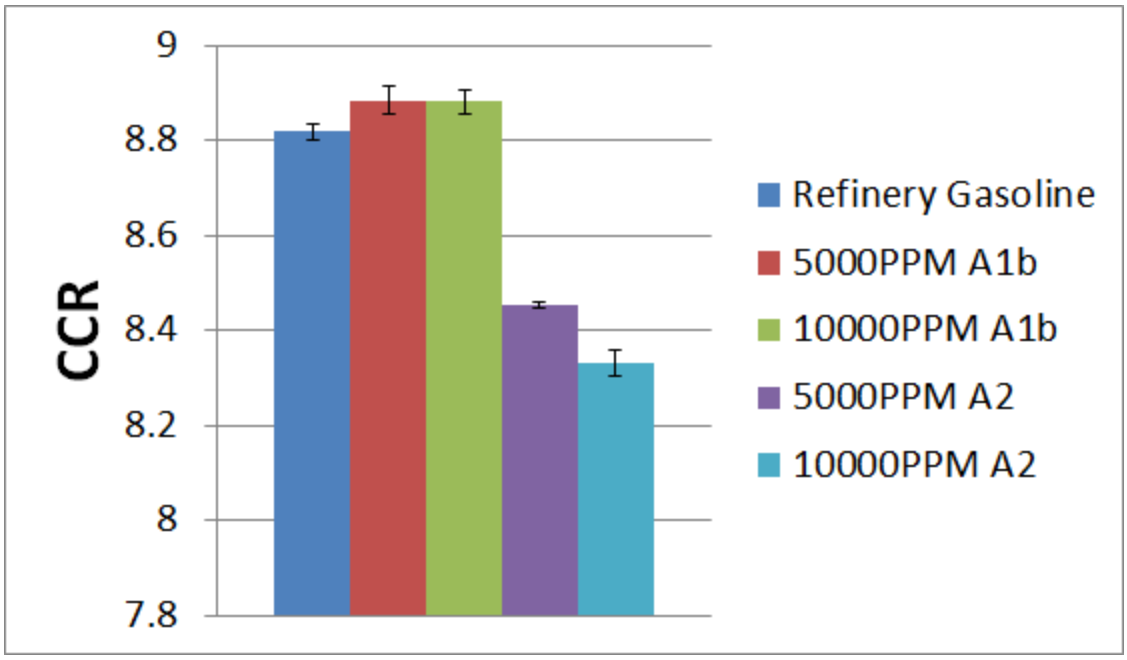

Figure 53: Impact of additive 1b and additive 2 on the critical compression ratio of refinery gasoline.

The first day, additive 1b and 2 were tested. This test followed typical critical compression ratio procedure. It can be seen that additive 1b appears to have a slight positive impact on the critical compression ratio. However, it must be noted that the equivalence ratio control problems that have been mentioned still persisted. This resulted in some cycles having very large knock value while other cycles did not experience a knocking event. So these knocking intervals tended to average to the same value that the other cases did. However, the other cases experienced knock at a more consistent rate. The baseline refinery gasoline had a critical compression ratio of just over 8.8. When additive 1 was added to the fuel, the critical compression ratio increased slightly too nearly 8.9. This is a very minute change. Although the critical compression ratio is higher, this did not translate into a large efficiency increase as discussed below. For additive 2, the critical compression ratio dropped to nearly 8.4 for the 5000 PPM case and to 8.3 in the 10000 PPM case. These results strongly suggest that additive 2 has a

negative impact on the critical compression ratio. This result is contrary to the RCM heat release analysis discussed above and in more detail in (Boissiere, 2016).

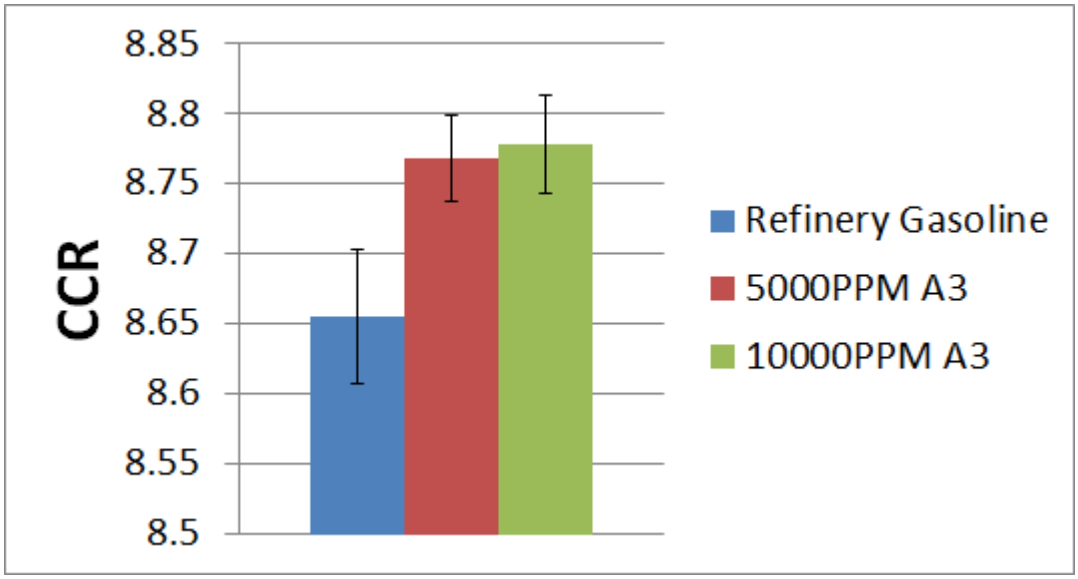

Figure 54: Impact of additive 3 on the critical compression ratio of refinery gasoline.

On the second day, the critical compression ratio of additive 3 was tested. In much the same way as additive 1b, additive 3 slightly increased the critical compression ratio by a magnitude of 0.1. Additive 1b increased the critical compression ratio by the same amount. The data Table 9 is a comparison of the power output and other parameters of the engine while the engine was knocking at KI=20. This table is of importance because the values follow the same trend when the engine is not knocking but at different compression ratios. For example, for baseline refinery gasoline at a compression ratio of 8, there will most likely be no knock (KI<1), and the engine operation will be steady. But if the compression ratio is increased to 8.1, then the engine will display slight knock (KI approximately equal to 2). If 10000 PPM of additive 3 is added to the refinery gasoline, the knock might cease (KI<1). So comparing the fuels at the point just before knock will show the maximum power output of the engine when knock is not present. The thought in comparing the fuels when the engine is experiencing heavy knock is the same as the compression ratio is varying between the tests. Although the engine will output less power

when it is not knocking, the relationships between the base fuel and the additive cases are thought to remain intact. Table 9 shows how each additive changes the engine output metrics from the refinery gasoline base fuel.

Table 9: Shows the percentage change that each additive has on the base fuel.

All values are in %	5000a1b	10000a1b	5000a2	10000a2	5000a3	10000a3
Avg. Peak Loc.	-1.1	0.5	-5.0	-1.4	4.2	5.2
Avg. NMEP	0.4	-0.1	0.5	-1.0	-0.1	-0.7
Brake Thermal Efficiency	0.4	-1.3	-1.0	-1.8	0.6	0.5

It is important to keep in mind that the equivalence ratio of the additive 1b case fluctuates more than the other cases, so might explain the variation in the data. For example, in terms of the peak pressure location data, the 5000 PPM case resulted in advancement of the peak pressure location, while the 10000 PPM retarded the location of the peak pressure. For additive 2, the brake thermal efficiency decreases with increased concentration of the additive. Additive 2 increases the NMEP for 5000 ppm but decreases for 10000 ppm. This result is explained by the variation in fuel flow observed during these tests. As for the average peak pressure location for additive 2, there is the largest change between the 5000 PPM case and the 10000 PPM case as compared to the baseline. The 5000 PPM case exhibits a 5% advance of the location of peak pressure, which suggests that this additive promotes knock. This large extreme advance in peak pressure location is not observed for the 10000 PPM additive 2 case, but this can again be attributed to the slightly lower equivalence ratio that the 10000 PPM case experienced during testing. For additive 3, the positive attributes were seen in the location of peak pressure as well as the thermal efficiency. The location of peak pressure clearly shows how the additive delayed the onset of knock and as the location of peak pressure was delayed 4.2% versus the baseline fuel for the 5000 PPM case and 5.2% for the 10000 PPM case. Although the NMEP was slightly

lower than the base fuel, this can again be attributed to a slightly lower fuel flow rate. The engine efficiency increase at this specific condition was shown to be about 0.5 percent. This is a small increase, which is only slightly greater than the thermal efficiency error values that were found from the uncertainty testing. This result suggests that there may be a slight benefit to using additive 3 when compared to pure refinery gasoline, but further testing of the additive at different engine conditions will be needed to verify these results.

The final test that was conducted with the gasoline fuel additives was the lean limit test. These experiments were conducted by changing the fuel flow rate while maintaining the same air flow. For this testing, the engine was reconfigured such that ambient air was used. The air was heated prior to entering the venturi tube. This modification was made so that the small air flow surges that were observed in the air intake while using the building air set up were eliminated. The engine is highly unstable when operating at lean conditions so it was necessary to eliminate as many factors that could contribute to the engine instability as possible.

The test plan for these experiments was to test all of the additives in the highest concentration (10000 PPM) in the refinery gasoline blend and to compare the results to the baseline. The equivalence ratio was reduced by 0.04 between each point and two separate sweeps were done for each fuel and additive combination. The engine conditions are tabulated in Table 10.

Table 10: Engine conditions use for lean limit testing of gasoline fuel additives.

Engine Conditions	
Equivalence Ratio	Vary
Ignition Timing	23 °BTDC
Compression Ratio	7.5
Intake Pressure	Ambient (≈86kPa)
Intake Temperature	45°C
Base Fuel	Refinery Gasoline

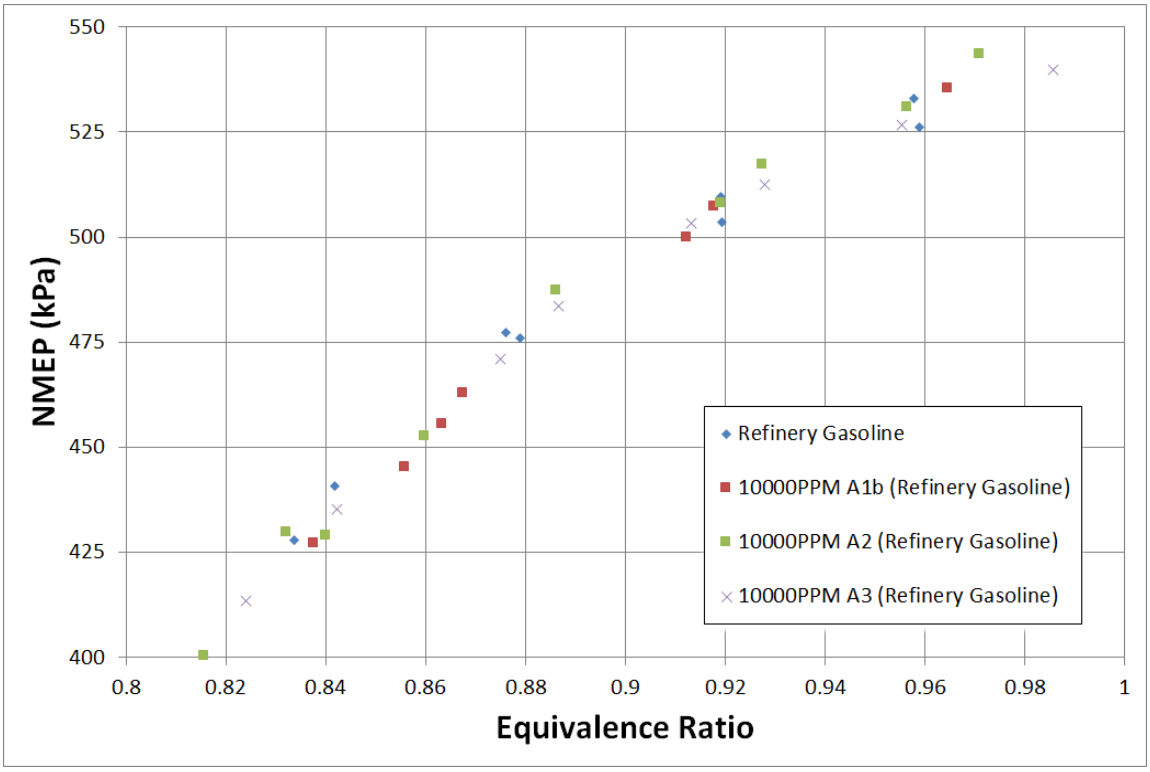

Figure 55: Shows how NMEP changes with equivalence ratio from 0.98 to 0.82.

Figure 55 is a plot of NMEP versus equivalence ratio for all of the additive cases. Clearly, none of the additives resulted in increases in NMEP at decreased equivalence ratios. All of the points fall directly along the same downward trend, with no outliers. Similar results

were found for all of the major engine conditions such as peak pressure, location of peak pressure, brake thermal efficiency and mass fraction burned (MFB 0-10 and MFB 10-90). However, there is slight separation in the engine stability data such as the NMEP COV. Since the average NMEP value is not changing between the cases, the difference must stem from the difference of standard deviations of the data. So, a larger COV value, in this case, is the direct result of a larger standard deviation and thus a more inconsistent engine. Figure 56 is a plot of NMEP COV versus equivalence ratio.

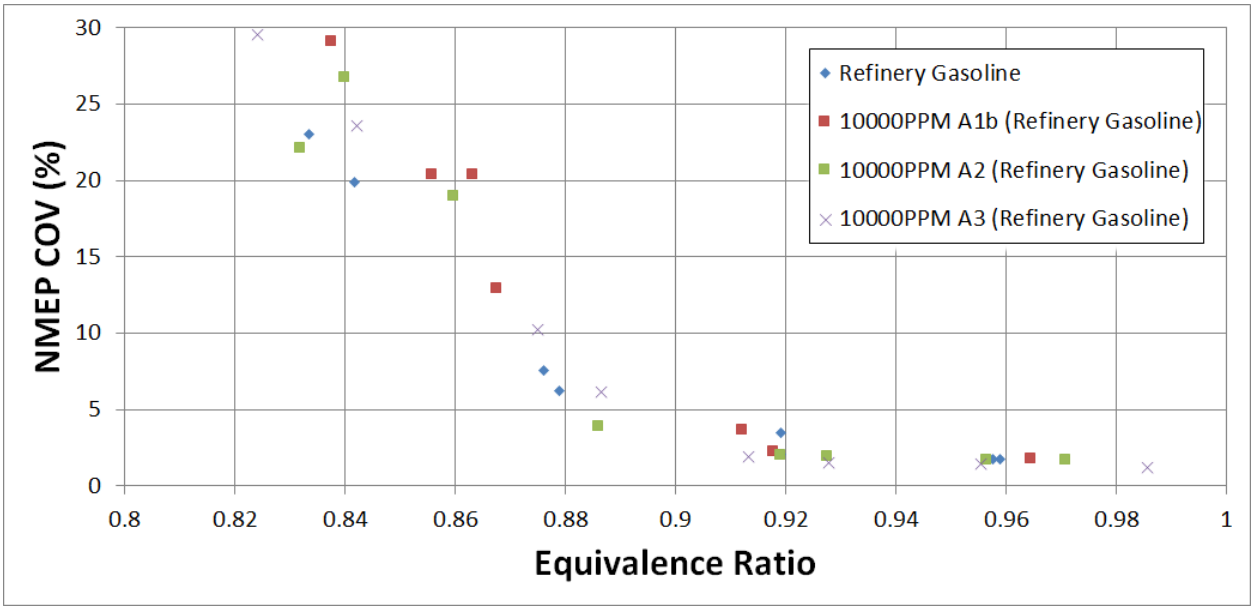

Figure 56: Shows how NMEP COV changes with equivalence ratio. Misfire begins to occur between an equivalence ratio of 0.86 and 0.88. Misfire has a drastic impact on NMEP COV.

Figure 56 shows that the NMEP COV values as a function of equivalence ratio are similar for the baseline and the additives, but there are slight differences as the lean limit is approached. In the published literature [48], there is a method of lean limit definition in which a semi-arbitrary point is chosen, such as NMEP COV = 10%, and a horizontal line is drawn. Then, a linear interpolation is done between the first point below and the first above this horizontal line for each of the additives. The point at which the additive linear fit lines cross the horizontal NMEP COV line, is defined as the lean limit. Figure 57 is a plot of this technique.

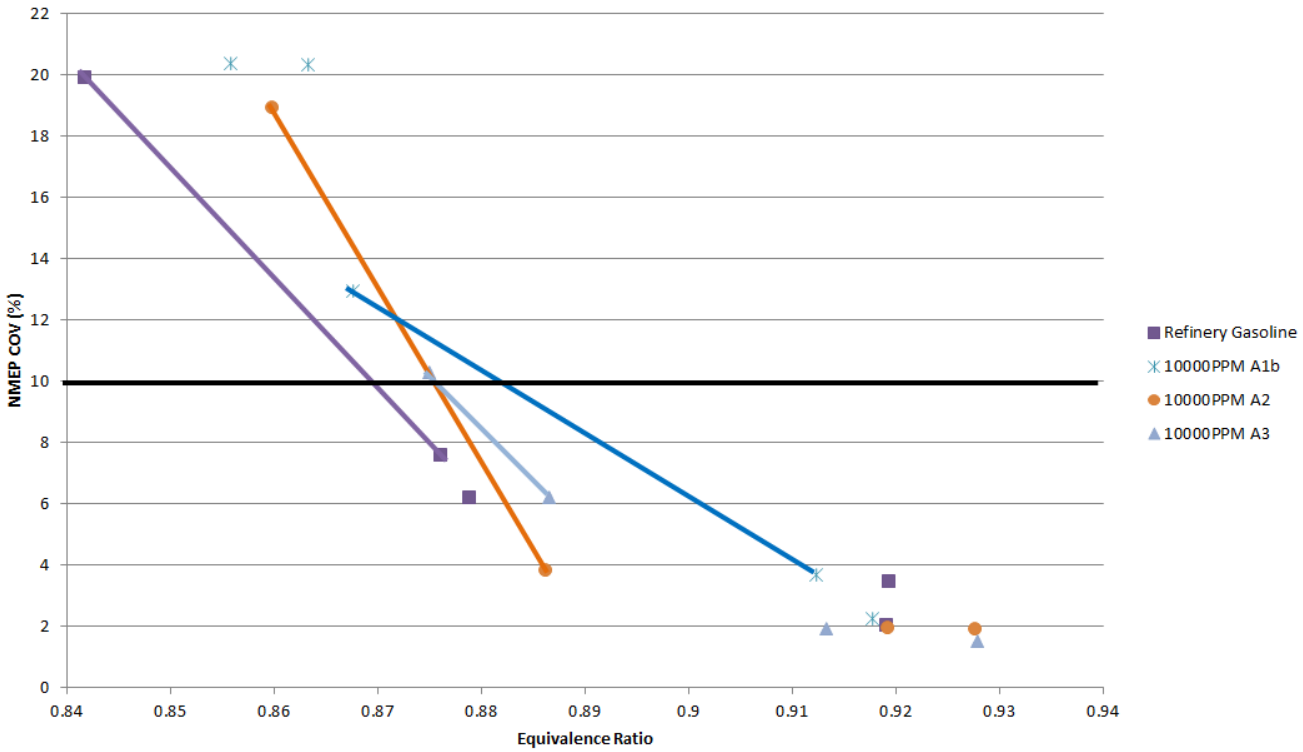

Figure 57: Shows how a linear interpolation method can be used to determine the lean limit.

Based on this method, the results suggest that the additives slightly increase the lean limit, which not a desirable effect. The purple line represents the baseline refinery gasoline. If the additives were to increase the lean limit, all of the other lines would cross the NMEP COV = 10% line to the left of the purple line, but this is not the case. The baseline condition, by this metric, has a lean limit at an equivalence ratio of 0.87, while the both additives 2 and 3 have a lean limit at equivalence ratio of 0.875 and additive 1b has a lean limit at an equivalence ratio just above 0.88. This result indicate that the additives have a slightly negative impact on the lean limit. Although these differences are very small, it can be concluded that the additives do not extend the lean limit. These data are not entirely conclusive as there was only one engine condition that was tested. The method for defining the lean limit is not perfect, and the sample size and difference are both small. Nevertheless, in this case, the additives appear to show a negative trend.

Although the linear interpolation is a good starting point for data analysis, the linear interpolated lines intersect, so the determined effect on the lean limit depends on the point at which the lean limit is defined. So, an additional analysis method was used in which a polynomial was fit to the NMEP COV vs. equivalence ratio data. This analysis shows nearly the same lean limit values (where each curve crosses the NMEP COV = 10%). However, this technique results in a consistent ranking of lean limit for each fuel , regardless of the choice of critical "lean limit" of 8%, 10%, or 12% NMEP COV. The polynomial technique is shown in Fig. 58.

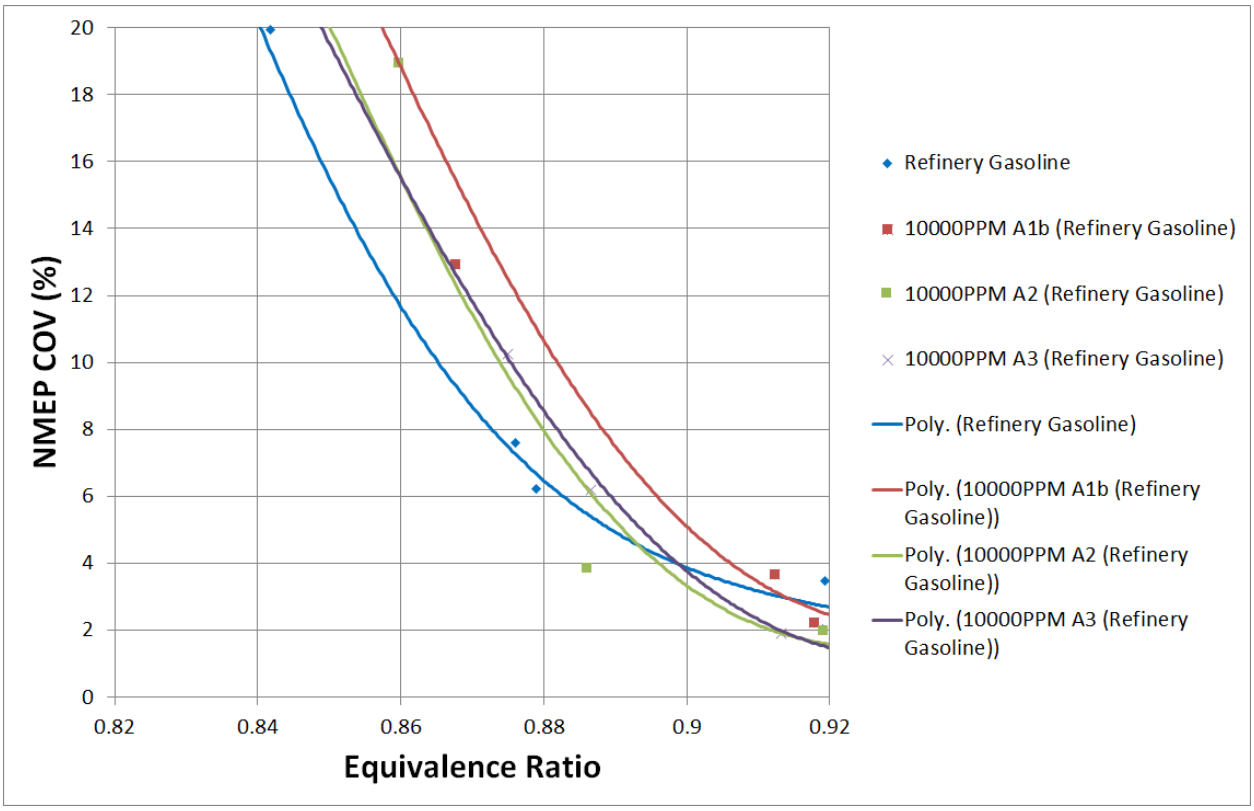

Figure 58: Polynomial fit method can be used to determine the lean limit. The point where the curve fit lines cross the NMEP COV = 10% line are deemed the lean limit of the fuel.

Fitting the data with a polynomial curve fit again shows the same trend that the additives increase the lean limit. The values that are found (when the lean limit is defined by the NMEP COV =10%) are nearly identical.

In an effort to better define how the gasoline fuel additives affect the lean limit, another equivalence ratio sweep was done. This sweep had a smaller window as the equivalence ratio only varied between 0.84 and 0.9, so there is a higher density of points at equivalence ratios at which the NMEP COV begins to increase dramatically. All of the engine conditions were held constant from the previous lean limit testing.

Figure 59 reflects that pinning down the equivalence ratio of the additive 1 case was not done. The baseline refinery gasoline points have a much tighter spread than the additive 1 case. At an NMEP COV of 6% and 4%, there are five additive 1 points that line up horizontally over a range in equivalence ratio of 0.86 to 0.9. Even though this equivalence ratio range is much larger than the range that was observed for the baseline, the additive is not tending to extend the lean limit as the points generally overlap.

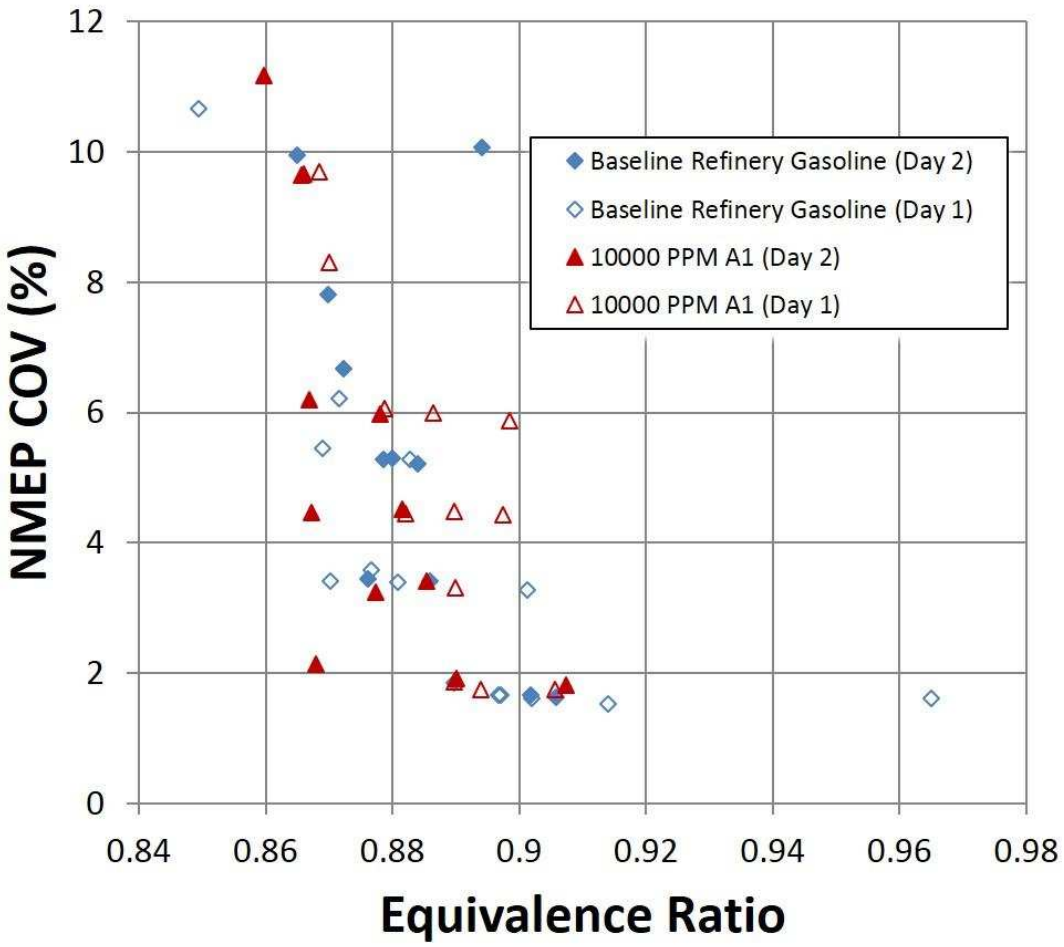

Figure 59: NMEP COV versus equivalence ratio for the baseline refinery gasoline and additive 1. The additive causes large fluctuations in the AFR control which makes pinning the equivalence ratio down difficult. This is represented by the Additive 1 points lined up horizontally.

Figure 60 shows how the presence of additive 2 in 10000PPM concentrations affected the lean limit of the refinery gasoline. Additive 2 does slightly extend the lean limit. This is initially seen at the onset of sharp NMEO COV increase, shown in Fig. 60, at an equivalence ratio of 0.88. The points with additive 2 have a NMEP COV of 2% while the baseline refinery gasoline has an NMEP COV of 3%. The additive delays the onset of NMEP COV increase. Also, at an equivalence ratio between 0.86 and 0.88 and an NMEP COV between 4 and 6%, the additive 2 points are leaner than the baseline refinery gasoline points. This indicates again that additive 2 is positively impacting the lean limit.

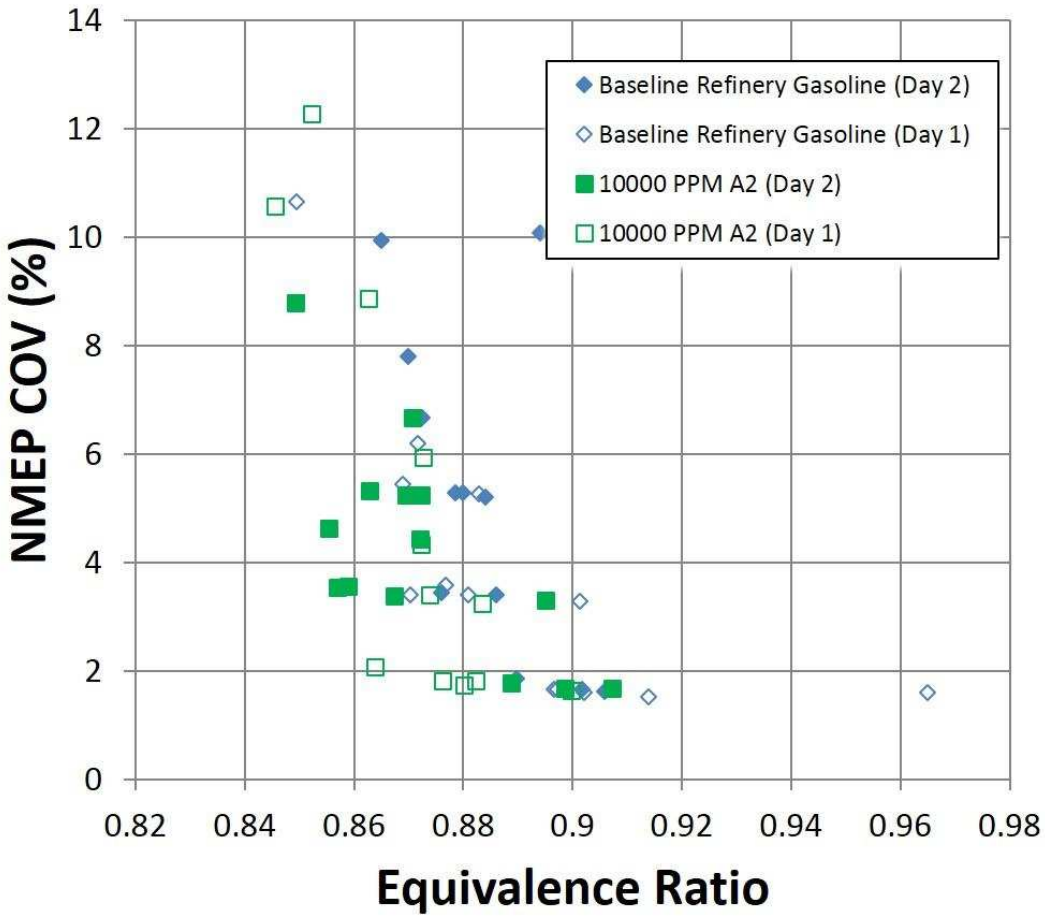

Figure 60: NMEP COV% versus equivalence ratio comparison between the baseline refinery gasoline and additive 2 in 10000PPM concentration.

Figure 61 shows the impact of additive 3 on the lean limit. Although additive 3 does not show the same initial extension of lean limit that additive 2 does (equivalence ratio of 0.88 in Fig. 60), additive 3 shows a consistent difference around the equivalence ratio between 0.85 and 0.86 mark. The additive case and the baseline case show the same rapid increase in NMEP COV% trend but the increase happens for the additive case at leaner conditions. This trend is repeated consistently over both testing days and for all of the points. This is conclusive that additive 3 has a positive impact of extending the lean limit.

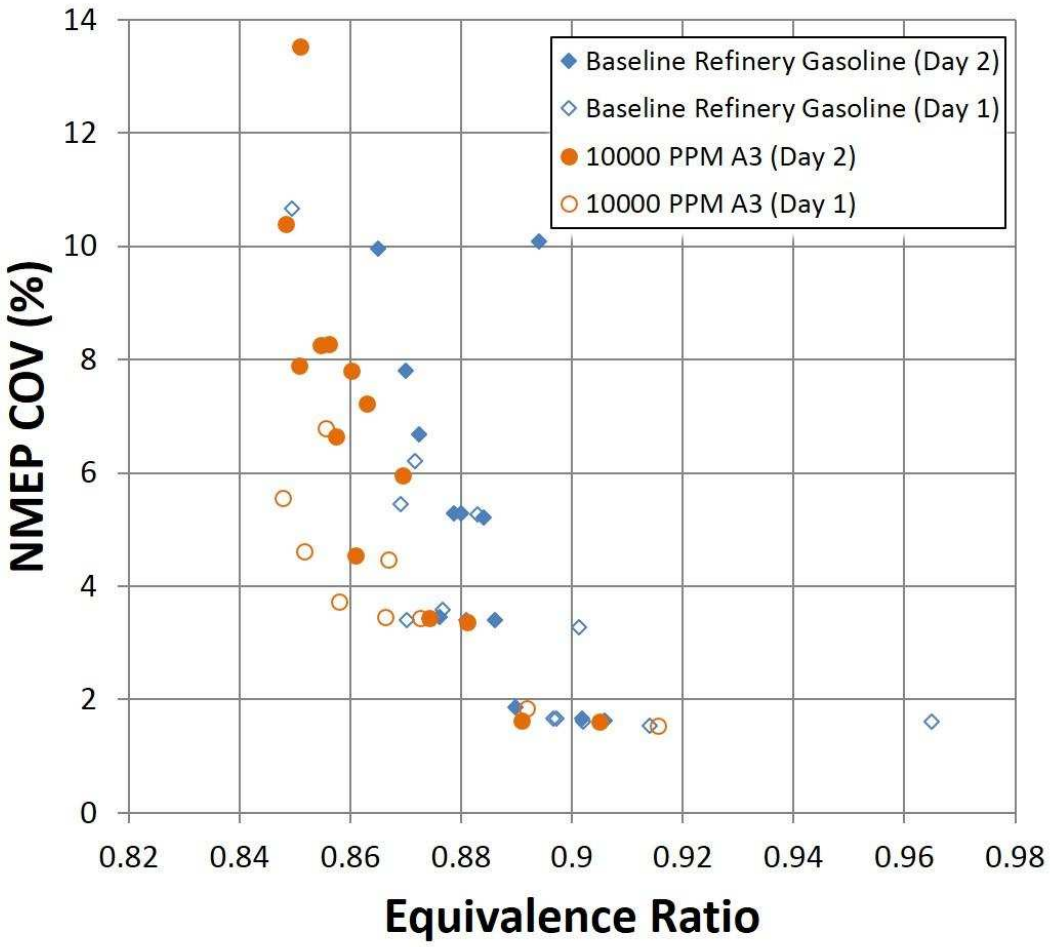

Figure 61: NMEP COV% versus equivalence ratio for additive 3. Additive 3 extends the lean limit.

3.2 Natural Gas Additive Results

The primary goal of the natural gas testing was to find a liquid additive that would extend the lean limit. For the initial tests, the liquid additives were added to the engine intake using the low flow atomizing nozzle. This method was used because it allowed for quickly adjusting the mol% liquid additive, which allowed for additive concentration sweeps to be conducted quickly. The experimental procedure started at 0% additive and then increasing percentages of additive were added to the fuel/air mixture until the knock integral of the engine reached 40. The mol% percent that caused the knock integral of 40 was considered the maximum mol% that would be tested in the engine. Five data points were then taken between 0 mol% and the maximum mol%.

A sample plot of knock integral versus mol% for NM and DTBP additives are shown in Fig. 62. DMM additive was not tested because it could not be controlled with the Ex-air nozzle because the DMM destroyed the internal O-rings. EHN is also not shown on this plot because the maximum mol% EHN that could be injected into the fuel stream before condensation occurred was 0.01% and at this concentration there was no effect on knock.

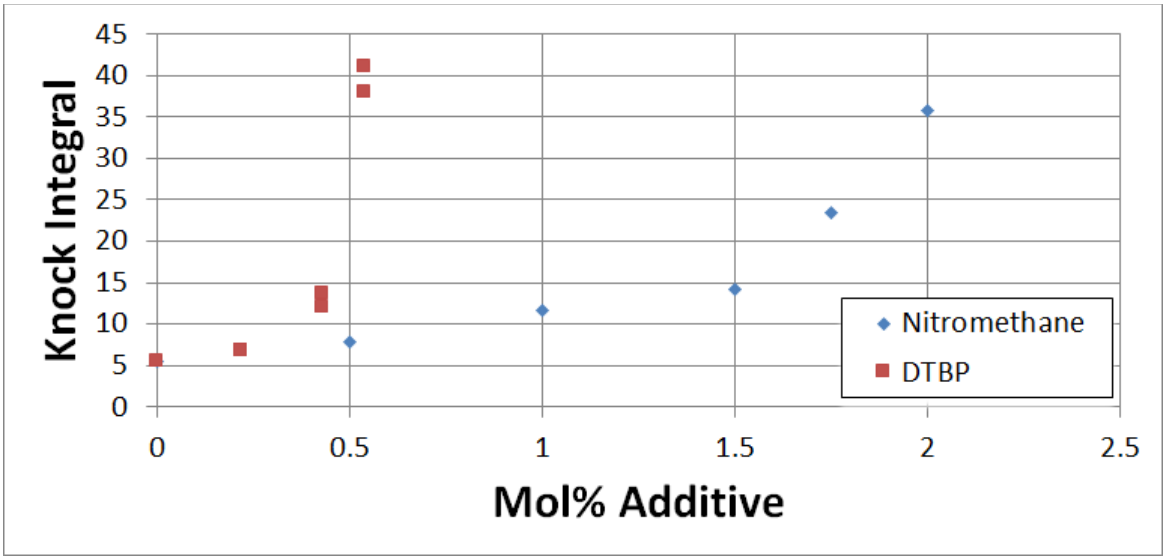

Figure 62: Knock integral versus additive mol% for natural gas fuel additives. The additives cause knock when in high concentrations.

The main objective of natural gas testing was to lower the lean limit of the engine while still producing the same power. To test the additive effectiveness at achieving this goal, equivalence ratio sweeps were performed. These tests aimed to keep NMEP constant at 1000 kPa. To accomplish this goal, the fuel flow rate was held constant for all tests and the air flow rate was increased, thereby decreasing the equivalence ratio. Initially, the lean limit was defined as the point at which the peak pressure COV reached 11. When this definition of lean limit was used, there were only slight differences between the baseline and additive cases, as can be seen in Figure 63.

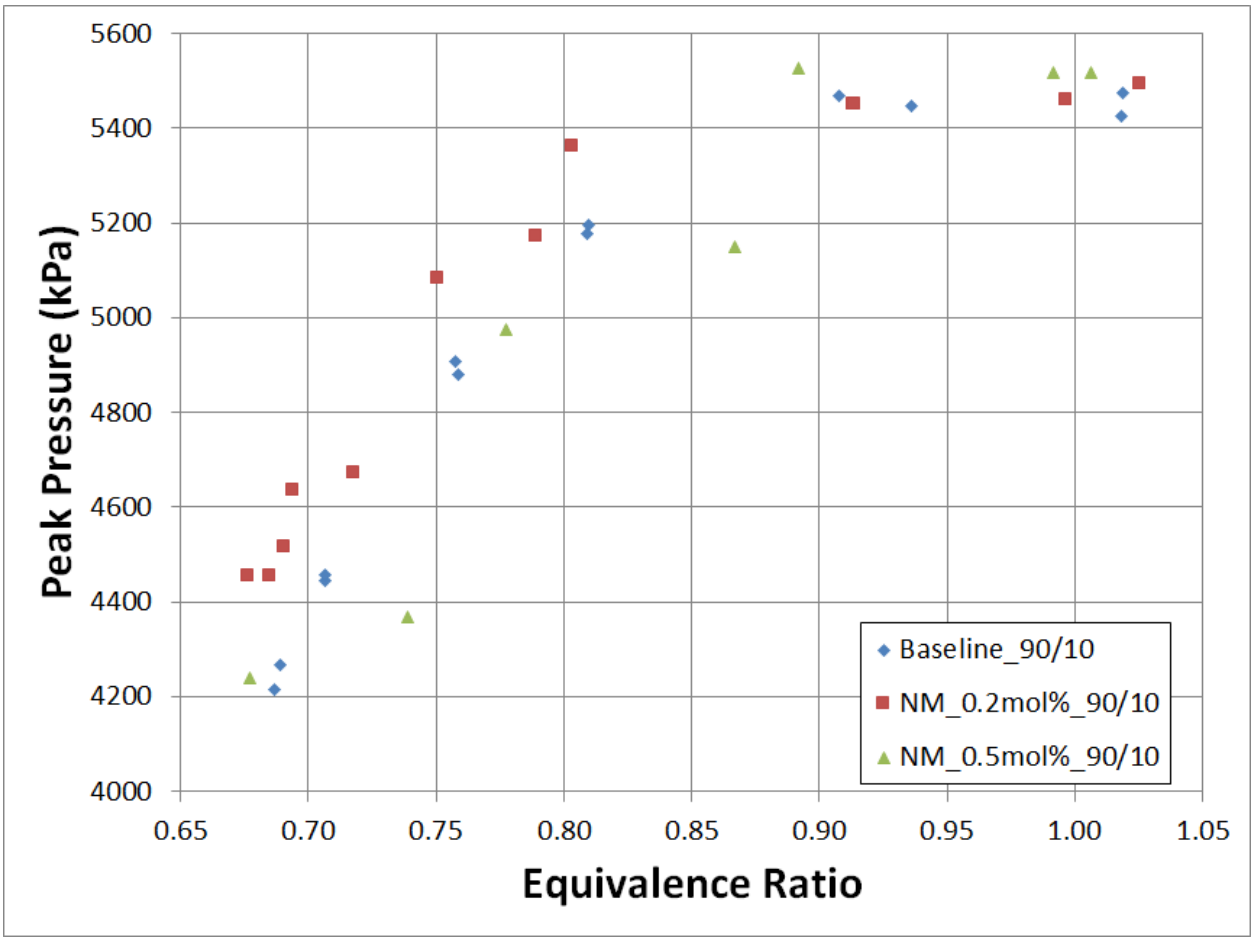

Figure 63: Peak pressure versus equivalence ratio for methane and methane with additive.

Figure 63 shows how the equivalence ratio affected peak pressure while NMEP was held constant. These tests were terminated when the peak pressure COV was 11. This plot shows that

it was difficult to decipher between the baseline and the additive points. So, this is the point where it was decided to change the base fuel from 90% methane/10% ethane to pure methane. This choice was made because ethane is more reactive than methane, so there was a chance that the effect of the additives was masked by the presence of the ethane. Also, instead of defining the lean limit based on peak pressure COV, the engine was operated until it could no longer hold load, which showed how lean each mixture could operate. A sample of cycle-to-cycle NMEP is shown in Fig. 64 for the baseline methane case to demonstrate how the engine output power varies with equivalence ratio.

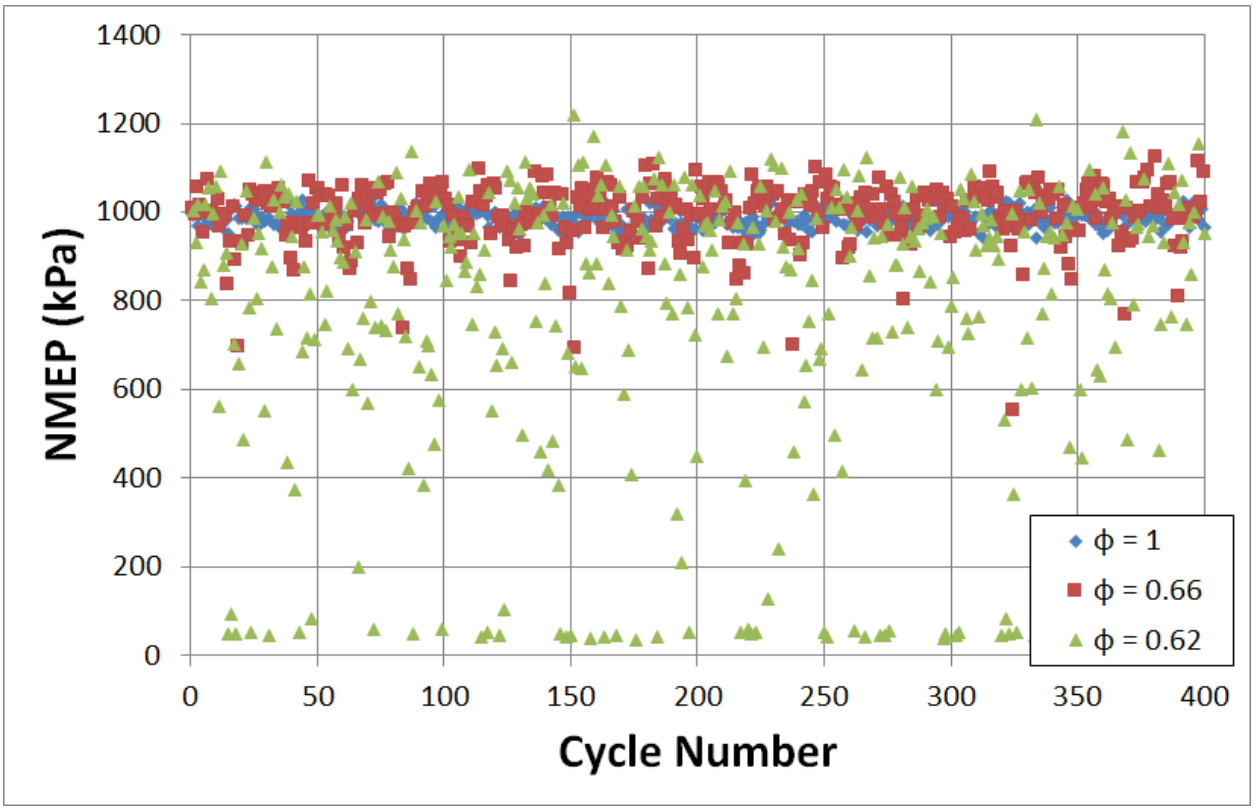

Figure 64: Shows how cycle-by-cycle NMEP changes with different equivalence ratios. There is a large different between the 0.66 points and the 0.62 points.

Figure 64 shows how the cycle-to-cycle NMEP changes during an equivalence ratio sweep. When the equivalence ratio is close to 1, the cycle-to-cycle standard deviation of NMEP is low and close to the target of 1000 kPa. As the mixture gets leaner, the cycle-to-cycle variation

in NMEP increases. This increase continues until, at some point, there is not enough fuel present to sustain flame propagation. At this point, the engine begins to misfire and the engine cannot hold load, as represented by the green triangles in Figure 64. Even at stoichiometric conditions, the NMEP oscillates over the sample because both fuel flow and airflow are controlled by PID loops. These loops are constantly correcting to hold the specified equivalence ratio. The result is that some cycles have a higher equivalence ratio than desired and some cycles have a lower equivalence ratio than desired. This control system performs well when the engine is holding load but starts to falter when the engine does not have consistent combustion. This problem arises because the fuel and air flow rates are controlled using the exhaust constituents. The result is that there are large variations in equivalence ratio when there is not consistent combustion.

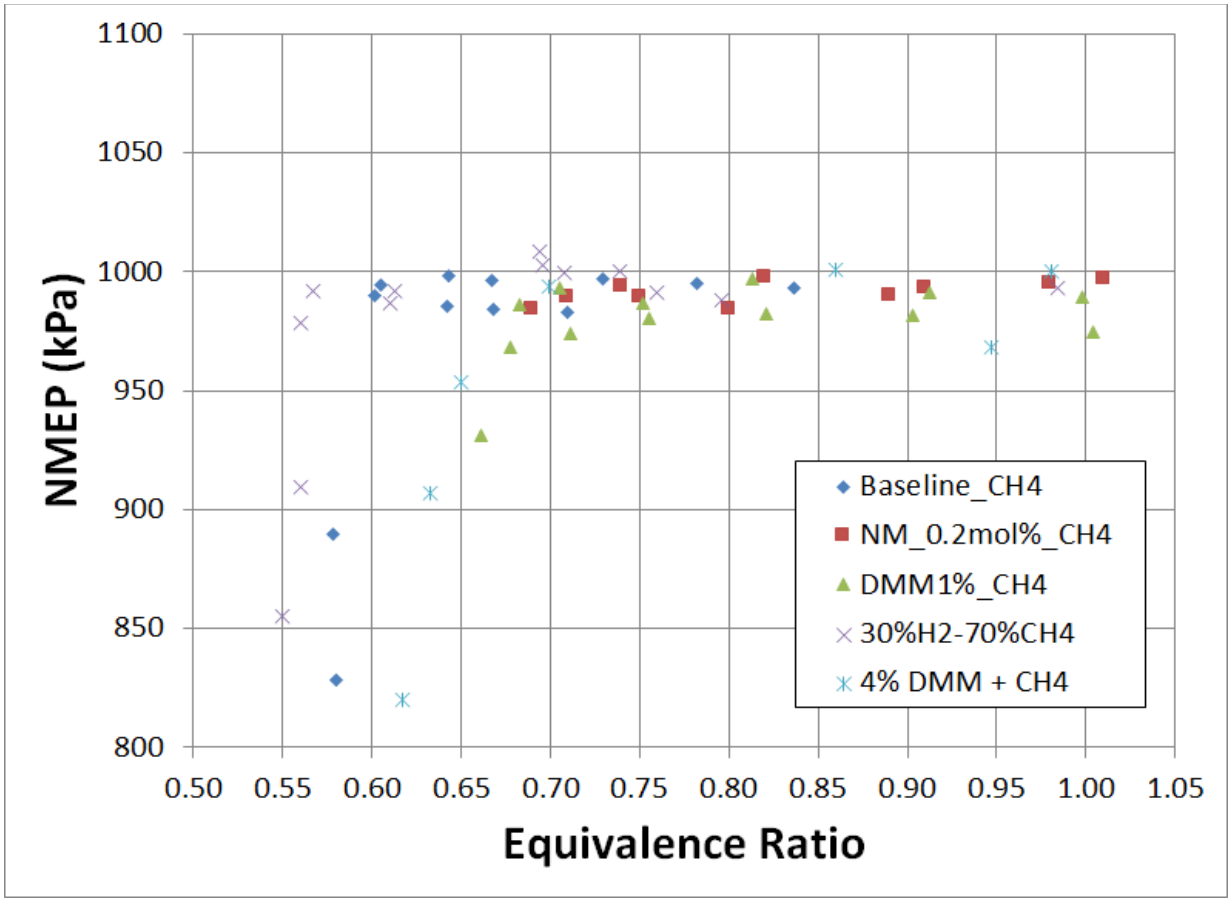

Figure 65: NMEP versus Equivalence Ratio. The hydrogen additive allows the engine to hold load at leaner conditions while the other additives tend to richen the point at which the engine can hold load.

Figure 65 is a plot of NMEP versus equivalence ratio for a methane baseline and methane plus additive fuel blends. This plot illustrates how the fuel additives affect engine operation at lean conditions. Running pure baseline methane allowed for the engine to hold an NMEP of 1000 kPa above an equivalence ratio of 0.61. Traditionally, hydrogen (H_2) has been used as a natural gas fuel additive and this plot shows that the addition of 30% hydrogen into the fuel stream allows the engine to operate leaner, extending the lean limit to 0.57. This testing aimed to find an additive that would act in natural gas in much the same way as H_2 does.

The novel additives do not show the same behavior at lean conditions as hydrogen. When 1 mol% DMM was added to the fuel, the engine could only hold load at an equivalence ratio above 0.68, and at 4 mol% DMM the leanest operable equivalence ratio was 0.7. Based on these results, it can be concluded that DMM is not an additive that is capable of extending the lean limit of natural gas.

Nitromethane was tested at a concentration of 0.2mol% for this study. Again no lean limit extension qualities were found. There were no test points taken when the engine was unable to hold load when nitromethane was the fuel additive. However, the following three plots help to show that the lean limit of the methane and nitromethane was realized.

Figure 66 shows how the average peak pressure changes over an equivalence ratio sweep. If the minimum operable equivalence ratio is taken from Figure 65, and those same minimum equivalence ratios are compared in terms of average peak pressure, it is found that the engine could not hold load if the average peak pressure was below 3500 kPa. The minimum operable peak pressure for the baseline, 30% H_2, 4% DMM and 1% DMM are 3750, 3950, 4230 and 3790 kPa, respectively. When 0.2% nitromethane is operated at an equivalence ratio of 0.69, the location of peak pressure is 24°ATDC and the average peak pressure is 3790 kPa, which is at the

tail end of the range that all other combinations failed. This peak pressure information in conjunction with the average peak pressure location as seen in Fig. 67 complete the picture. Figure 64 shows average location of peak pressure versus equivalence ratio. For methane, the latest location of peak pressure observed was 24 degrees after top dead center (ATDC). In this case, when the location of peak pressure is 24 degrees ATDC, the engine is still holding load, as this occurs at an equivalence ratio of 0.61. As the equivalence ratio is decreased further, the engine is no longer able to hold load and the location of peak pressure advances as the location of peak pressure of a misfire stroke is at TDC. When 0.2% nitromethane was tested, the location of peak pressure was also 24°ATDC. In fact, 24°ATDC was latest that any of the additive cases were able to hold load The final component of this analysis resides in Figure 68 which compares peak pressure COV versus equivalence ratio. This plot shows that as the mixture is leaned, the peak pressure COV increases faster for the nitromethane case when compared to pure methane case. The nitromethane case became unstable at richer conditions than the pure methane. The combination of analysis of the NMEP, peak pressure, location of peak pressure, and peak pressure COV versus equivalence ratio combine to show that nitromethane, in the tested concentration, is not an additive that is capable of decreasing the operable lean limit as desired.

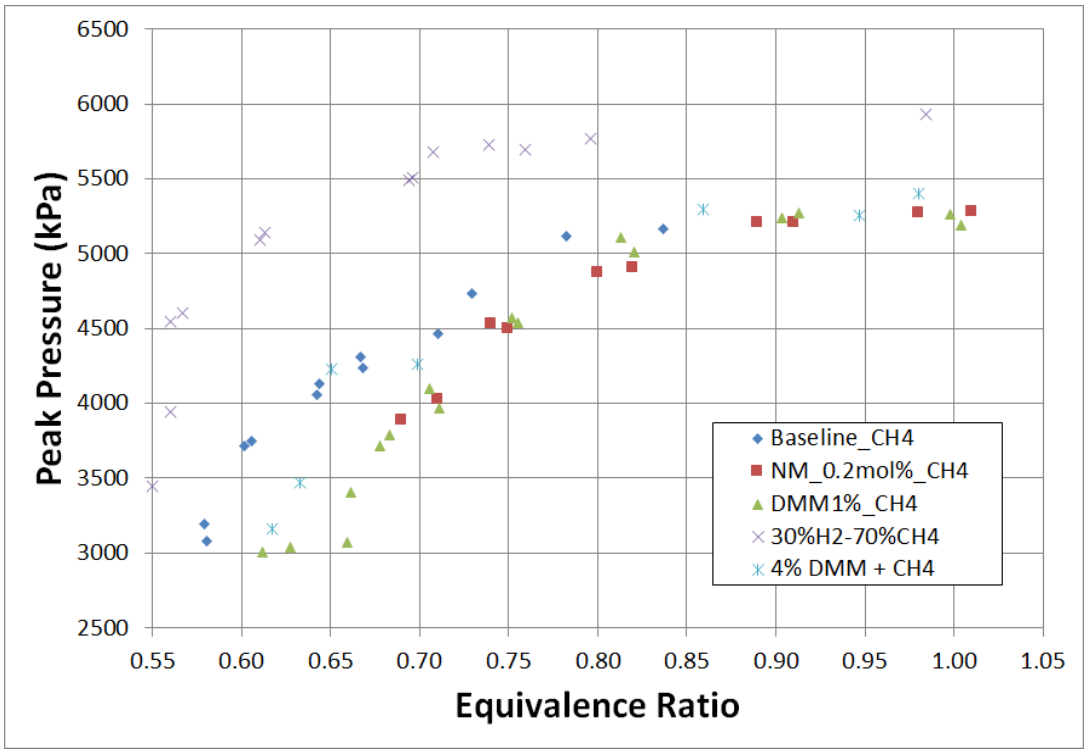

Figure 66: Peak pressure versus equivalence ratio for comparison pure methane and all additives. Hydrogen increases the peak pressure. The novel fuel additives decrease the peak pressure at lean conditions.

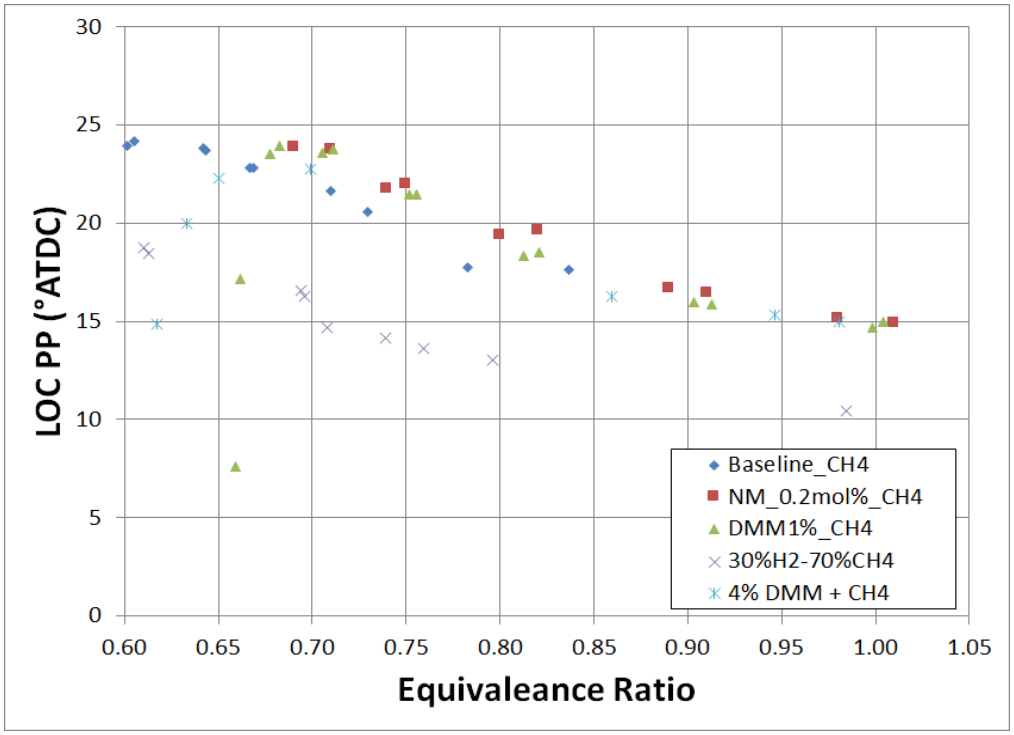

Figure 67: Location of peak pressure versus equivalence ratio comparison for pure methane and all additives.

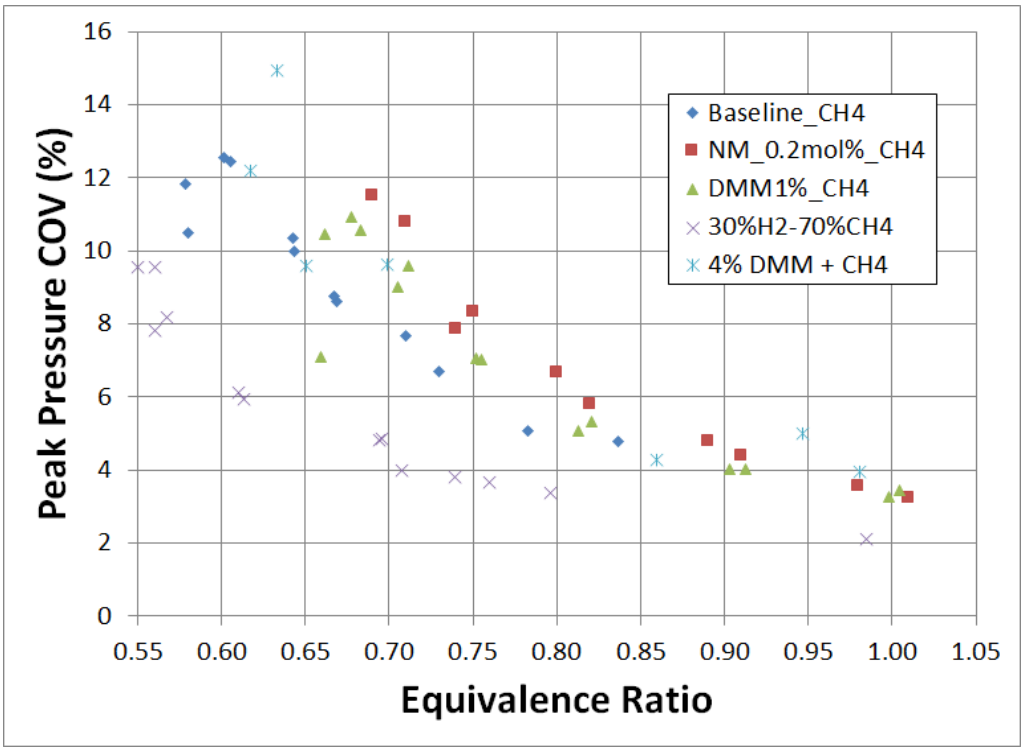

Figure 68: Peak pressure COV versus equivalence ratio comparison for pure methane and all additives.

EHN and DTBP were not tested during the lean limit testing. EHN was not tested because the vapor pressure was too low for the bottle mixing method to be used. EHN has a vapor pressure of just 27Pa at 20°C. Due to liquid condensing on the inside of the bottle, this vapor pressure results in a maximum mol% of EHN to be 0.002% when the bottle is filled to 160 psi, which is not a sufficient amount of the fuel to be tested. In order to a higher mol% additive, the bottle pressure would have to be less than 160 psi. This causes an insufficient fuel pressure so the engine would not be able to run. Similarly to EHN, DTBP was eliminated from consideration also because of a low vapor pressure. Although DTBP has a vapor pressure that is orders of magnitude higher than that of EHN, the maximum amount that could have been used was 0.1mol%. This number was deemed too small to have a significant effect on lean limit.

Emissions data were collected in tandem with pressure data during the natural gas equivalence ratio sweeps. Data was collected with both a 5-gas analyzer and a Fourier transform infrared spectroscopy (FTIR). The following section analyses additive effect on emissions.

The total hydrocarbon (THC) brake specific emission is shown in Figure 69. This figure shows the publicized trend of THC emission plots (Verma, 2016). At low equivalence ratios, there is a lot of THC because there is a lot of excess air, so the fuel may not burn completely, leaving behind THC. At richer conditions, equivalence ratios of approximately 0.65 to 0.95, there is a relatively flat portion. This exists as the there is an advantageous ratio of fuel to air, so the fuel burns more completely thus leaving behind less THC. At rich conditions, an equivalence ratio over 1, the THC concentrations begin to take off. This is because there is not enough air for the fuel to burn and thus the fuel never reacts.

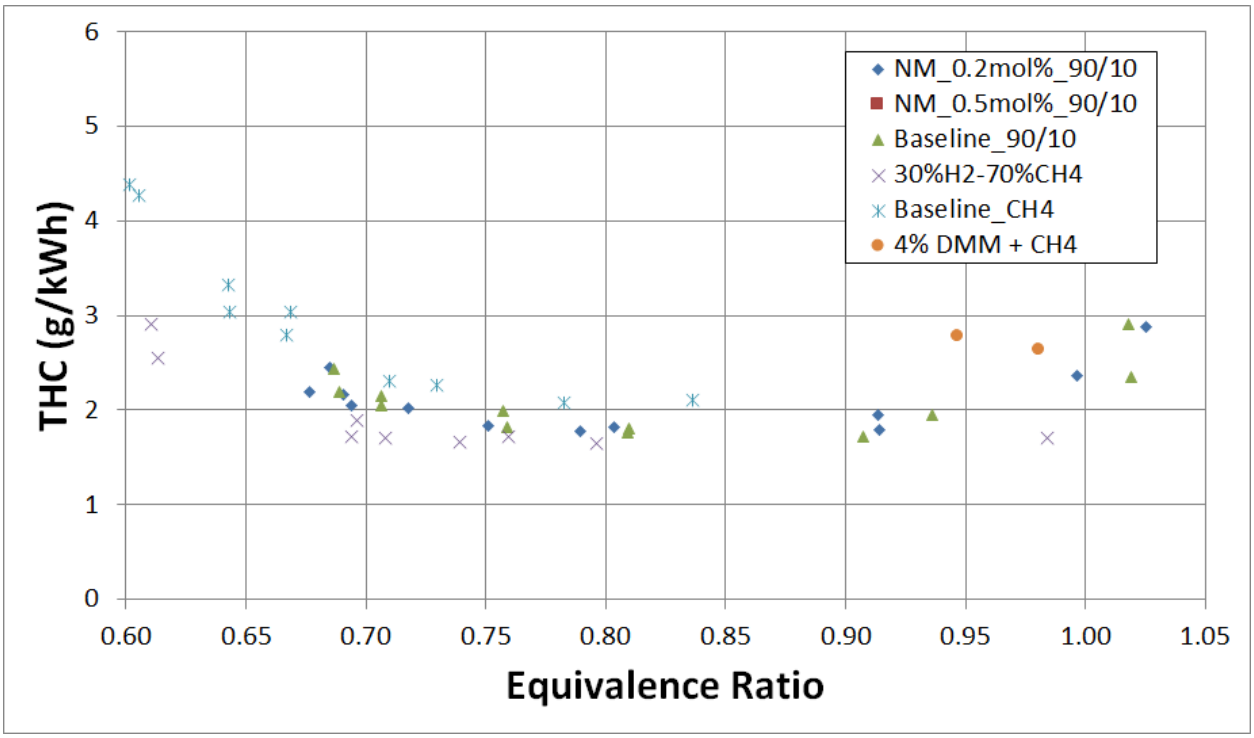

Figure 69: THC production versus equivalence ratio comparison for pure methane and all additives.

Figure 69 shows how the additives had negligible effect on the THC output. This would imply the additives did not contribute to a more complete burn of the fuel and air mixture. Ideally, if the additives were to have a positive impact on THC emission output then the additive curves would be below the baseline curve. This plot can be misleading as the square points use a baseline that is 90% methane and 10% ethane while the diamond points use a baseline that is pure methane. It is important to show that nearly all of the 90% methane and 10% ethane baseline points are overlapping, which indicates no discernable additive effect. While analyzing the blue diamond 100% methane points, the hydrogen reduced THC output when compared to the baseline.

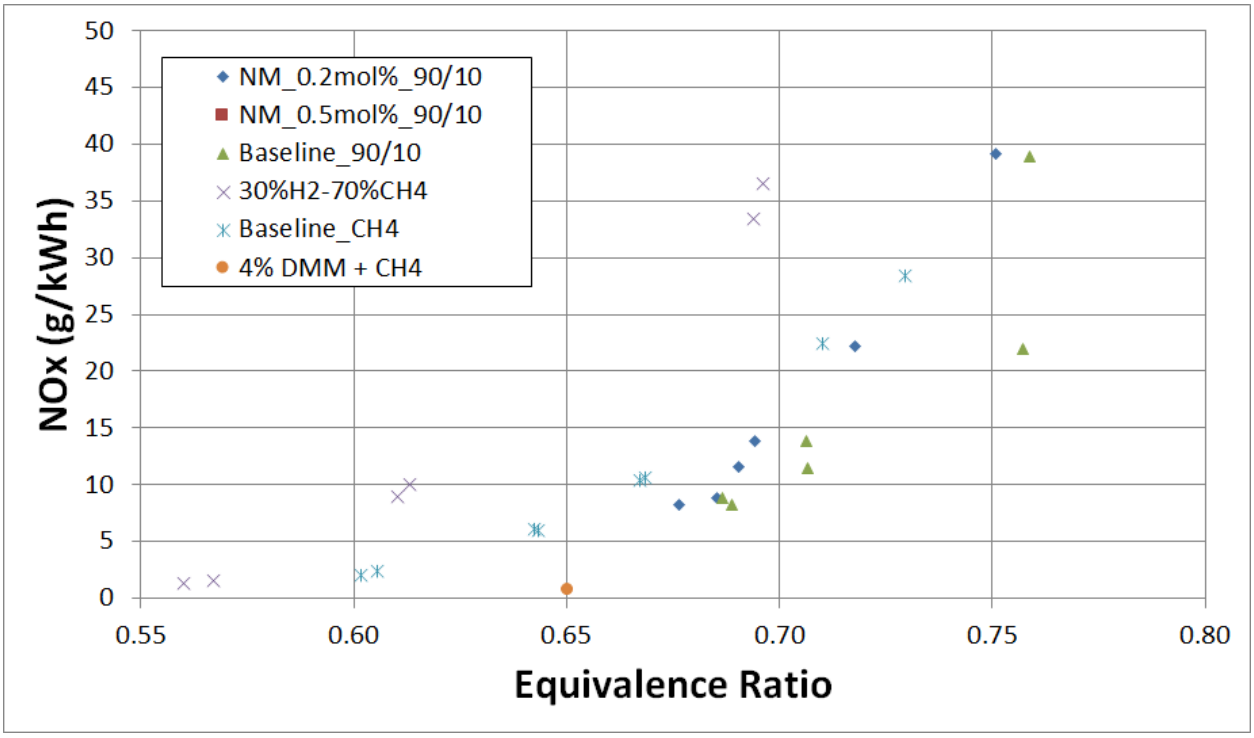

Figure 70: NOx production versus equivalence ratio comparison for pure methane and all additives.

The NO_x data for the equivalence ratio sweeps are shown in Figure 70. NO_x is more prevalent when combustion is very hot as it takes a lot of energy to break an N_2 bond. It then follows that the hydrogen case would produce more NO_x as that flame burns hotter. However,

the hydrogen case makes up for this added heat release as the hydrogen allows for leaner operation. During lean operation the mixture in the cylinder is significantly cooler as the excess air proves to just cool the mixture as it does not react. This means that when the engine is operating at an equivalence ratio of 0.7, the hydrogen case will have the highest NO_x pollution. For example, at an equivalence ratio of 0.61 the hydrogen case emits 8.91 g/kWh of NO_x while the baseline methane case only emits 2.34 g/kWh of NO_x. Conversely, when the engine is operating as lean as possible, the hydrogen will emit the lowest NO_x pollution as there is significantly more excess air that serves to cool the mixture in the cylinder. At the leanest conditions with which the engine can hold load, the hydrogen case emitted 1.37 g/kWh of NO_x while the leanest case of the baseline methane emitted 2.07 g/kWh of NO_x; this represents a 34% reduction in NO_x emittance. Therefore, the hydrogen case clearly shows a reduction in NO_x emittance when the engine is operating lean.

For the novel additives, the effect on NO_x formation and emission is minimal. The 90/10 points with and without additive tended to produce slightly less NO_x emission when compared to the methane baseline. The difference between the 90/10 baseline and the 90/10 with nitromethane case is small, but the additive case tends to produce more NO_x emissions than the baseline case. This can be explained through chemical composition. The baseline fuel is composed of purely of carbon and hydrogen. However, when nitromethane is present, the fuel now contains nitrogen. This nitrogen is single bonded to an ethyl group and an oxygen, and double bonded to an oxygen. See Figure 26 for a molecular diagram. The C-N bond is much weaker than the N_2 triple bond found in pure nitrogen. Therefore, this molecule provides a simpler path to creating NO_x as all that has to happen is the C-N bond must be broken and NO_2

will be created. This molecule is a very strong molecule and will not be broken at the temperatures that are found in a cylinder during lean engine operation.

This additive analysis shows that there is a slight drawback to using nitromethane as an additive to the methane base as NO_x is poisonous to humans. This comes on the heels of the data analysis that the nitromethane increases the lean limit. Under these very specific engine conditions, nitromethane was not effective as an additive that will improve the combustion efficiency and power of an engine operating on natural gas.

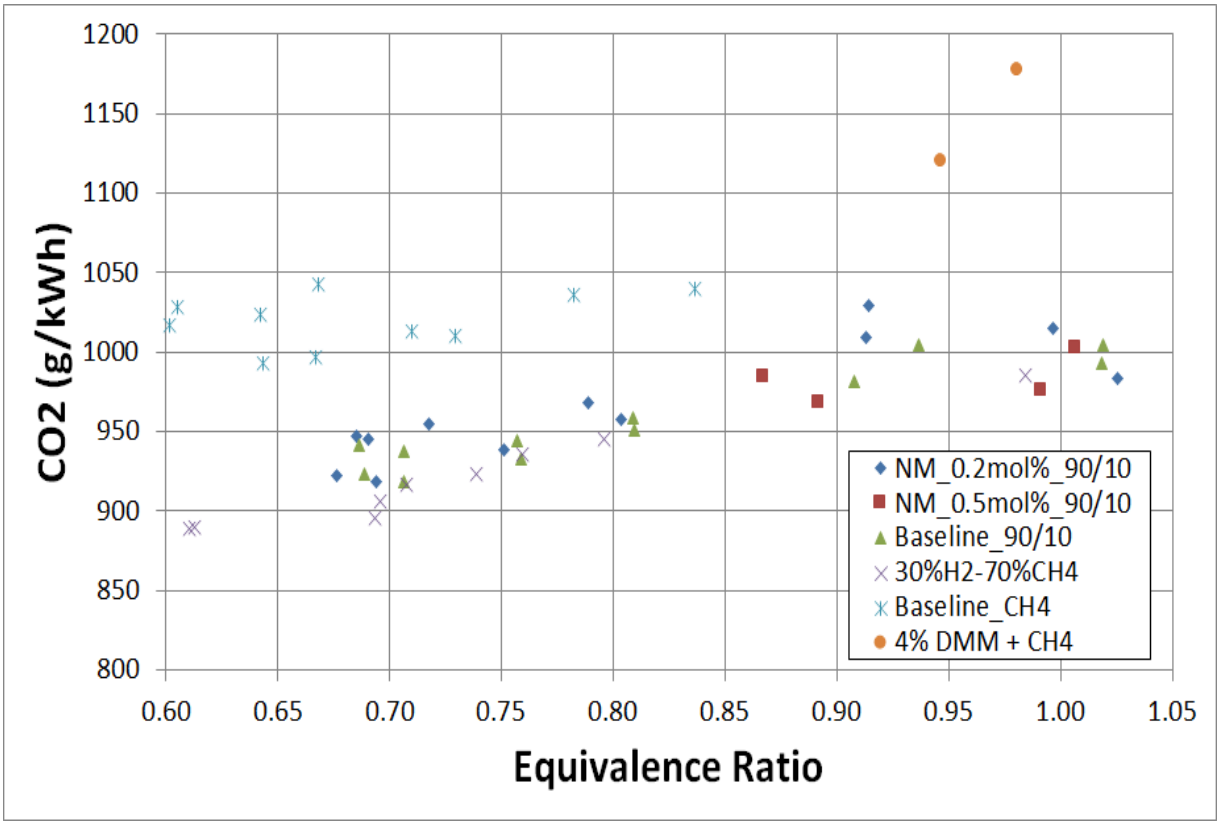

Figure 71: Carbon Dioxide production versus equivalence ratio comparison for pure methane and all additives.

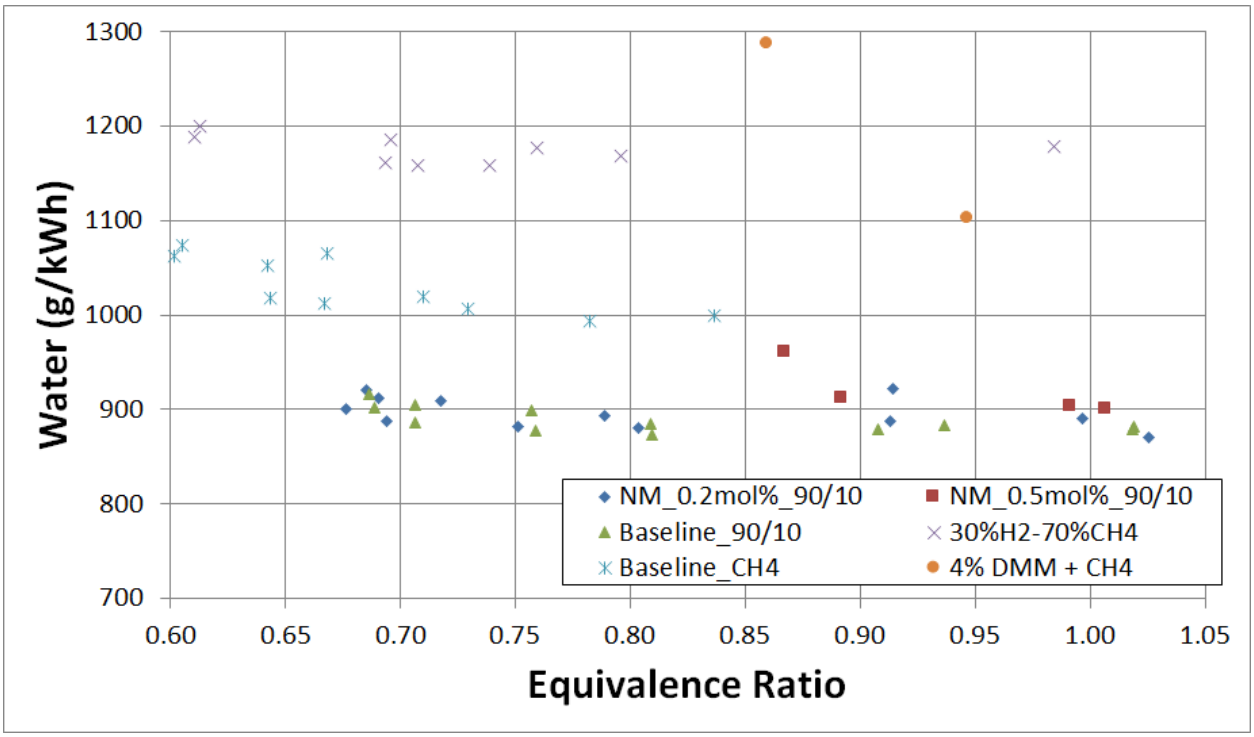

Figure 72: Production of water versus equivalence ratio comparison for pure methane and all additives.

The CO_2 and H_2O charts are analyzed here at the same time as they are both the largest in presence and have ties to each other. The presence of hydrogen significantly affects the amount of CO_2 that is emitted. This is less to the effect the hydrogen has on combustion and more on the fact that the hydrogen is more prone to make H_2O as opposed to CO_2 because hydrogen does not contain carbon or oxygen. Once the initial oxygen atoms split, it just needs to join with two hydrogen radicals. These hydrogen radicals are extremely prevalent as 30 mol% of the fuel is pure hydrogen and the majority of the remaining fuel is also hydrogen. This result is clearly seen from in both the CO_2 and the H_2O plots. Hydrogen seems to help these emissions on all fronts. As far as the new additives go, there is still no separation between the baseline 90/10 case and the additive case. These additives appear to clump around the baseline, which could be a cause of the additives being in too low of concentration to have a substantial impact on combustion

products, and there is not a significant difference between methane and air compared to pure nitromethane.

For the baseline methane condition, there is likely much more CO_2 in the exhaust when compared to the case with hydrogen as there is more carbon in the fuel. When this much hydrogen is added to the base fuel it changes the landscape of the fuel that is entering the chamber. If the fuel were to be entirely hydrogen, then the ideal theoretical exhaust outputs would be H_2O and N_2 and compared to methane where the exhaust products would be N_2, CO_2, and H_2O. This shows why the CO_2 emissions are lower and H_2O emissions are higher when hydrogen is present.

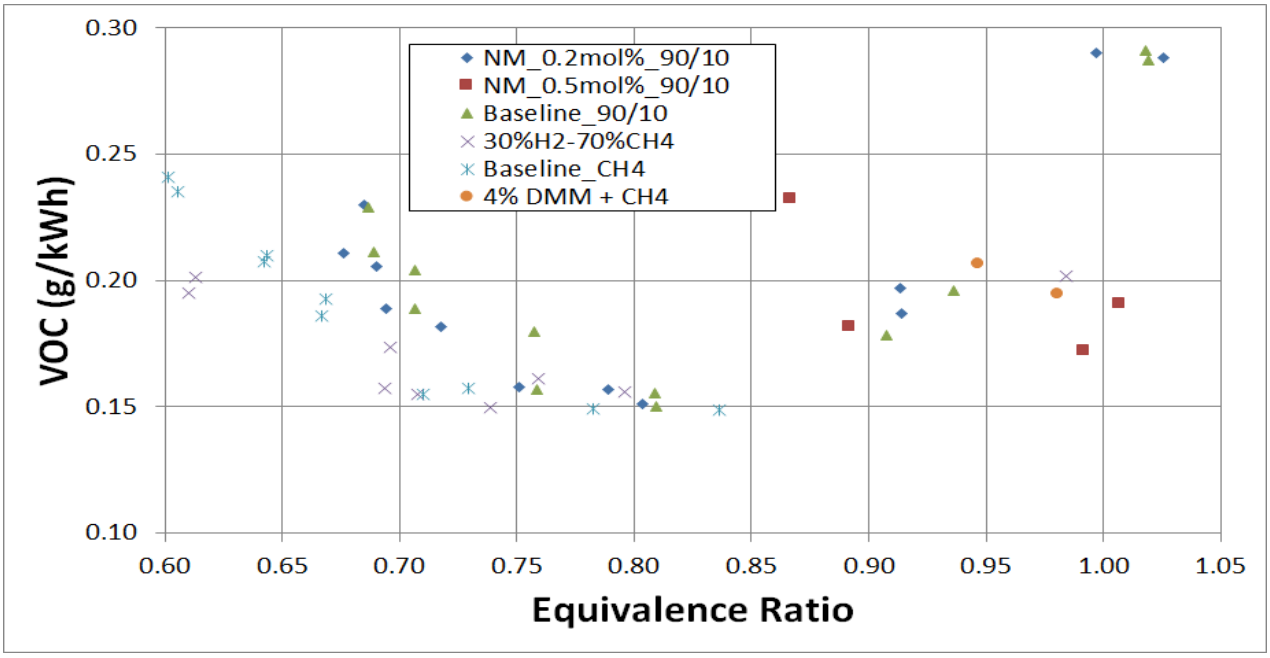

Figure 73: Production of volatile organic compounds versus equivalence ratio comparison for pure methane and all additives.

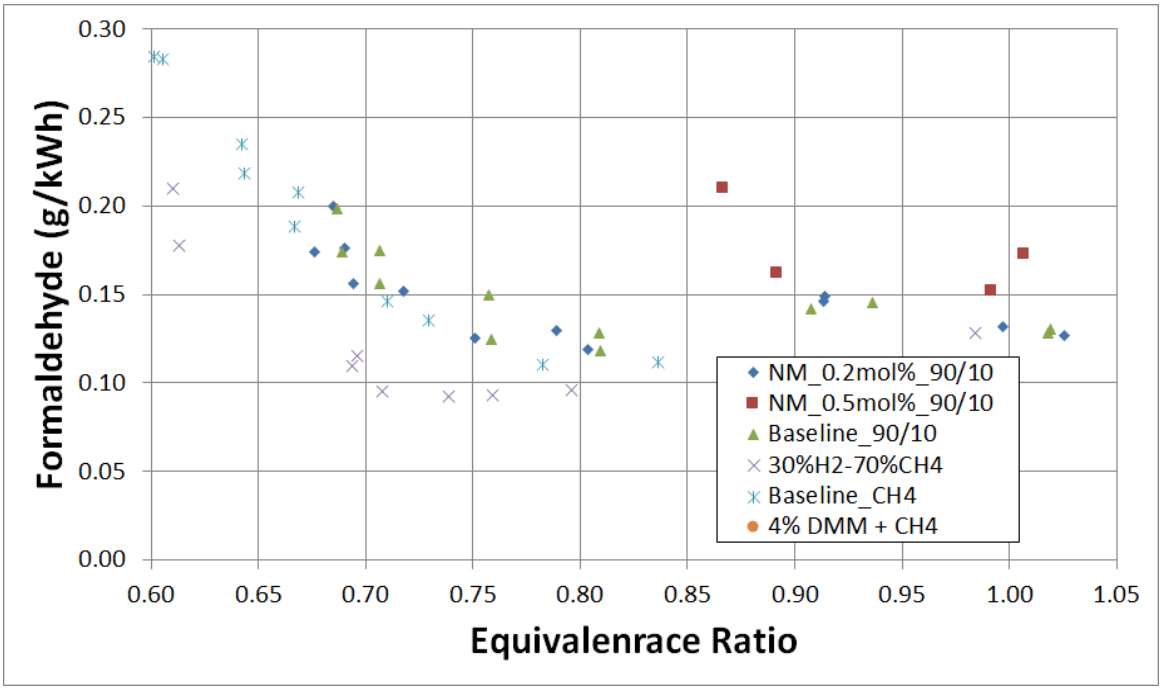

Figure 74: Production of Formaldehyde versus equivalence ratio comparison for pure methane and all additives.

Formaldehyde and volatile organic compounds (VOCs) arre compared at the same time her as they provide the same data structure, have nearly the same values and originate from the same combustion properties. Volatile organic compounds consist of ethylene, propene and propane. These molecules are highly reactive. For the baseline, all the fuel that is put into the engine is in the form of methane (99.99% purity). In order to measure VOC's in the exhaust of the engine these molecules must have been formed in the cylinder or in the exhaust piping. This is in opposition to gasoline type fuels in which long chain hydrocarbons are injected into the cylinder and the incomplete combustion causes the long chain hydrocarbons only being partially devoured into shorter chain hydrocarbons. Both Figure 73 and 74 show that formaldehyde and VOC's increase with decreasing equivalence ratio. This occurs because of the incomplete burning of the fuel and air in the cylinder. For example, a methane molecule may only lose one or two hydrogens which would create a polar molecule, and then combine with another partially combusted polar molecule. If the equivalence ratio were to be closer to stoichiometric than this

molecule would tend to continue to decompose, and it the presence of oxygen would form one CO_2 molecule and two H_2O molecules.

It would be better for engine efficiency if the exhaust products to contain less VOC's and formaldehyde. All of the VOC compounds and the formaldehyde contain higher enthalpy energies, which means that the more VOC's and formaldehyde that is measured in the exhaust the less chemical energy was released during combustion. As seen in Figure 73 and 74, the only additive to show that there is less formaldehyde and VOC's in the exhaust products is hydrogen. This result is only slight. When hydrogen is in the fuel, there are more OH radicals created. The OH radicals are the radicals that are responsible for breaking down the carbon fuel and are the main reason for the creating of H_2O within the cylinder. When hydrogen is in large concentration in the fuel as is when it is used as an additive and there is an excess amount of air, the hydrogen readily breaks apart and releases a lot of heat, which causes the oxygen to decompose. These two separate radicals combine to form OH radicals. These radicals then either recombine with another hydrogen, which either comes from the base methane or from a radicalized H_2. Because OH is prone to scouring hydrogen radicals, the case with a hydrogen is more likely to make water and less likely to make larger molecules such as formaldehyde and VOC's. There is little change between the baseline cases and the novel additive cases. This is the result because of the similarity between the base methane and the additives. The additives are a slightly larger molecule than the base fuel, but they are not long chain hydrocarbons, so they have to go through the same adhesion process to form the larger VOC molecules as the base fuel. Therefore, it is largely unexpected for these additives to contribute to the VOC or formaldehyde formation.

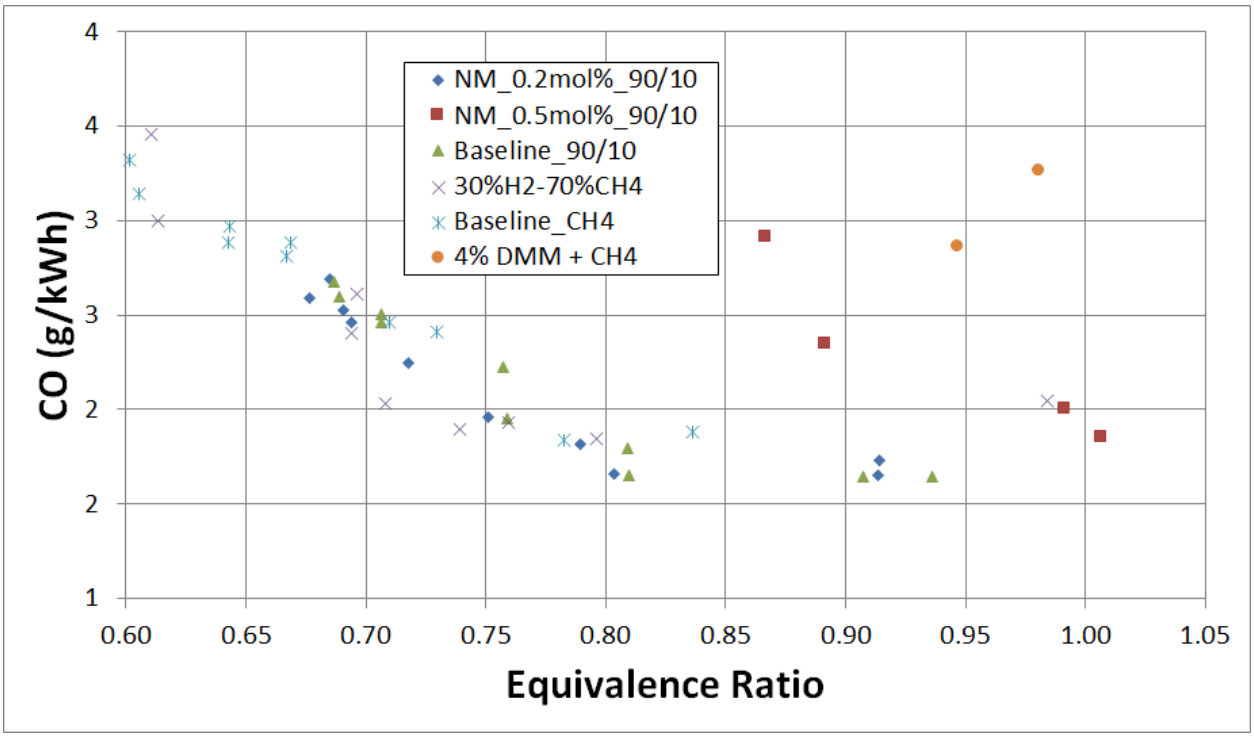

Figure 75: Production of Carbon Monoxide versus equivalence ratio comparison for pure methane and all additives.

Carbon monoxide is fatal to humans. When analyzing Figure 75, it can be observed that all of the data follows the same linear trend from an equivalence ratio around 0.8 to the lean limit. This is consistent across all base fuels and additive combinations; no additive has a large impact on CO emission.

4 Conclusions and Future Work

Natural gas and gasoline fuel additives were tested in a CFR engine. These fuel additives were intentioned to increase power and decrease the lean limit. For the natural gas fuel additives, the primary hypothesis for the fuel additives was that the lean limit would be extended. By holding the power of the engine constant and decreasing the equivalence ratio, this hypothesis was tested and it was concluded that the additives did not have the desired effect. The only fuel additive that showed promise was hydrogen, but this additive is not novel to this research. For the gasoline additives, the hypothesis was that the additives would increase the critical compression ratio, engine power and extend the lean limit. For additives 1b it was found that this additive decreases AFR control, slightly increases the critical compression ratio by 0.5% and does not have a discernable effect on the lean limit. Additive 2 showed a significant decrease in critical compression ratio of 5.5%, had no effect on NMEP and showed lean limit extension. Additive 3 showed an increase in critical compression ratio of 1.4%, showed a decrease of NMEP of 1% and showed lean limit extension. The main conclusions are, additives 2 and 3 show promise as a gasoline additive but need more testing while additive 1b tends to condensate in the fuel.

4.1 Further Engine Improvements and Testing

In continuing with this project, there are many more tests and engine configurations that would need to be used in order to fully classify each additive. Engine power will change with load and speed. Allowing the engine speed to change may show that the additive have a positive effect that at the current engine speed is not observable. The timing between the cycles will increase or decrease, which will affect how long the chemistry has to take place. There is a

possibility that at the relatively slow 940 RPM of the CFR is not utilizing the additive effectively. The CFR has an RPM that is more comparable to a car idling at a stop light than a car that is cruising down the road. So it may be beneficial to test these additives in another engine that has the capability to change speed so that the power can be measured at different speeds as well as being able to see how the engine handles RPM transients with and without the additive. In order to conduct this testing, either the CFR needs to be modified with a Variable Frequency Drive (VFD) or a different engine must be used. A VFD will allow the engine to be removed from the generator frequency which is a powered by the grid. This installation would allow testing for engine stability when there are RPM transients.

The second improvement to the CFR for gasoline testing would be to add a way to change the load. In the current carburetor set-up, the engine operates at maximum load all of the time. The engine pulls in all of the air and fuel that it can every cycle. Putting a throttle valve on the engine intake would allow the operator to restrict how much air and fuel would enter the chamber at a time. However, this set up still comes with restrictions in that the maximum load that the engine can be run at is atmospheric. With the natural gas CFR set-up, the engine has the capability to run at pressures that are greater than the atmospheric pressure. If this were to be made possible for the gasoline set-up there would need to be large scale changes. Most notably, the carburetor would need to be replaced by a fuel injector. The carburetor is naturally aspirated, and the fuel line is open to the atmosphere. This means that if the airline was to be pressurized to above ambient conditions, the fuel would be forced in the opposite direction of the venturi tube and there would be no fuel in the air stream. So a fuel injector would need to be installed. This would be a big project, but would be a much more accurate model of a modern car as all new

commercial cars use a fuel injector and a lot of new cars have a turbo that increases the air pressure in the vicinity of the air intake.

In addition to the changes that could be done for the gasoline system, a few changes would be useful for the natural gas system. For much of the RCM testing, there was a laser used as a spark plug. This is how it was found what the minimum ignition energy of the fuel/air mixture was and that the additives were having an effect. It is well documented that at lean conditions the flame may not propagate due to the fact that there is a lot heat transfer from the flame to the spark plug. This means that the spark plug is quenching the flame kernel within the cylinder. For CFR operation, there was a standard off the shelf spark plug used. This spark plug has a small area between the anode and the cathode, which is not ideal for finding the lean limit. So if there could be a different spark plug used that either increased the volume between the anode and the cathode, or eliminated them altogether (laser) then there would be a more consistent test apparatus with the RCM. Eliminating the spark plug would make for more comparable data.

Further improvement to the engine would include updating the ignition system to allow for more precise ignition timing. Currently the cycle-to-cycle variation in the ignition timing is about 1 crank angle degree. This variation is the reason why the location of peak pressure has such a large COV. Updating this system would lead to more repeatable results and tighter data trends.

Finally, further testing would of course include more additives. Just because none of the eight additives that were tested in this work proved to have a significant effect on engine power and efficiency, does not mean that there is not an additive out there that will. The only way to create a new and improved fuel is trial by fire to find to find the best possible combination.

Bibliography

1. U.S. Department of Energy. Independent Statistics and Analysis from the United States Energy Information Administration (2016). (U.S. DOE, 2016)

2. United States Environmental Protection Agency. Where the Energy Goes: Gasoline Vehicles (2016). (U.S. EPA, 2016)

3. N. Rahmat, A. Abdullah, A. Mohamed. Recent progress on innovative and potential technologies for glycerol transformation into fuel additives: A critical review. Renewable and Sustainable Energy Reviews Volume 14, Issue 3 (2010). (Rahmat, 2010)

4. M. Al-Hasan. Effect of ethanol-unleaded gasoline blends on engine performance and exhaust emission. Energy Conversion and Management V. 44 I. 9 (2003). (Al-Hasan, 2003)

5. R. Silva, R. Cataluna. Effect of additives on the antiknock properties and Reid vapor pressure of gasoline. Fuel 84 (2005) 951–959. (Silva, 2005)

6. D. Splitter, R. Reitz, R. Hanson. High Efficiency, Low Emissions RCCI Combustion by Use of a Fuel Additive. 2010 SAE Int. J. Fuels Lubr. Volume 3 Issue 2. (Splitter, 2010)

7. G. Genchi, E. Pipitone. Octane Rating of Natural Gas-Gasoline Mixtures on CFR Engine. 2014 SAE International doi:10.4271/2014-01-9081. (Genchi, 2014)

8. S. MacAllister, J. Chen, y. Fernandez. Fundamentals of Combustion Processes. 2011. ISBN: 978-1-4419-7942-1. (MacAllister, 2011)

9. A. Winkler, P. Dimopoulos. Catalytic activity and aging phenomena of three-way catalysts in a compressed natural gas/gasoline powered passenger car. Applied Catalysis B: Environmental 84 (2008) 162–169. (Winkler, 2008)

10. J. Eng. Characterization of Pressure Waves in HCCI Combustion. SAE Technical 2002-01-2859. (Eng, 2002)

11. A. Martins, Rodrigo A. Rocha. Cold start and full cycle emissions from a flexible fuel vehicle operating with natural gas, ethanol and gasoline. Journal of Natural Gas Science and Engineering 17 (2014) 94e98. (Martins, 2014)

12. P. Geng, H. Zhang. Combustion and emission characteristics of a direct-injection gasoline engine using the MMT fuel additive gasoline. Fuel 144 (2015) 380–387. (Geng, 2015)

13. S. Jang, J. Choi. Comparison of fuel consumption and emission characteristics of various marine heavy fuel additives. Applied Energy 179 (2016) 36–44. (Jang, 2016)

14. Schifter, U. González, C. González-Macías. Effects of ethanol, ethyl-tert-butyl ether and dimethyl-carbonate blends with a gasoline SI engine. Fuel 183 (2016) 253–261. (Schifter, 2016)

15. F. Ma, Y. Wang, H. Liu. Effects of hydrogen addition on cycle-by-cycle variations in a lean burn natural gas spark-ignition engine. International Journal of Hydrogen Energy 33 (2008) 823 – 831. (Ma, 2008)

16. G. Verma, Ra. Prasad. Experimental investigations of combustion, performance and emission characteristics of a hydrogen enriched natural gas fuelled prototype spark ignition engine. Fuel 178 (2016) 209–217. (Verma, 2016)

17. J. Ji, S. Lin. Experimental study on initial temperature influence on flame spread characteristics of diesel and gasoline–diesel blends. Fuel 178 (2016) 283–289. (Ji, 2016)

18. F. Ma, Y. Wang. Experimental study on thermal efficiency and emission characteristics of a lean burn hydrogen enriched natural gas engine. International Journal of Hydrogen Energy 32 (2007) 5067 – 5075. (Ma, 2007)

19. N. Rosi, J. Eckert. Hydrogen Storage in Microporous Metal-Organic Frameworks. Materials and Methods (2003) vol 300. (Rosi, 2003)

20. R. Pandey, A. Rehman, R. Sarviya. Impact of alternative fuel properties on fuel spray behavior and atomization. Renewable and Sustainable Energy Reviews 16 (2012) 1762–1778. (Pandey, 2012)

21. M. Pacheco, C. Marshall. Review of Dimethyl Carbonate (DMC) Manufacture and Its Characteristics as a Fuel Additive. Energy & Fuels 1997, 11, 2-29. (Pacheco, 1997)

22. A. Dillon, K. Jones, T. Bekkedahl. Storage of Hydrogen in single-walled carbon nanotubes. Nature (1997) vol 386. (Dillon, 1997)

23. F. Ma, Y. Wang. Study on the extension of lean operation limit through hydrogen enrichment in a natural gas spark-ignition engine. International Journal of Hydrogen Energy 33 (2008) 1416 – 1424. (Ma, 2008)

24. S. Binjuwair, A. Alkudsi. The effects of varying spark timing on the performance and emission characteristics of a gasoline engine: A study on Saudi Arabian RON91 and RON95. Fuel 180 (2016) 558–564.(Binjuwair, 2016)

25. L. Barreto, A. Makihiraa, K. Riahi. The hydrogen economy in the 21st century: a sustainable development scenario. International Journal of Hydrogen Energy 28 (2003) 267 – 284. (Barreto, 2003)

26. A. Maria, W. Cheng. Understanding Knock Metric for Controlled Auto-Ignition Engines. SAE (2013) doi:10.4271/2013-01-1658. (Maria, 2013)

27. R. Sierens, E. Rosseel. Variable Composition Hydrogen/Natural Gas Mixtures for Increased Engine Efficiency and Decreased Emissions. Engineering for Gas Turbines and Power (2000) Vol. 122 / 135. (Sierens, 2000)

28. H. Watson, P. Phuong. Why Liquid Phase LPG Port Injection has Superior Power and Efficiency to Gas Phase Port Injection. SAE 2007-01-3552. (Watson, 2007)

29. D. Wise. Investigation into producer gas utilization in high performance natural gas engines. 2013. Dissertation. (Wise, 2013)

30. J. Anstrom, K. Collier. Blended hydrogen–natural gas-fueled internal combustion engines and fueling infrastructure. Compendium of Hydrogen Energy (2016). (Anstrom, 2016)

31. M. Reyes, F. Tinaut, A. Melgar. Characterization of the combustion process and cycle-to-cycle variations in a spark ignition engine fueled with natural gas/hydrogen mixtures. International Journal of Hydrogen Energy (2015) e1. (Reyes, 2015)

32. M. Ruzal-Mendelevich, D. Katoshevski, E. Sher. Controlling nanoparticles emission with particle-grouping exhaust-pipe. Fuel 166 (2016) 116–123. (Ruzal-Mendelevich, 2016)

33. B. Fan, J. Pan, W. Yang. Effects of hydrogen blending mode on combustion process of a rotary engine fueled with natural gas/hydrogen blends. International Journal of Hydrogen Energy (2016) 1 e1 5. (Fan, 2016)

34. B. Korb, S. Kawauchi, G. Wachtmeister. Influence of hydrogen addition on the operating range, emissions and efficiency in lean burn natural gas engines at high specific loads. Fuel 164 (2016) 410–418. (Korb, 2016)

35. M. Kamil, M. Rahman. Performance prediction of spark-ignition engine running on gasoline-hydrogen and methane-hydrogen blends. Applied Energy 158 (2015) 556–567. (Kamil, 2015)

36. W. Yinhui, Z. Rong, Q. Yanhong, P. Jianfei. The impact of fuel compositions on the particulate emissions of direct injection gasoline engine. Fuel 166 (2016) 543–552. (Yinhui, 2016)

37. V. Pradeep, Shamit Bakshi, A. Ramesh. Direct injection of gaseous LPG in a two-stroke SI engine for improved performance. Applied Thermal Engineering 89 (2015) 738e747. (Pradeep, 2015)

38. M. Nora, H. Zhao. High load performance and combustion analysis of a four-valve direct injection gasoline engine running in the two-stroke cycle. Applied Energy 159 (2015) 117–131. (Nora, 2015)

39. W. Yinhui, Z. Rong, Q. Yanhong, P. Jianfei, L. Mengren, L. Jianrong, W. Yusheng, H. Min, S. Shijin. The impact of fuel compositions on the particulate emissions of direct injection gasoline engine. Fuel 166 (2016) 543–552. (Yinhui, 2016)

40. L. Hamilton, J. Cowart. Cranking-Startup Intake Port and In-Cylinder Mixture Preparation Behavior in a CFR Gasoline Engine. JSAE 20077049 SAE 2007-01-1833. (Hamilton, 2007)

41. K. Morganti, T. Mun Foong, M. Brear. Design and Analysis of a Modified CFR Engine for the Octane Rating of Liquefied Petroleum Gases (LPG). SAE (2014) doi:10.4271/2014-01-1474. (Morganti, 2014)

42. H. Watson, P. Phuong. Why Liquid Phase LPG Port Injection has Superior Power and Efficiency to Gas Phase Port Injection. SAE 2007-01-3552. (Watson, 2007)

43. Jüri Olt, Villu Mikita. Cylinder Pressure Characteristics of Turbocharged and Naturally Aspirated Diesel Engines. Procedia Engineering 100 (2015) 350 – 359. (Olt, 2015)

44. L. Siwale, L. Kristóf, A. Bereczky. Performance, combustion and emission characteristics of n-butanol additive in methanol–gasoline blend fired in a naturally-aspirated spark ignition engine. Fuel Processing Technology 118 (2014) 318–326. (Siwale, 2014)

45. B. Bunting, K. More, S. Lewis, T. Toops. Phosphorous Poisoning and Phosphorous Exhaust Chemistry with Diesel Oxidation Catalysts. SAE (2005) 01-1758. (Bunting, 2005)

46. H. Spikes. The history and mechanisms of ZDDP. Tribology Letters, Vol. 17, No. 3, October 2004. (Spikes, 2004)

47. A. Morina, A. Neville, M. Priest, J. Green. ZDDP and MoDTC interactions in boundary lubrication—The effect of temperature and ZDDP/MoDTC ratio. Tribology International 39 (2006) 1545–1557. (Morina, 2006)

48. F. Amrouche, P. Erickson, J. Park, S. Varnhagen. Extending the lean operation limit of a gasoline Wankel rotary engine using hydrogen enrichment. International Journal of Hydrogen Energy 41 (2016) 14261-14271. (Amrouche, 2016)

49. C. Sung, H. Curran, Using Rapid Compression Machines for Chemical Kinetics Studies, Progress in Energy Combustion Science (2014) 1-18. (Sung, 2014)

50. A. Beattie, M. Moore, A. Goldberg. “Tetraethyl-Lead Poisoning.” The Lancet volume 300, Issue 7766 (1972). (Beattie, 1972)

51. J. Dec. Advanced compression-ignition engines – understanding the in-cylinder process. Proc. Combust. Inst. 32(2), 2727-2742 (2009). (Dec, 2009)

52. C. Dumitrache, M. Baumgardner, A. Boissiere, A. Maria, J. Roucis, A. Marchese, A. Yalin. A Study of laser induced ignition of methane-air mixtures inside a Rapid Compression Machine. Proceedings of the Combustion Institute (2016). (Dumitrache, 2016)

53. A. Boissiere. Effect of Additives on Laser Ignition and Compression Ignition of Methane and Hydrocarbons in a Rapid Compression Machine (2016). (Boissiere, 2016)

54. M. Baumgardner, S. Sarathy, A. Marchese. Autoignition Characterization of Primary Reference Fuels and n-heptane/n-Butanol Mixtures in a Constant Volume Combustion Device and Homogeneous Charge Compression Ignition Engine. Energy Fuels (2013), 27 (12), pp7778-7789. (Baumgardner, 2013)

55. R. Reitz, G. Duraisamy. Review of high efficiency and clean reactivity controlled compression ignition (RCCI) combustion in internal combustion engines. Progress in Energy and Combustion Science (2015). (Reitz, 2015)

56. Kokjohn, S. L., Hanson, R. M., Splitter, D.A., Reitz, R. D., Int. J. Engine Res. 12(3), 209-226 (2011). (Kokjohn, 2011)

57. Hockett, A. G., Hampson, G., Marchese, A. J., Int. J. Powertrains (2016). In press. (Hockett, 2016)

58. Waukesha CFR F-1 & F-2 Research Method (F-1) Motor Method (F-2) Octane Rating Units Operation & Maintenance, Second Edition. 1998. (Waukesha, 1998)

59. Z. Huang, Y. Ren, D. Jiang, L. Liu, K. Zeng, B. Liu, X. Wang. Combustion and emissions characteristics of a compression ignition engine fueled with Diesel – dimethoxy methane blends. Energy Conservation and Management 47 1402-1415, 2006. (Huang, 2006)